

AUS Repository

Liposomal drug release using ultrasound and modeling release dynamics for model predictive controller design

Item Type	Thesis
Authors	Moussa, Hesham Gamal
Download date	2026-05-20 17:29:43
Link to Item	http://hdl.handle.net/11073/7841

LIPOSOMAL DRUG RELEASE USING ULTRASOUND AND MODELING
RELEASE DYNAMICS FOR MODEL PREDICTIVE CONTROLLER DESIGN

by

Hesham Gamal Moussa

A Thesis Presented to the Faculty of the
American University of Sharjah
College of Engineering
in Partial Fulfillment
of the Requirements
for the Degree of

Master of Science in
Electrical Engineering

Sharjah, United Arab Emirates

June 2015

© 2015 Hesham Gamal Moussa. All rights reserved.

Approval Signatures

We, the undersigned, approve the Master's Thesis of Hesham Gamal Moussa.

Thesis Title: Liposomal drug release using ultrasound and modeling release dynamics for model predictive controller design

Signature

**Date of Signature
(dd/mm/yyyy)**

Dr. Nasser Qaddoumi
Professor, Department of Electrical Engineering
Thesis Advisor

Dr. Ghaleb Hussein
Professor, Department of Chemical Engineering
Thesis Advisor

Dr. Hassan Mir
Associate Professor, Department of Electrical Engineering
Thesis Committee Member

Dr. Amani Al-Othman
Assistant Professor, Department of Chemical Engineering
Thesis Committee Member

Dr. Nasser Qaddoumi
Head, Department of Electrical Engineering

Dr. Mohamed El-Tarhuni
Associate Dean, College of Engineering

Dr. Leland Blank
Dean, College of Engineering

Dr. Khaled Assaleh
Director of Graduate Studies

Acknowledgments

As I come to the end of this journey of my life where I had the opportunity to study and experience a completely new world, I have to pay my gratitude to those who helped me as I went.

All my special gratitude and thanks are due to my advisors Prof. Ghaleb Husseini and Prof. Nasser Qaddoumi who contributed to the success of this work through their continuous support and encouragement and their wise and professional advising on the matter of the thesis.

I would also like to mention how grateful I am to have worked with Prof. Ana Martins. Without her dedication and enthusiasm, I could have not reached where I am now. She taught me a lot and always made me feel like a friend. I would like also to extend my gratitude to Dr. Nabil Abdel Jabbar for his support and assistance that contributed in the making of this thesis.

My thanks are also due to the faculty of engineering and the electrical engineering department for giving me this opportunity and for the limitless and profound support they provided. I would like also to acknowledge the University for providing me with the graduate teaching assistantship that made it possible for me to continue my graduate studies at AUS.

Also, a special thanks to my teammate and friend Salma Elgaili who did not spare an effort in supporting and assisting me in my journey. Last but not least, I have to acknowledge with the warmest regards my family, friends and colleagues who supported me all along and made my journey days as enjoyable as ever.

Dedication

The price of success is hard work and dedication and blessing from God, so never lose hope. This is dedicated to everyone trying hard to succeed but the time is yet to

come.....

Abstract

Chemotherapy is widely used for cancer treatment; however, it causes unwanted side effects in patients such as fatigue, weight loss, pain, hair fall and nausea. Those side effects are due to the fact that most of the currently used therapeutic agents are in fact toxic to several organs, including the heart. In addition, many of them lead to the death of both cancerous and healthy cells. In the traditional way of treatment, when the patient was injected with the drug, a high dosage was required so that enough could reach the cancer cells and destroy them. These high dosages, however, can cause more harm than benefit, since they are responsible for the death of many healthy cells. To avoid these adverse effects, nanocarriers, called liposomes, have been developed, which can be loaded with the chemotherapeutic agents, and can be chemically modified to circulate for long periods in the blood stream while encapsulating the drugs and resisting any premature leakages. Additionally, ligands can be conjugated to their surface, allowing for their specific binding to receptors overexpressed on the surface of cancer cells and the subsequent internalization via endocytosis. Using ultrasound (US) as a triggering mechanism, the release of the drug is controlled temporally and spatially as it is induced inside the cells, hence avoiding drug release in systemic circulation, which in turn reduces the undesired side effects of conventional chemotherapy. US is of great interest to be used as a triggering technique as there is a lot of published work proving its usability in causing release from liposomes. Most of the work uses low frequency US as it causes the release at lower power densities; however, it is hardly focused unlike US at higher frequencies. The developed liposomes were tested against low frequency US (20 kHz) and focused-US at 1 MHz and 3 MHz and the results were compared to the literature. Moreover, the kinetics of the release were modeled to be used for many applications such as control systems and elimination of the need for further exhaustive laboratory experimentation.

Search Terms: *Ultrasound, drug release, triggering, PEGylated-liposomes, drug delivery systems, HIFU, Neural Networks, Model Predictive Control*

Table of Contents

Abstract	6
List of Figures	9
List of Tables	11
CHAPTER 1: Introduction	12
CHAPTER 2: Liposomes	16
2.1. Introduction.....	16
2.2 What are liposomes?	17
2.3. Liposome stability - stealth liposomes.....	20
2.3.2. <i>Colloidal stability</i>	21
2.4. eLiposomes	23
CHAPTER 3: Triggering Techniques	25
3.1. Triggering methods.....	26
3.1.1. <i>Temperature-triggered release – thermosensitive liposomes</i>	26
3.1.2. <i>Enzyme-triggered release</i>	32
3.1.4. <i>Light-triggered release</i>	40
3.1.5. <i>Magnetoliposomes</i>	43
CHAPTER 4: Ultrasound	48
4.1. Physics of ultrasound	48
4.2. Ultrasound applications	51
4.3. Ultrasound behavior in matter	53
4.4. Transducer design	60
4.4.1 <i>Concept of Piezoelectricity</i>	60
4.4.2. <i>Piezoelectric material properties</i>	62
4.4.3. <i>Radiation Field of Piston Transducer</i>	67
4.4.4. <i>Unfocused circular transducer</i>	71
4.4.5. <i>Focused circular transducer</i>	72
CHAPTER 5: Ultrasound in Drug Delivery	75
5.1. Interaction of ultrasound with liposomes.....	75
5.1.1. <i>Hyperthermia</i>	75
5.1.2. <i>Cavitation</i>	77
5.1.3. <i>Collisional mechanism</i>	81
5.1.4. <i>Acoustic droplet vaporization</i>	82
5.3. Advantages and shortcomings of US as a trigger in DDSs.....	86

5.4. Liposomes and ultrasound: clinical uses.....	87
CHAPTER 6: Experimental Work	90
6.1. Experimental Setup.....	90
6.2. Expected results based on literature.....	91
6.3. Methods	92
6.3.1 <i>Synthesis of PEGylated liposomes</i>	92
6.3.3. <i>Experimental procedure for the low frequency online experiments</i>	99
6.3.4. <i>Comparison between low and high frequency ultrasound as a triggering modality</i>	102
CHAPTER 7: Modeling and Control.....	104
7.1. Background on Neural Networks Modeling	104
7.2. Model Predictive Controlling	108
CHAPTER 8: NN-MPC and Results.....	110
8.1. Procedure and Setup	110
8.2. Sample results	116
CHAPTER 9: Conclusion and Recommendation	121
References.....	123
Appendix A	139
Vita	143

List of Figures

Figure 1. The general structure of a PEGylated liposome.	18
Figure 2. Formation of liposomes of different sizes and levels. LMV, multilamellar vesicle; SUV, small unilamellar vesicle; LUV, large unilamellar vesicle; GUV, giant unilamellar vesicle.....	19
Figure 3. Stability of PEGylated liposomes. Collisions are prevented by adding PEG chains to the surface of liposomes, which act as springs during collisions. .	22
Figure 4. Ultrasound-triggered release from eLiposomes.	24
Figure 5. The two major triggering techniques. Internal triggers and external triggers	25
Figure 6. Nature of acoustic wave propagation: shear and longitudinal.....	49
Figure 7. Image showing a successive cycles of high and low pressure areas formed due to the motion of a piston in a medium of particles.	50
Figure 8. Representation of a sinusoidal wave.	51
Figure 9. Layered model of the human body simplified into three main layers.....	59
Figure 10. Wave propagation behavior at boundaries between layers of different acoustic impedances.....	59
Figure 11. Ultrasound wave behavior in a multilayer medium	60
Figure 12. PZT ultrasound system showing the PZT powder placed between two metal plates	62
Figure 13. Transmission line model for Ultrasound PZT probe	64
Figure 14. Circular Disk Ultrasound Probe	67
Figure 15. Division of the circular PZT disk into very small sub-disks and analysis of the US waves radiated from those points at a certain point in space distanced from the origin by “r”	69
Figure 16. Radiation pattern of different probes at different half angles.....	70
Figure 17. The actual field pattern of the circular disk transducer versus that of the theoretical one.....	72
Figure 18. The focused ultrasound probe and the corresponding radiated wave,.....	73
Figure 19. Different types of cavitation processes.....	80
Figure 20. Liposomes loaded with microbubbles.	81
Figure 21. Complete drug delivery system explaining the objective of this work.	90
Figure 22. Experimental setup for sonication of the liposomes from down below	95

Figure 23. Sample results showing the fluorescence level against offline sonication for a period of 1 hour divided into 4 equal portions of 15 minutes each.....	96
Figure 24. Calcein release kinetics from PEGylated liposomes at pH 7.4 using 1-MHz US.	97
Figure 25. Calcein release kinetics from PEGylated liposomes at pH 7.4 using 3-MHz US.	98
Figure 26. Calcein release curve versus time of sonication.....	100
Figure 27. Calcein release curve when using ultrasound on/off cycle of 10/10 seconds.....	102
Figure 28. The structure of the simple neural network.....	106
Figure 29. Back propagation training of neural networks with a delay of 2 samples.	107
Figure 30. Basic components of a model predictive controller	109
Figure 31. Square pulses indicating the periods at which the US is on or off as well as what power density is being used	111
Figure 32. The mimicking US pulses plotted against the corresponding release curve.....	112
Figure 33. The release curve after cleaning and fitting using NN back propagated training.	113
Figure 34. Simulink block of the NN predictive controller used to build the NN-MPC.....	115
Figure 35. Full NN-MPC system setup.....	115
Figure 36. Finding the reference curve out from the data base of collected release curves	116
Figure 37. Finding the reference curve out from the data base of collected release curves	117
Figure 38. The proposed US pattern that shall be used in case of ideal performance	118
Figure 39. Sample results from the NN-MPC: Reference signal.....	118
Figure 40. Sample results from the NN-MPC: Corresponding system output	119
Figure 41. Sample results from the NN-MPC: Controller moves.	119

List of Tables

Table 1. Ultrasound: range of frequencies and respective applications [188].	52
Table 2. Acoustic absorption in fresh water, seawater and air (at sea surface normal conditions) at 10 kHz and 1 MHz. From [173].	57
Table 3. Average attenuation coefficients in tissue (from [208]).	57
Table 4. Attenuation of human tissue at 1 MHz. Adapted from [208, 209].	58
Table 5. Tabulated results of the sample given in figure 23.	96

CHAPTER 1: Introduction

In the past decade, there has been increased interest in the area of drug delivery especially for the treatment of cancer, an often terminal disease that can have devastating symptoms. In 2012, cancer was reported as the leading cause of death in Europe and North America. It was also regarded as the second leading cause of death in the less developed countries, especially in Africa. Statistics of estimated cancer incidence, mortality and prevalence worldwide are well documented by GLOBOCAN, a project of the International Agency for Research on Cancer, part of the World Health Organization (WHO) [1]. Unfortunately, this disease can be very difficult to treat, and sometimes even impossible. Tumors can strike in two forms, either malignant or benign. In both forms, tumors result from an abnormal growth of cells. In the case of benign tumors, this abnormal growth usually forms a stable, non-moving mass that can be removed from the body through surgery. On the contrary, in the case of malignant tumors, i.e., cancer, the growing cells can spread in the body, causing metastasis, increasing the number of affected organs and interfering with vital body functions.

Treatment varies according to the tumor type: in the case of benign tumors, surgery is usually performed to remove the tumor, although there is no guarantee that all cells are removed. Likewise, in the case of a cancerous tumor, it is still possible to remove the whole tumor if it is contained within a specific area, but in the case the cancer goes into metastasis, it may not be feasible to do so [2]. In some cases, no surgery is possible, especially when the tumor is located in inaccessible or vital areas (e.g. brain tumors). These facts led medical doctors and scientists to try to develop assistive treatments that can help in stopping cancer from spreading inside the body which led to the development of chemotherapy. The German chemist Paul Ehrlich was the first to use the term chemotherapy in the 1900s [3]. He was also the first to use animal models for testing newly developed chemical medicines. These pioneering discoveries led to the true revolution of chemotherapeutic agents used for cancer treatment as we know it today [3]. However, it was not until the 1960s that chemical medicines were considered effective against cancer. Prior to that, surgery and radiotherapy were dominant in the treatment of cancer. In 1960, scientists discovered that the use of chemotherapy, in addition to surgery, increased the possibility for a successful recovery of cancer patients [3]. However, chemotherapy, although a great discovery, can also cause several health problems to those undergoing treatment. This is due to the fact that the chemicals used

are not selective, i.e., they affect not only cancerous cells, but also healthy cells in the body. Hence, patients treated with anti-neoplastic chemical agents suffer from several serious side effects due to the death of vital healthy cells, such as hair loss, fever, fatigue, weight loss and lowered immunity [2, 4].

Since scientists believe in the essentiality of using chemotherapy for cancer treatment, researchers have directed considerable attention to reducing its side effects. One of the methods used to overcome these unwanted effects was to lower the toxicity of the chemicals through identification of the effective agents and the removal of unwanted chemicals before administration. Another approach consisted of carefully checking the vitals of the patient and testing for allergic reactions, before he/she was declared eligible to undergo chemotherapeutic treatment [2]. However, the greatest advances in this field were, possibly, due to the collective work of medical scientists and engineers who used their technological and scientific knowledge to design efficient Drug Delivery Systems (DDS).

Nanoparticles are an essential part of a DDS. They have a durable chemical composition that is compatible with bodily fluids, and can be designed to circulate in the body for extended periods of up to several days [5]. The role of these nanoparticles is to encapsulate the chemotherapeutic agent in their core, so that it does not interact with healthy cells in the body. Nanoparticles are designed based on two targeting methods, passive and active, both of which make them capable of accumulating in cancerous tumors preferentially. This, in turn, reduces the dosage that would be needed to treat the tumors if the free drug were to be used. Once the nanoparticles accumulate at the diseased site, external or internal means of triggering are used to release their content, by disrupting their membrane, which causes the drug to leak out. Hence, the release trigger is the complementary part of many DDSs. Examples of nanoparticles are liposomes, micelles, dendrimers, archaeosomes, solid lipid nanoparticles and other carrier systems [6, 7], with the most widely researched being the first two. Examples of external triggers are ultrasound (US), electromagnetic waves (light-triggering) and magnetic fields, while internal triggers include pH, temperature and enzymes [8].

Furthermore, for every DDS, release experiments are conducted to determine the relation between US parameters and the release rate. Therefore, any experiment will involve the adjustment of one of the US parameters such as intensity or frequency to study its effect on the release curve. This process will yield multiple release curves

which can be used as a reference for medical doctors employing the DDS to help them choose the proper US parameters that can be used to achieve a certain level of release within a certain period of time. Hence, developing models based on the collected release data would prove to be beneficial especially if a controller is to be designed to control the US during the online sonication process. Also, those models work as a method by which a release curve can be predicted even if it is not one of the initial curves used to develop the model.

The objectives of this thesis are as follows:

1. To design a focused US probe capable of operating at 1 and 3 MHz frequencies while providing waves of high power densities.
2. Test the release of the model drug calcein from the newly developed PEGylated liposomes against the two frequencies and various power densities in offline experiments.
3. Explore the reasons behind the release of the calcein from the liposomes at those frequencies.
4. Test and study the dynamics of the release of the model drug calcein from the newly developed PEGylated liposomes when sonicated with 20 kHz US at different intensities in the continuous mode in online experiments.
5. Develop a generic ANN model relating different US parameters and the corresponding release trend for the 20 kHz online experiments.
6. Use the developed model to design a controller that can adjust the sonicators parameters to follow a certain desired output based on the neural network model predicative controller (NN-MPC).

In this thesis, the focus is on liposomes as the drug carrier and high frequency US as a triggering technique while reviewing briefly the history of triggering techniques. Hence, in the next chapters, the chemical aspect of liposomes and the way they are formed is discussed followed by a chapter that reviews different nanocarriers and their corresponding triggering techniques. Then in chapter four, a review of the physics of ultrasound is presented that will help in understanding the ways it can induce drug release from nanocarriers. This review also helps in understanding the procedure used in designing the ultrasound probe used in this thesis. Chapter five then discusses ultrasound applications in drug delivery and explores the ways it interacts with

liposomes. Then, in chapter six, the experimental procedure followed for the release experiments and the results for those experiments with discussions are presented. Chapter seven then introduces the modeling and control concept and details the online low frequency release experiments conducted to develop the ANN model. Chapter 8 will then summarize the release results and the method by which the model was developed. It also includes the NN-MPC designed to control the release from a simulated *in vitro* situation.

CHAPTER 2: Liposomes

2.1. Introduction

A full DDS is composed of two main parts. The first part is related to the carrier vehicles that circulate in the body, and then deliver their contents to the desired location. These carriers include liposomes, micelles, dendrimers, archaeosomes, solid lipid nanoparticles and others [9-11], but in this work, only liposomes are discussed. The second part of the DDS is the controlled release of the drug from the nanocarriers using triggering methods [8].

To improve the utility of these nanovehicles, so they can circulate in the blood stream and accumulate at the desired location, targeting techniques are used to modify their surface so that they can sense their way in the body and accumulate preferentially at the tumor site. There are two broad types of targeting techniques, namely passive and active (ligand) [5, 8, 12, 13]. In *passive targeting*, the vesicles accumulate preferentially at the tumor site based on several malignancy physical parameters, including pH level, capillary size, enzymatic concentration, and leaky vasculatures [14]. Additionally, solid tumors have damaged lymphatic drainage systems. Together, these factors promote the extravasation and accumulation of macromolecules and nanoparticles at the tumor site, a phenomenon known as the enhanced permeability and retention effect (EPR) [15, 16]. This type of targeting requires longer circulation periods allowing for the carrier to accumulate at the targeted location before release occurs [5, 8] (see Section 2.3. Liposome stability - stealth liposomes). Furthermore, in passive targeting, the carriers can also be designed to respond to the intended trigger. Hence, the physical environment in which the drug is introduced can be used both as a targeting parameter and as a triggering technique, as will be discussed later. Nonetheless, while controlling the release using physical parameters may prove challenging, it may be a desirable feature in case most of the loaded drug dosage contained in the carriers is to be completely released [5, 9, 12, 17, 18].

The nanocarriers can also be designed in such a way that they have higher affinity towards certain cancer cells, when compared to their affinity towards healthy cells. This is done using ligands that can biochemically recognize certain features of cancerous cells (namely receptors), thus allowing them to specifically bind to those cells. This type of targeting is termed *active targeting*. Active targeting can be further

divided into three levels: first-order, second-order, and third-order targeting [13]. First-order targeting usually refers to organ targeting, where the carriers are programmed to accumulate in a certain organ and release the drug in the desired region. This is the lowest form of active targeting as it is not sufficiently selective. Second-order targeting, cell targeting, is more selective as the carriers bind to the surface of the cells inside the organ where the drug can be released. This form of targeting is more focused, yet not very selective because the drug is released over the whole region, including healthy cells in the vicinity of the cancer tissue. The third and most selective active targeting form is called subcellular targeting. The carriers used in this form have the ability to select specific cells, enter their cytosol, and release their contents afterwards [19, 20]. Using third-order targeting, only cancerous cells are treated with the chemotherapy, while the adjacent healthy cells are usually spared the cytotoxicity of the anti-neoplastic agent [12, 13, 18].

2.2 What are liposomes?

In the early 1960s, Alec Bangham, a British scientist, was conducting experiments with phospholipids when he recognized spherical structures developing when water was added to the phospholipid film. Later, he discovered that those spherical structures, known as liposomes, were hollow and could encapsulate chemicals [17, 21, 22]. Liposomes are drug delivery vehicles in the nanosize range which can be used to encapsulate chemotherapeutic drugs until reaching the location of diseased tissues inside the body. They are comprised of phospholipid bilayers similar to cell membranes (Figure 1), which is an advantage when compared to other nanoparticles. Phospholipids are molecules that have two parts, a hydrophilic head and a hydrophobic tail. This composition allows for both hydrophobic and hydrophilic drug encapsulation by the liposomes. Hydrophobic drugs can be loaded between the lipid layers where no water is present, while hydrophilic agents can be loaded in the aqueous core of the liposomal structure. Additionally, liposomes have the advantage that chemical flags (ligands) can be attached to their surfaces to achieve more specific active targeting [21, 23].

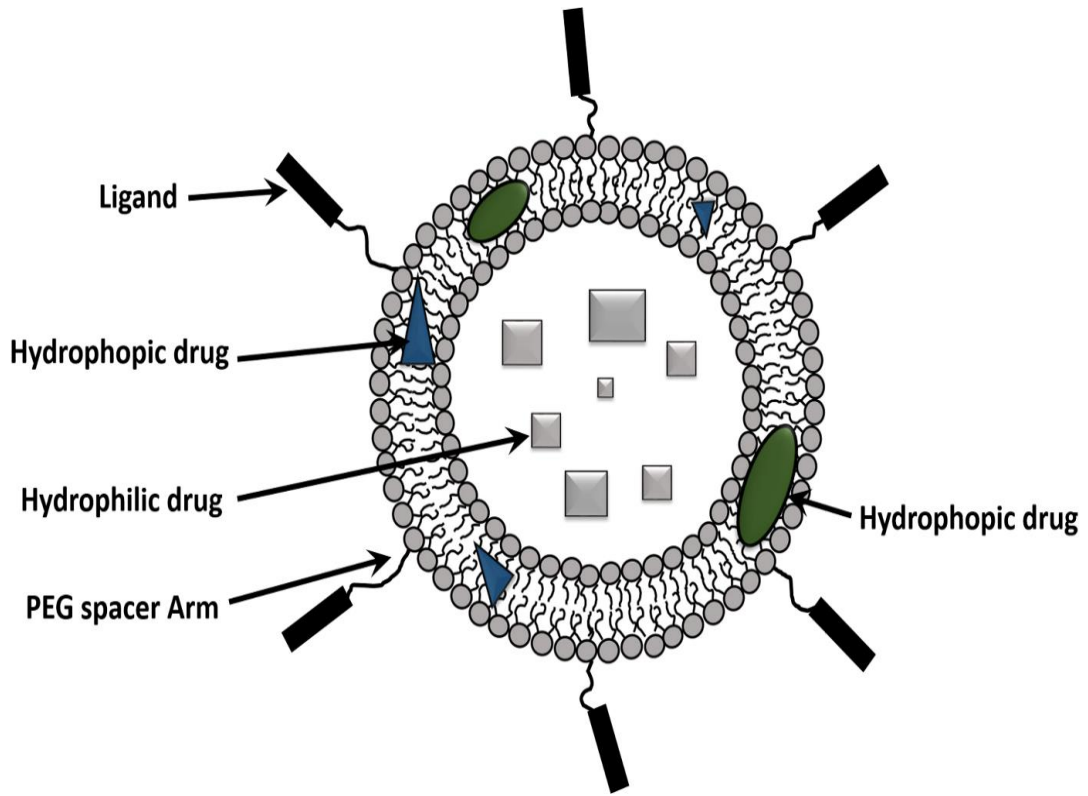


Figure 1. The general structure of a PEGylated liposome.

The lipids that form liposomes have certain features that determine the structure of the resultant carrier. Those features include the packing parameter which is the ratio of the cross-sectional areas of the hydrophobic to the hydrophilic regions of the lipid and can be calculated as follows [17, 24]:

$$PP = \frac{V}{L \cdot A} \quad (1)$$

where V and L are the volume and the length of the hydrophobic part while A refers to the area of the hydrophilic part. In order to form a functional liposome, the packing parameter needs to be between 0.74 and 1.0 [25]. If this threshold is met, using the right technique, full liposomes called multilamellar vesicles (MLVs), can be formed [26]. MLVs are relatively big in size and their main advantage is that they are stable. Unilamellar vesicles (ULVs) can be produced from the MLVs by physical means, e.g. high intensity focused US (HIFU). These ULVs can be further classified into three types: small unilamellar vesicles (SUVs), large unilamellar vesicles (LUVs), and grand or giant unilamellar vesicles (GUVs) [27] (Figure 2). The most appropriate vesicles for drug delivery are the ULVs due to their average size and their ability to encapsulate all types of drugs [24].

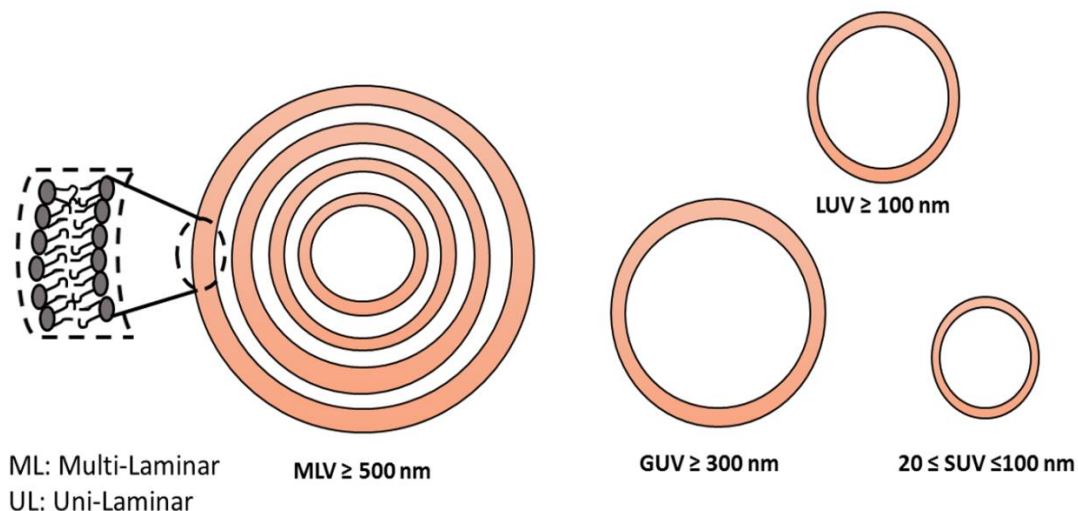


Figure 2. Formation of liposomes of different sizes and levels. *LMV*, multilamellar vesicle; *SUV*, small unilamellar vesicle; *LUV*, large unilamellar vesicle; *GUV*, giant unilamellar vesicle.

Other features of liposomes, including thermotropic behavior, phase transition temperature (or temperature range), and maximum transition temperature (T_m), are also determined by the lipid composition and their packing parameters. These features determine the permeability of the liposomes and their sensitivity to temperature. When liposomes are formed, the lipid bilayer goes through a two-phase transition stage. The lipids can change from a solid-ordered state (SO), sometimes referred to as the gel phase, where each element is discrete and not attached to other elements in a harmonious way forming a crystalline structure, to a liquid-ordered state (LO) where the layer becomes more flexible and homogenous. When the lipids forming the liposomal membrane are all in the SO state or in the LO state, the liposomes are considered to be tight, allowing almost no drug release. However, as the lipid transitions from one state to another, at some point, some of the lipids will be in the SO state while others will be in the LO states. When this happens, in a state referred to as liquid-disorder (LD), the lipids are arranged in such a way that allows the formation of pores in the shell through which the drug starts to diffuse out, i.e., release begins. This transition happens due to a temperature change that leads to the solidification or liquefaction of the lipids. This phenomenon occurs at T_m , during which the maximum change in heat capacity happens and most of the thermal energy is used to re-organize the lipids. This transition temperature is determined based on the packing parameter and the lipid composition of the liposomes. Similarly, other liposomal features depend

entirely on the lipid composition hence reasserting the importance of the chemical formulations of those nanocarriers [17, 24, 28].

The fact that the liposomal membrane is similar to that of human cells gives it the advantage of being more easily accepted by the human body. Nonetheless, these membranes can still be attacked by the macrophages that patrol the blood constantly, which can identify them as dead cells or foreign structures, thus contributing to their elimination. At the same time, this fact can actually be advantageous in some cases. Some diseases, such as systematic fungal infection and leishmaniase, are due to the infection of macrophages; hence they can be treated by delivering liposome-encapsulated toxic drugs directly into the mononuclear phagocyte system [23]. To treat other diseases, a new strategy had to be devised, and this issue was resolved with the synthesis of a new type of liposome called *stealth* liposomes [23, 29-31].

2.3. Liposome stability - stealth liposomes

A crucial characteristic that needs to be addressed when dealing with drug nanocarriers is their stability. Stability is essential since non-stable carriers will prematurely release their toxic content once the patient receives the medication.

Stealth liposomes are high-stability, long-circulating liposomes [23, 29-31]. The inclusion of saturated phospholipids and cholesterol in the composition of liposomes increases their stability, but does not prevent their binding to proteins. To increase the blood circulation time of liposomes, these vehicles are usually coated with a layer of a synthetic polymer called polyethylene glycol (PEG) (Figure 1), which protects them from binding serum proteins, and thus from being recognized by the mononuclear phagocyte system.

The stability of a liposome is mainly dependent on three factors: chemical composition, colloidal stability, and biological stability, all of which are inter-related [17, 30].

2.3.1. Chemical formula stability

Since liposomes are nano-sized carriers made of lipids, their chemical stability is highly dependent on the stability of these compounds, which are prone to oxidation and hydrolysis [17]. Both unsaturated and saturated hydrocarbon chains can suffer oxidative processes, although the latter only occurs at high temperatures. In the

presence of oxygen, this process, termed lipoperoxidation, develops quickly and may lead to the rupture of the hydrocarbon chains. Such reactions cause deformations in the surface of the liposomes that lead to their destabilization. The chemical stability of the liposomes determines their shelf-life and can be enhanced by the addition of antioxidants and chelators of metal ions [30].

Another chemical process that jeopardizes the stability of liposomes is hydrolysis. This process can affect both the carboxylic esters, as well as the phosphate esters that are present in the liposomal structure. The hydrocarbon chains may be completely hydrolyzed leading to the formation of glycerophosphoric acid [17].

To increase the physicochemical stability of the liposomes, cholesterol units are added to the formulation, which, along with the presence of phospholipids containing saturated hydrocarbon chains, make them stiffer and less vulnerable to physical factors [8]. The use of cholesterol needs to be optimized so that the produced liposomes are stable enough to circulate for longer periods in the body, yet their breakdown is possible so that drug release can be achieved at the diseased location. It has been observed that liposomes with cholesterol in their composition have longer blood circulation time, which proves that chemical stability affects biological activity [31].

2.3.2. Colloidal stability

Colloidal stability refers to stability in the case of collisions between different liposomes and other components of the blood (including blood proteins). When liposomes are systemically introduced into the body, it is inevitable that they will collide with other particles. Those collisions may lead to their disruption and shear, allowing for the release of their contents. To avoid the occurrence of this disruption due to collisions, a surface chemical chain is attached to the surface of the liposomes through either grafting or absorption. The most widely used chemical chain is, as mentioned before, the PEG polymer, which is added to the formulation to generate sterically stabilized liposomes (SSL) (the stealth liposomes mentioned previously) [32]. The PEG polymer is a hydrophilic chain that is spread over the surface of the liposomes. These chains are capable of preventing the liposomes from colliding with other particles in the body using a repulsive force due to the compression of the chains between the two surfaces. Simply stated, those chains work as springs that create an opposing force when compressed to retain their original length (Figure 3). These polymers also protect

the liposomes against the mononuclear phagocyte system, lowering the possibility of the liposomes being ingested by the macrophages, as described earlier. Chain compression is entropically unfavorable allowing for the carriers to circulate in the blood for longer times [33].

However, the presence of these chains on the surface of the liposomes may pose a problem when the liposomes are used for active targeting. The ligands for targeting are usually shorter than the PEG polymers, which presents a challenge to the action of targeting as it prevents the ligands from binding to the receptors on the surface of the targeted cells [34]. Therefore, to achieve better targeting of PEG-coated liposomes, the targeting ligand is attached to the surface of the liposome through a PEG spacer arm. This allows the ligands to be extended further outside the dense PEG-coated surface and become more “visible” to the receptors, which reduces steric interference when binding to the target [28].

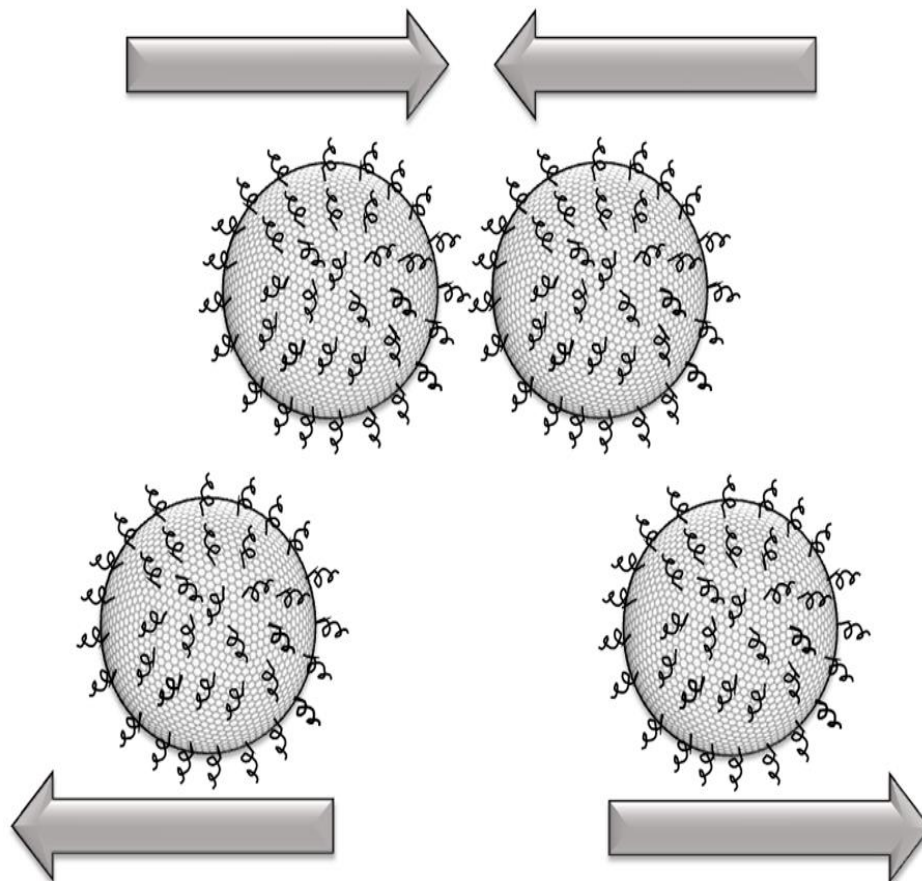


Figure 3. Stability of PEGylated liposomes. Collisions are prevented by adding PEG chains to the surface of liposomes, which act as springs during collisions.

2.4. eLiposomes

eLiposomes or emulsion liposomes are a new class of stealth liposomes, containing nanoemulsion droplets, which makes them more sensitive to ultrasonic triggering (i.e. more echogenic) [35-39]. This feature is an example of the type of modifications that the liposomes can undergo to improve their effectiveness as drug carriers. Once emulsions are vaporized, the size of the carrier increases by 125-fold which bursts it open, thus spilling its contents at the desired location. The emulsions can also act as bubbles that can cause cavitation, which is one of the mechanisms by which drug release from liposomes can be induced (discussed in section 4). However, here, only the structure of the eLiposomes will be discussed.

The main advantage of eLiposomes over other liposomes is the fact that they are more sensitive to US, and hence release can be induced using low intensity waves [36, 38]. Liposomes are not inherently sensitive to acoustic waves [40]. However, when air bubbles are present in the vicinity, release can occur. This is due to the fact that these bubbles are affected by US-induced cavitation (Section 4.2.2), which leads to the induction of a massive force that causes the liposomes to shear open and release their content. This discovery inspired research on acoustically sensitive liposomes. Additionally, eLiposomes are smaller in size than normal microbubbles which is an advantage when considering leakage (via the EPR effect) in the vascular network of tumors [35]. Their size, also, makes them suitable for ligand-stimulated uptake into cells through endocytosis [37].

In the first attempts to use US to trigger the release from liposomes, the microbubbles, considered as US contrast agents, were introduced in the solution with the liposomes. However, in order to trigger their release, the bubbles had to be of a certain size and composition. It was challenging to deliver them to the targeted site with the liposomes, as they were bigger in size and easily eliminated by the pulmonary pressure, which introduced various constraints when the system reached the clinical phase [41]. As a solution to this problem, it was then suggested to introduce nanoemulsions into the liposomal structure, to make them more echogenic [37]. Those nanoemulsions are usually made of perfluorocarbons (inert), the two most common being perfluorohexane (PFC₆) and perfluoropentane (PFC₅), both possessing low vapor pressures [35, 37]. The main advantage of these perfluorocarbons is their non-toxic nature (they are currently being investigated as blood substitutes) and their stability in

aqueous solutions. They also have relatively low vapor pressures, which makes them sensitive to the pressure waves induced by the acoustic field [36, 38].

Vapor can be compressed by increasing the external pressure, which forces its atoms to come close together. However, if the external pressure is reduced, the vapor will expand to regain its normal atomic spacing. The emulsions are designed to contain the perfluorocarbon under a certain pressure level at a certain temperature in the form of a liquid. When the external pressure is forced below the vapor pressure, the emulsion will expand and the perfluorocarbon will change from liquid to gas, and since the emulsions are loaded inside the liposomes, they will in turn expand. This expansion leads to the formation of pores in the membrane of the liposomes (which are capable of bursting the liposome open), which causes the release of the drug [39] (Figure 4). The size of the nanoemulsions has been described to be as small as 30 nm [37] and as large as 500 nm [38]. As mentioned above, when the US is in the rarefaction phase (low pressure cycle), the pressure will be below the vaporization pressure of the perfluorocarbon, forcing it to vaporize, leading to the expansion or even the complete destruction of some nanoemulsions. Hence, eLiposomes are considered useful carriers when US is used as a trigger. Several research studies showed that, when using US as a trigger, drug release from eLiposomes increases, when compared with the release from “normal” liposomes [35, 36, 38].

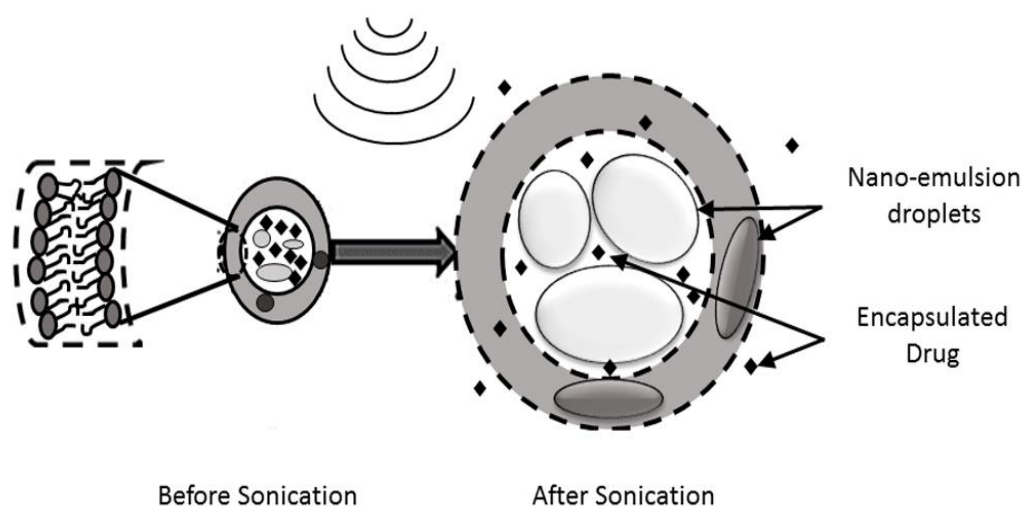


Figure 4. Ultrasound-triggered release from eLiposomes. Ultrasound affects the encapsulated nanoemulsions causing them to expand during the low pressure cycle, leading to the expansion and eventually the disruption of the liposomal lipid bilayer.

CHAPTER 3: Triggering Techniques

So far, this review focused mainly on the first part of the drug delivery system, i.e., the carrier. Although this is a crucial part of the system, stimuli or techniques controlling the release of the therapeutic agents from the carriers are equally important. This form of targeting is referred to as triggered targeting. The objective of a DDS is to deliver the drug to the desired location in the body and to control the release of its content, thus minimizing the side effects of the drug. This section focuses on the different techniques used to trigger the release from the nanocarriers, and in particular from liposomes. Summarized in Figure 5, there are two types of triggering means: internal triggers including the pH level, temperature, and time, and external triggers including light, electromagnetic waves, magnetic fields and US [42]. Since US is the main focus of this review, section 4 will be dedicated to the discussion of this triggering technique. It is important to note that some external triggers either directly affect the carriers or are used to induce an internal trigger. For example, electromagnetic waves can be used to directly trigger release or they can be used to heat up the area and cause release through a temperature increase (an internal trigger) [43].

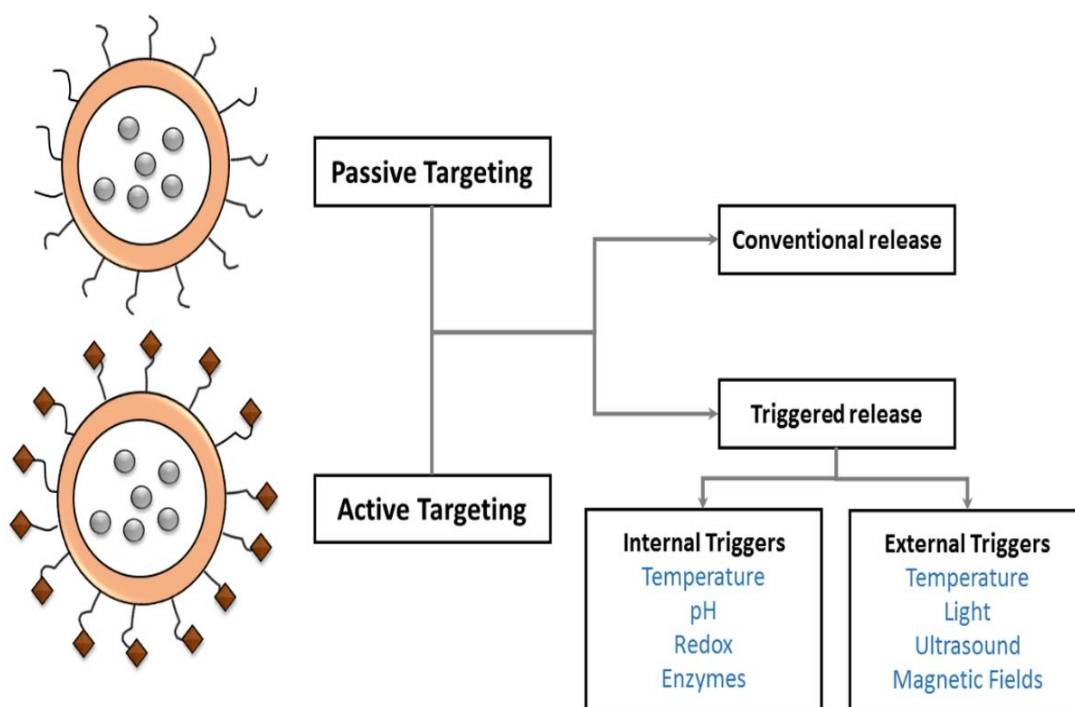


Figure 5. The two major triggering techniques. Internal triggers and external triggers are used to control drug release from different liposomal carriers modified to be sensitive to a specific trigger.

Triggering is defined as the method by which the release of drug is controlled, and it includes the period of release, the amount to be released and the location of the release. An efficient DDS can be obtained by targeting the carriers, and encapsulating a chemotherapeutic agent, until it reaches the cancer cells, followed by its triggered release at the desired site, thus increasing the efficacy of the treatment [42]. Each triggering technique is used along with a specific type of carrier that is designed to respond to it. For example, magnetoliposomes are easily triggered by magnetic fields because their chemical composition includes active agents that are sensitive to these external fields, namely super-paramagnetic elements including iron [44]. Similarly, other types of nanocarriers have specific agents in their chemical composition that make them sensitive to certain triggering signals [37].

3.1. Triggering methods

3.1.1. Temperature-triggered release – thermosensitive liposomes

This type of trigger is the most widely used to release drugs encapsulated in liposomes, and it has been extensively reviewed in the last few years [45-49]. Since most triggering techniques revolve around the concept of thermal release, extensive research has been directed towards developing liposomes that are thermally sensitive. Liposomes are made of lipids that have a thermal threshold above which they start to melt. This causes the surface of the liposomes to become porous, allowing the encapsulated drug to be released. Nonetheless, not all liposomes behave in this manner. Thermally-triggered liposomes have a defined chemical composition that makes them vulnerable to temperature; hence they are termed “temperature sensitive liposomes” (TSLs) or “thermosensitive liposomes” [49-54]. As the name suggests, TSLs are sensitive to an increase in the local temperature, a process known as hyperthermia, which can be induced via external triggering techniques including US, magnetic fields, microwaves or infrared light [54-57]. If the temperature increase is adequate, so that the temperature reached is higher than the thermal point of the liposomes, it will cause release of the drug within the target at the desired location, hence the side effects due to the toxicity of the chemotherapeutic agent are decreased. Usually, the designed TSLs have a thermal point in the range of 39-43° C depending on the type of lipids used in the synthesis [49, 58]. This temperature range is higher than the temperature of the human body (37° C on average), which makes TSLs desirable drug carriers, since they

are perfectly stable in the body and will not release their contents unless mild hyperthermia is induced.

TSLs were first reported in 1978 by Yatvin *et al.* [59] and tested in an *in vitro* model. The original formulation contained 1,2-dipalmitoyl-*sn*-glycero-3-phosphocholine (DPPC) and 1,2-distearoyl-*sn*-glycero-3-phosphatidylcholine (DSPC). However, with this formulation, release was not specific and occurred everywhere the temperature of the tissues exceeded a certain threshold. Hence further research was done to design thermosensitive targeted liposomes, (TSLs) that circulate in the body, and are aimed towards a targeted destination. To accomplish this, liposomes were first stabilized by adding extra saturated fats and cholesterol to their composition [60]. Also, to increase their circulation time in the body, hydrophilic polymers or glycolipids, such as PEG or monosialoganglioside G_{M1}, were added to the composition, yielding stealth TSLs [61]. These hydrophilic polymers act as a shield against blood plasma and macrophages, avoiding elimination processes including phagocytosis and endocytosis, hence increasing the circulation time of the carrier in the blood stream. By adding these two extra components, functional triggered TSL liposomes were produced. Further improvements were achieved with the incorporation of lysolipids and temperature-sensitive polymers. Actually, the first TSLs that had the potential to be used in clinics were described in 2000 by Needham and co-workers [62], and were composed of DPPC and DSPE-PEG₂₀₀₀, modified with *lyso*-phosphatidylcholine (*lyso*-PC).

Thermosensitive liposomes may be divided into three broad groups: traditional TSL (TTSL), lysolipid TSL (LTSL) and polymer-modified TSL (PTSL) [49].

TTSLs make use of the fact that all lipids have a transition temperature, hence the liposomal lipid bilayer undergoes phase transitions according to the temperature, as described in Section 2.2. Liposomes can be designed to melt at a certain temperature, by carefully planning their formulation [8]. However, it is possible to modify the membrane of the liposomes to make them more sensitive to temperature by adding different molecules to their formulation such as in the case of LTSL which contains lysolipid-modified membranes. Lysolipids are lipids that contain only one, not two, hydrocarbon chains, which makes them more prone to form highly curved micelles resulting in stabilized defects in the membrane when the T_m is approached [49]. One example of a lysolipid is 1-myristoyl-2-palmitoyl-*sn*-glycero-3-phosphocholine

(MPPC), which has been combined with DPPC to create liposomes used in *in vitro* and *in vivo* studies showing promising results [49].

On the other hand, PTSLs are liposomes with a formulation that includes natural or synthetic thermosensitive polymers [63, 64]. These polymers have a specific lower critical solution temperature (LCST), above which the polymer changes phases, transitioning from hydrophilic to hydrophobic [8, 49, 58]. When liposomes coated with these polymers are subjected to temperatures above the LCST, the phase change of the polymer chains makes them contract, destabilizing the liposomal lipid bilayer, and making these regions leaky, thus causing the release of the liposomal drug load [63, 64]. There are several groups of polymers, based on the chemistry of their groups, but the most widely studied is poly(N-isopropylacrylamide) (poly(NIPAM)), which has a temperature threshold of 32° C [65]. Poloxamers such as Pluronic®, well known in the field of polymeric micelles, have also been used as temperature sensitizers in liposomes.

The first studies using poly(NIPAM) and derivatives [66-68] demonstrated that it was possible to anchor these polymers to the surface of liposomes, enhancing their thermosensitivity. The combination of poly(NIPAM) with different co-monomers changes its basic LCST, e.g., the transition temperature of the copolymer of N-isopropylacrylamide and octadecylamine (poly(NIPAM-co-ODA)) is 29°C, while that of the copolymer of N-isopropylacrylamide, acrylic acid and octadecylamine (poly(NIPAM-co-AA-co-ODA)) was determined to be 37°C [69]. These studies also revealed that the sensitivity to temperature was highly dependent on the liposomal composition, since liposomes with PC showed low release, while when the temperature-sensitive DPPC was incorporated into the liposomes, the release significantly increased [66]. Further studies showed that the release could be further improved when 1,2-dioleoyl-*sn*-glycero-3-phosphoethanolamine (DOPE) was used [68, 69]. The main advantage of DOPE carriers is their unique hexagonal II shape in physiological conditions, forming inverted micelles instead of stable bilayers. This destabilizing effect can be balanced by combining them with temperature-sensitive polymers, creating stable TSLs when the temperature is below the LCST of the polymers. Above the LCST, the polymer chains collapse and release from these TSLs can be triggered prematurely [63]. In any case, liposomes conjugated with these polymers are TSLs with an LCST below the physiological temperature of the human

body, preventing their clinical use as drug carriers [49, 63]. For *in vivo* drug delivery, the liposomes must show release at temperatures slightly higher than the physiological temperature. Kono *et al.* [64] used a combination of poly(NIPAM) with poly(acryloylpyrrolidine) (poly(APr)), a polymer with a LCST around 50° C, to produce a polymer with a LCST of ~40°C. Calcein-containing DOPE-liposomes, stabilized by the above mentioned copolymers, were then tested for temperature-triggered release. The results confirmed the sensitivity of the liposomes to changes in the temperature, mainly due to the structural change that the copolymers undergo, which causes the membrane to be leaky and allow for the release of the loaded drug. Release was measured using the fluorescence emission over time technique, at temperatures lower and higher than the copolymers' LCST. Almost no release was observed at temperatures below the LCST, but as the temperature reached and exceeded the LCST, significant release was measured. Additionally the authors reported that the bio-distribution of these liposomes could be potentially controlled by the presence of the copolymers [64, 67]. In fact, above the LCST, liposomes covered with the copolymer tend to aggregate, since their surface becomes hydrophobic. If present below the LCST, however, the polymer grafts will act similar to PEG, reducing the interaction between the liposome and blood proteins, which can increase their circulation time.

Simultaneously, Nishita and co-workers [70] reported a study using TSL containing cisplatin, triggered with localized hyperthermia, used to treat murine tumors. The results showed that cisplatin was more effective when combined with TSL possessing a LCST of approximately 42°C. It was observed that the cisplatin effect was enhanced by temperature, as the concentration inside the tumor, within 30 minutes of administration, was 3.4 times higher than when normal liposomes were used. Also, heating the tumor site resulted in an increased retention of the drug which in turn enhanced its effect. This study highlighted the importance of this type of liposomes and encouraged further research in this field.

Later, Paasonen and co-workers [71] used poly(N-(2-hydroxypropyl)methacrylamide mono/dilactate) (pHPMA mono/dilactate) polymer, with a LCST of 42°C and studied the effect of its incorporation on TSLs loaded with the fluorescent model drug calcein. Liposomes coated with the polymer showed enhanced calcein release at 43°C, when compared with the non-coated ones. This

enhanced release could be possibly attributed to the precipitation of the polymer, which leads to the liposome aggregation, with subsequent destabilization of the bilayer.

A very important factor to consider when using TSLs is the choice of the proper triggering techniques capable of causing an increase in the surrounding temperature, thus causing the drug release from these nanocarriers. As mentioned earlier, there are internal and external triggering techniques that can be used to induce release from liposomes. Until now, the TSLs that have been described in this section were designed to tolerate physiological temperatures until they arrived at the tumor site and released their contents. Nonetheless, this presents a challenge because the difference in temperature between the tumor sites and the rest of the human body may not be significantly different. Thus the idea of externally triggering the release from TSLs was considered as a possible solution to this problem. This was done by designing TSLs with thermal thresholds higher than the body temperature, usually in the range of 39 - 45 °C [46].

One of the first external heating means used in research were microwaves: electromagnetic waves with a frequency range of 0.3 to 300 GHz, with relatively short wavelengths [72]. Microwaves are capable of heating by interacting with particles, especially in dielectric material, causing energy absorption and subsequent conversion to thermal energy. In fact, the thermal energy is converted from a mechanical-electrical interaction between the fast alternating electric field created by the microwave, and the rotation of the dipole of the atom. This energy conversion is referred to as dielectric heating [73]. The frequencies dedicated to achieving local heating using microwaves are 915 MHz, for industrial use, and 2.45 GHz for domestic use [74]. At these frequencies, liquids, especially water, undergo extensive dielectric heating. This concept forms the basis of the function of the microwave ovens used nowadays, and easily explains why dry food is hardly heated by microwaves, while the heating of wet food is easily achieved. The same concept can be used to trigger the release of agents from TSLs by locally heating the tumor region using externally applied microwaves [75]. Heating the human body with microwaves is easily achievable since the body mostly consists of water. The TSLs accumulate at the tumor site through the EPR effect or by active targeting and then the temperature can be raised using focused microwaves, which leads to localized release. Nonetheless, microwaves penetration is constrained by skin depth, which is defined as the distance that the microwave can penetrate in the

body until all its energy is absorbed and converted into heat. The skin depth δ is approximated by equation (2) [76, 77]:

$$\delta = \text{sqrt}\left(\frac{2*\rho}{\mu_o*\mu_r*\omega}\right) = \text{sqrt}\left(\frac{\rho}{\mu_o*\mu_r*\pi*f}\right) = \text{sqrt}\left(\frac{1}{\mu_o*\mu_r*\pi*f*\sigma}\right) \quad (1)$$

where ρ is the *resistivity of the conductor*, σ is the conductance of the conductor ($\rho=1/\sigma$), ω is the *angular frequency of the field* ($= 2\pi \times \text{frequency}$), μ_r is the *relative magnetic permeability of object*, and μ_o is the *permeability of free space* [72].

As seen in the above equation, δ is inversely proportional to the frequency of the microwave; hence, the higher the frequency, the more superficial the heating. On the other hand, δ is directly proportional to the resistivity of the subjected body, but inversely proportional to its magnetic permeability (equal to the permeability of the free space). Since the resistivity of the human body is low, the penetration is somewhat constrained. Furthermore, since the body is mostly composed of water, it will heat up quickly from the outside to the inside. Consequently, if the targeted tumor site is deep in the body, the skin will overheat when attempting to achieve the required triggering temperature. This presents a challenge when it comes to treating a deep internal tumor, yet it is very effective with surface cancers such as skin cancer. In fact, microwaves are used alongside radiotherapy to induce whole-body hyperthermia that can assist in the elimination of skin cancer or superficial tumors [75].

Another method that can be used to generate local heating is referred to as an infrared sauna [78]. Similar to microwaves, infrared signals are waves that carry energy that can be absorbed by the body and converted into heat. However, although infrared is a safer option compared to microwaves, it has limited applications. As the name sauna suggests, the waves cannot be localized, hence providing an overall heating of the body. Otherwise, infrared saunas are just normal saunas with a more sophisticated heating system than the classic charcoal or electric heaters. Recently, far-infrared saunas were developed [78]. The main advantage of this type of sauna is that it does not heat up the air in the room, but still heats up the body. This feature is appreciated by patients who cannot tolerate normal saunas especially since the treatment requires long exposure times. Similar to microwaves, this method can induce hyperthermia that can lead to a controlled release from TSL. Although these saunas are a safe option and can be used for the treatment of superficial tumors, the disadvantage of having longer sessions

compared to microwave sessions makes them one of the last resources by which temperature-controlled release can be achieved.

Other techniques that use alternating magnetic fields (AMF) or light signals can also be used to induce an elevated temperature at the tumor site; however, each technique needs a specially modified liposome that is sensitive to the specific triggering. The use of magnetic fields to produce local heating at tumor sites was first introduced in Europe in 1957 by Gilchrist and co-workers [79], who suggested the use of magnetic sensitive materials that can be activated using AMF and produce heat. The idea was then developed and applied to cancer treatment, with magnetic fields being used to heat the tumor cells and cause hyperthermia, usually in the range of 42-45 °C, thus causing their death [48, Thiesen, 2008 #621]. Magnetic nanomaterials used for hyperthermia are very diverse, and several have been described, from the well-studied iron oxide-based to metallic nanomaterials based on Mn, Fe, Co, Ni, Zn, Mg and their oxides [48]. When TSLs were introduced, magnetic fields were considered a method by which local heating could be achieved from an external source, thus achieving controlled release. The practice was to introduce targeted TSL that contain the therapeutic agents through normal means such as injections or tablets. On the other hand, the ferromagnetic elements had to be delivered with the highest accuracy possible. Unfortunately, this proved rather challenging. In fact, if such accurate delivery was possible, then why not use this delivery technique to deliver the active therapeutic agent directly? Therefore, the idea was abandoned. Additionally, although this technique outperforms the other techniques in terms of safety, it is not the preferred technique and is extremely challenging. Later, with the introduction of magnetic-sensitive liposomes, called magnetoliposomes, the use of magnetic fields as an external thermal triggering technique was further researched [44, 80-82] (discussed in Section 3.1.5).

3.1.2. Enzyme-triggered release

The main goal of a DDS that utilizes liposomes as the carrier is to break down the lipid bilayer, thus allowing the encapsulated drug to escape into the tissue or even penetrate directly into the cell cytosol. As described, the liposomes are designed to be stable and robust yet sensitive to a certain stimulus that allows for the controlled release of their contents. Hence, it is wise to look at the environment in which the liposomes

are introduced and exploit every possible factor that can be used as a trigger. Some of the most important factors that have been investigated are the enzyme concentrations and pH levels [83].

It is critical to keep in mind that the cellular environment is dynamic and may change if affected by cancer. This can be used as an advantage in case the tumor site environment shows, when compared to healthy body tissues, an elevated level of one of the factors that can be used as a target. For instance, the activity of certain enzymes may be increased solely at the tumor site, so liposomes can be designed to target the site, where drug release can be triggered using those enzymes. This enzyme-triggered release is an internal triggering technique in which the liposomes are programmed to *search* for the location with elevated enzyme activities and accumulate at that location. Liposomes sensitive to enzymes are called bio-responsive, since they are chemically modified to be affected by a biological trigger. Additionally, they are programmed to initiate release when the enzyme level is above a certain threshold. For this purpose, the enzymes of interest are those that can disturb the liposomal surface and induce release. Usually lipases are used to hydrolyze the phospholipids that compose the liposomes, but cancer-associated proteases can also be used, when the liposomes have stabilizing polymers attached via peptide bonds [84]. Phospholipases are enzymes that catalyze the hydrolysis of phospholipids. Several studies were performed to prove the possibility of designing a successful DDS that is based on liposomes as carriers and phospholipase activity as the trigger (reviewed in [85]). The works of Luk *et al.* [86] and Nieva *et al.* [87] showed that phospholipase C induces the aggregation and fusion of liposomes. However, it was observed that this enzyme activity is not high in tumors. Phospholipase A2 (PLA2), on the other hand, is upregulated in infectious and inflammatory diseases and high concentrations of this enzyme have been found in tumors [88, 89]. PLA2 enzymes catalyze the hydrolysis of aggregated lipids, but not the hydrolysis of single lipid molecules, hence they are a perfect choice for an enzyme triggered release from liposomes. Additionally, it was observed that the lysolipids and fatty acids that form during the reaction catalyzed by PLA2 act as permeability enhancers, hence increasing drug transport across the biological membranes [90-92].

PLA2 enzymes are sensitive to surface charge, hence liposomes can be made more sensitive to their action by modifying their surface with lipopolymers, creating what are called LiPlasomes [85]. LiPlasomes are liposomes designed to be susceptible

to hydrolysis by PLA2 enzymes, which are composed of uncharged DSPC, anionic DSPG (1,2-distearoyl-*sn*-glycero-3-phosphatidylglycerol), and the lipopolymer DSPE-PEG2000 (1,2-distearoyl-*sn*-glycero-3-phosphoethanolamine-N-poly(ethylene glycol)-2000) [85]. This is a good example of enzyme triggered release as the *in vitro* and *in vivo* results suggested the feasibility of using such carriers along with chemically modified prodrugs to achieve successful rates of cancer treatment [93, 94]. Unfortunately, the results obtained with cisplatin-LiPlasomes in a phase 1 clinical trial, showed no significant differences between the treatment with the free drug and the encapsulated drug [95]. However, this approach is promising and further developments of the formulation are being pursued.

Meers and co-workers [96] reported another enzyme activity that can be used as a trigger, having an enhanced fusogenicity when close to cancer cells. Elastases are proteases that catalyze the hydrolysis of elastin, a fiber present in connective tissue. They have specificity for uncharged amino acids, e.g. alanine and valine [97]. Additionally, it is known that cancer, as well as inflammations, are associated with an increase in this enzyme [98]. Hence, liposomes were designed with a targeting moiety composed of small peptides that are sensitive to the action of elastase [96]. These liposomes contain DOPE, which is not stable at the physiological temperature, neutral pH and average salt concentration. However, since DOPE is zwitterionic under these conditions, when attached to peptide chains, it becomes negatively charged, which increases its stability, making it possible to synthesize stable liposomes that can circulate in the body. When these liposomes reach the vicinity of the tumor site, the peptides are hydrolyzed by elastase, allowing DOPE to return to its zwitterionic form. Additionally, these liposomes are designed to contain trace amounts of positively charged lipids. Hence, upon enzymatic cleavage the liposome becomes positively charged. The charge reversal assists in the process of liposomal binding to cell membranes, since most cells are negatively charged. This is the first step that leads to the fusion of the liposomes and the targeted cells, and can occur before or after endocytosis [96]. A similar strategy was described by Davis and Szoka [99] who created alkaline phosphatase-sensitive liposomes, with a release mechanism similar to the one described in [96].

Another successful bio-responsive DDS is exemplified by estrogen-modified liposomes that target prostatic carcinomatous tissues, where the concentration of

phosphatase is higher than in normal tissues. The liposomes modified and treated with stilboestrol diphosphate, a phosphorylated synthetic estrogen, are targeted towards the prostatic tumor. Once there, the phosphatase can interact with stilboestrol diphosphate causing the liposomal membrane to be sheared and the contents to be released [8].

A different, but also an interesting approach, consists of using phospholipid building blocks in liposomal formulation as a prodrug. The prodrugs released after the degradation of the phospholipids are activated at the tumor site by overexpressed enzymes [93]. For example, it is possible to design prodrugs similar to lipids that can form liposomes, and use lipases to trigger their release at the target site [85].

From what has been described thus far, it is clear how important it is to exploit the cancer region in a search for the best triggering technique to be used, as well as the chemical formulation of the liposomes, which makes them sensitive to a certain trigger. The importance of the chemical formula was emphasized recently, in a review paper by de la Rica and co-workers [84]. Another factor that has been extensively studied when exploiting the tumor environment is the pH level, which is reviewed next.

3.1.3. pH-Triggered release

As discussed in the previous section, liposomes synthesized using DOPE linked to a peptide chain can be activated by the catalytic action of specific enzymes, namely elastase [96]. A version of these liposomes which contained pH-dependent cationic lipids was designed to be more sensitive to elastase. After elastase activation and the fusion of the liposomes with the cells, the low pH of the endosomes allowed the destabilization of the liposomes causing the subsequent release of the liposomal contents. This is an example of pH-triggered release from pH-sensitive liposomes (reviewed in [100-103], first described by the group of Yatvin [104]. pH-sensitive liposomes are stable at physiological pH but, under acidic conditions, they become destabilized and have fusogenic properties, which causes the release of the encapsulated molecules [102]. As for the triggering mechanism, the pH change can be either caused by a lower pH level in the environment close to the tumor, or possibly by the help of enzymes, as described in the fusogenic liposome work presented by Meers [96].

It has been observed that the pH level around tumor sites is usually more acidic, around 6.5, than in healthy tissues with an extracellular pH in the vicinity of 7.4 [83]. Hence, pH-triggered liposomes could be designed to release their contents once they

reach the tumor site. However, the most acidic sites in the tumor are often distant from its microvasculature, and hence, are reached with difficulty by liposomes. Consequently, the triggering of liposomes was redesigned to occur after endocytosis [105], inside endosomal vesicles, where the pH is usually lower than 5. This prevents the liposomes from getting into the lysosomal phase, where the biological activity of the drug can be decreased or lost by the action of hydrolases and peptidases [100, 101, 103, 106]. Furthermore, several reports indicate that in these liposomes, the encapsulated drugs are efficiently transferred from the endosomes to the cytoplasm of the target cell [107, 108]. Several mechanisms may be involved in this intracellular transfer: pH-induced fusion of the liposome and endosome membranes, with direct release into the cytosol; destabilization of endosomal membranes caused by the destabilization of the liposomal membranes, and drug leakage into the cytosol; destabilization of the liposome and release inside the endosome, followed by diffusion or translocation of the molecules to the cytosol [100].

Essentially, there are four classes of pH-sensitive liposomes, in accordance with the mechanism which utilizes pH as a trigger [100-103].

The first class makes use of polymorphic lipids such as phosphatidylethanolamine (PE) and derivatives (e.g., DOPE), in combination with amphiphilic compounds that contain one acidic group, forming stabilized liposomes at neutral pH [28]. This class of liposomes and the pH-triggering mechanism has been extensively reviewed (see, for example, Karanth, 2007 #495; Simoes, 2004 #489). Unlike most phospholipids, PE has a cone shape, due to its small headgroup, which is poorly hydrated [109], and tends to adopt a hexagonal form. At neutral pH, the stabilizing amphiphilic compound is negatively charged and it increases hydration, which stabilizes the lipid in the lamellar form, preventing aggregation and fusion. At acidic pH, however, the amphiphile is protonated, hydration decreases and the PE reverts to the hexagonal phase, thus promoting fusion [110]. However, these are the least efficient pH-sensitive liposomes as they are rapidly cleared and easily destabilized by serum proteins. This is because, to make liposomes more stable so they can circulate for longer periods, modifications, such as the inclusion of cholesterol and PEG or its derivatives (which, as discussed in the previous section, has the ability to circumvent the stability issue of these liposomes), has to be added to the PE lipids. Nonetheless,

these modifications also make those liposomes less sensitive to pH changes; hence there is a tradeoff between stability and pH-sensitivity [111, 112].

The second class of pH-sensitive liposomes, named “caged” liposomes are formed from lipid derivatives that are chemically engineered to have pH-sensitive chemical bonds that are altered when the liposomes are subjected to an acidic environment. This leads to the destabilization of the liposomal membrane, which in turn leads to an increased permeability of the encapsulated molecules as well as increased fusogenicity [100, 101]. This class of liposomes is helpful when the fusion process occurs between the liposomes and the endosomes or lysosomes, as the pH inside these vesicles is low, thus causing the lipid derivatives to change form, which in turn allows the release of the drug. This class of pH-sensitive liposomes makes use of lipids such as *N*-acylated aminophospholipid derivatives, plasmalogens, and others, as recently reviewed by Ferreira *et al.* [101]. Compared to the previously described class of liposomes, these nanoparticles displayed higher levels of pH sensitivity in the presence of serum protein [113].

The third class of pH-sensitive liposomes follows the same triggering process described for the previous class, but uses peptides that are sensitive to acidic environments, or reconstituted fusion proteins, which are added to the liposomal composition, and are capable of destabilizing the membrane at low pHs [114]. These liposomes were developed based on the fact that viruses enter the host cells by binding to receptors overexpressed on their surface, followed by direct fusion with the membrane (endocytosis). The binding step is mediated by viral glycoproteins, and these were used as a first attempt to create modified liposomes called virosomes, in 1975 [115]. Afterwards, several synthetic peptides have been designed to interact with the liposomal bilayer in a pH-dependent way (reviewed by [100]), to create pH-sensitive liposomes.

The fourth and most developed class in this field incorporates pH-titratable polymers, which are susceptible to conformational changes at low pHs, into the liposomal composition, as reviewed by Felber and co-workers [116]. These polymers include the previously mentioned temperature-sensitive poly(NIPAM), poly(alkyl acrylic acid)s, modified poly(glycidol)s, polyphosphazenes and poly(malic acid)s. When thermosensitive liposomes were developed, it was observed that the combination of poly(NIPAM) with titratable monomers in liposomal systems increased the LCST

above 37°C, as described in Section 3.1.1. Simultaneously, it was observed that the liposomes also became pH-sensitive [117, 118]. Acrylic acid, methacrylic acid, propylacrylic acid, and N-glycidylacrylamide are some of these titratable monomers. At the neutral pH of blood, the carboxylic groups are ionized and the polymer exhibits an extended conformation. Inside endosomes, however, the acidic pH leads to the protonation of the carboxylic groups, which reduces the copolymer solubility, allowing the hydrophobic interaction with the liposome bilayer, and its consequent destabilization, which makes the liposome leaky [116]. Including PEG in the formulation increases liposome stability, as mentioned previously, but PEG usually decreases the fusogenicity and pH-sensitivity of the liposomes [103]. However, Leroux and colleagues [119] described the synthesis of serum-stable pH-sensitive liposomes, by inserting a modified NIPAM/methacrylic acid copolymer ((poly(NIPAM-co-MAA)) in the lipid bilayer of PEG-stabilized liposomes. The enhanced release of fluorescent markers or Dox from PC and PC/cholesterol liposomes at 37° C in acidic conditions similar to those found *in vivo* suggested the possibility of creating pH-sensitive liposomes using those copolymers, which can withstand human body conditions and successfully deliver the drugs to the tumor cells [100, 103]. Interestingly, it has also been observed that the inclusion of PEG on the liposome surface did not affect the contents release in an acidic environment indicating that these pH-sensitive liposomes can be stable in blood circulation. Unfortunately, there are not enough *in vivo* studies using these liposomes to allow for the prediction of their possible clinical uses [116].

Recently, a new type of pH-sensitive liposomes, called fliposomes, has been described [120-124]. These contain amphiphiles such as trans-2-morpholinocyclohexanol that undergo a pH-triggered flip, which disrupts the liposomal membrane allowing the release of the encapsulated molecules. The proposed mechanism involves a protonation-induced conformational change, and was described by Liu *et al.* [121]. These liposomes are highly stable in serum and, in weakly acidic medium, exhibit quick release [120, 123, 124].

In summary, pH-sensitive liposomes are liposomes that are chemically modified, either through the addition of PE agents, pH-sensitive lipids or peptides, or the attachment of titratable polymers, so that they become responsive to a change in pH, which makes their membrane leaky and/or increases fusogenicity, allowing for

drug release. Additional information on the different classes of pH sensitive liposomes and the advantages and disadvantages of each can be found in the review by Drummond *et al.* [100].

pH-sensitive liposomes have been used in *in vitro* and *in vivo* studies. For example, the groups of Mamasheva *et al.* and Shi *et al.* [113, 125] described the use of pH-sensitive liposomes with a folate moiety to target cancer cells *in vitro*. Several other *in vitro* studies have been extensively reviewed [100, 101, 103, 116]. *In vivo* studies using this type of liposomes are rare, however [101, 116]. Carvalho-Junior *et al.* [126] compared the efficiency of cisplatin administered in free form or encapsulated in stealth pH-sensitive liposomes, for the treatment of solid Ehrlich tumors in a mice model. Cisplatin is very cytotoxic, hence it causes several unwanted side effects. The authors observed a longer circulation of cisplatin in its encapsulated form, which led to a higher concentration of the drug in tumor tissue. Additionally, the retention of cisplatin by renal tissue was lower when using the encapsulated drug, which supports a promising role for pH-sensitive liposomes in the alleviation of the nephrotoxicity caused by cisplatin [126, 127]. Another study by the same group [128] confirmed that the use of these liposomes allows them to be used with higher doses of cisplatin, which leads to a significant decrease of the tumor volume, and increase of the tumor growth inhibition, without increasing the side effects, (when compared to non-pH sensitive liposomes and free cisplatin).

Paliwal *et al.* [129] synthesized pH-sensitive liposomes with an estrogen moiety for targeted delivery of Dox to estrogen-sensitive cancer cells (e.g., MCF-7). Their *in vivo* studies using female Balb/c mice showed an increased efficiency of these liposomes in the inhibition of tumor growth, when compared to non-pH sensitive liposomes and free Dox. Additionally, the use of these liposomes significantly reduced the cardiotoxicity of Dox, a well-known side effect of this drug.

The group of Ishida [130, 131] studied several different Dox-encapsulating pH-sensitive liposome formulations against human B cell lymphoma using mice xenografted with Namalwa cells. The non-targeted formulations showed no increased efficacy when compared to free Dox, but mice treated with targeted anti-CD19 (a B-lymphocyte antigen) formulations had an increased lifespan. The lifespan was slightly higher (1.5-fold) for mice treated with the targeted pH-sensitive liposomes when compared those treated with to the targeted regular liposomes. This modest result is in

contrast with *in vitro* assays obtained by the same group, and was considered to be due to the fast clearance of the liposomes in the blood.

3.1.4. Light-triggered release

Light usually refers to the part of the electromagnetic radiation spectrum that can be detected by the human eye. It comprises waves with wavelengths of 400 nm (violet light) to 700 nm (red light). Immediately adjacent to the visible light spectrum is ultraviolet (UV) light (100-400 nm) and near infrared (IR) light (650-1000 nm), which are usually also considered forms of light. Since light is a wave, it contains energy that can be converted to other forms of energy. Light presents several advantages that renders it as one important trigger for drug release: pulse duration, intensity, cycle and wavelength can be controlled, the beam can be focused at the targeted location, and a variety of tissues can be irradiated easily and without the need for surgical procedures [132]. Nonetheless, just like with any other type of trigger, the nanocarriers to be used must be modified to become sensitive to the triggering means. The principle(s) of phototriggering include light-induced isomerization or polymerization of photoreactive lipids and photosensitization by membrane anchored hydrophobic probes [133, 134]. In the early 1990s, scientists took an interest in developing liposomes that were sensitive to light and there was a breakthrough when they succeeded in creating what is currently known as photosensitive liposomes. Anderson and co-workers [135] were able to chemically modify the liposomal structure to include light sensitive lipids that change form when subjected to light. They were able to achieve a photoactivated drug release, by creating a liposomal formulation with the right concentrations of plasmalogen (1-alk-1'-enyl-2-acyl-sn-glycero-3-phosphocholine) lipids and zinc phthalocyanine (ZnPc), a photosensitizer. The mechanism involved the sensitized photooxidation of the vinyl ether linkage of the plasmalogen, followed by its cleavage, which changed the membrane permeability.

However, there are several biological constraints associated with photoactivated release such as biocompatibility, plasma instability, and near infrared sensitivity [136]. In 1996, a paper on triggerable plasmalogen liposomes was published to introduce a newly developed light-sensitive type of liposome that was able to avoid the side effects associated with the earlier photoactive drug release processes [136]. The authors synthesized plasmenylcholine liposomes that were sensitive to light with wavelength

in the spectrum band of 630 to 820 nm. This range was chosen due to the availability of sensitizers absorbing in this range, the fact that light in this range has a penetration depth of more than 0.8 cm for any tissue, the stability of the liposomes that can be preserved until they reach the targeted location, and the light sources in this band that were available. As in the previous work [135], a light sensitizer was added to the liposome formulation, to make it photosensitive. In this work, the authors used three type of sensitizers: the previously used ZnPc, tin octabutoxyphthalocyanine dichloride ($\text{SnCl}_2\text{Pc}(\text{OBU})_8$), and bacteriochlorophyll *a* (BChl_a). The effect of these compounds on the release kinetics was monitored, and the authors concluded that the increased release upon irradiation is due to the photooxidative cleavage of the plasmenylcholine vinyl ether bond which is close to the hydrophilic interfacial region. This event is responsible for liposome aggregation and membrane fusion, leading to the release of their payload of drug.

In 1999, Bisby and co-workers [137] reported the synthesis of a new type of light-triggered liposomes. In this work, the authors used a sensitizer called *Bis-Azo PC*, which is a synthetic phospholipid with acyl chains containing azobenzene moieties. When these lipid molecules were subjected to pulsed UV light, their form changed from the stable E-isomer, sterically compatible with a packed stable lipid bilayer, to the more bulky Z-isomer, which created pores in the membrane, allowing the leakage of the encapsulated drug. Later, the authors also reported that the addition of cholesterol to the composition increased the sensitivity of the liposomes, making it possible to use visible light for their photosensitization [138]. These results suggested the possibility of controlling the release rate through the wavelength-dependent release from cholesterol and non-cholesterol liposomes, by sequential exposure to visible and UV light. In a photo-triggered release, the composition of the liposomes is critical to their efficiency of response to the photo triggering process. This importance was highlighted in the work of Yavlovich *et al.* [139], which described the synthesis of photosensitive liposomes with a photopolymerizable diacetylene phospholipid ($\text{DC}_{8,9}\text{PC}$) (1,2- bis (tricoso-10,12-diyonyl)-*sn*-glycero-3-phosphocholine). Upon exposure to UV light (254 nm) release of calcein could be observed from DPPC/ $\text{DC}_{8,9}\text{PC}$ liposomes, but not from egg PC/ $\text{DC}_{8,9}\text{PC}$. The release was due to the UV-induced photopolymerization of the $\text{DC}_{8,9}\text{PC}$. Later, the same authors [134] were the first to report the *in vitro* killing of cancer cell cultures, following light-triggered release of Dox from these

photosensitive liposomes. The liposomes contained different concentrations of DPPC, DSPE-PEG2000, egg PC, and DC_{8,9}PC, and were subjected to UV (254 nm) or visible light (laser, 514 nm). It was successfully documented how differently composed liposomes have different release rates. This discovery ignited an interest in designing liposomes that can be completely controlled in terms of release rate, stability, targetivity, selectivity, and circulation time.

Aygun *et al.* [140] presented a very interesting work where scanning electron microscopy was used to study the photo-induced release from 1,2-dimyristoyl-*sn*-glycero-3-phosphocholine (DMPC) or DSPC liposomes stabilized by cholesterol and containing the photosensitizer ZnPC. The authors studied the effect of changing the liposome composition on the encapsulation capacity, morphology and photo-induced release properties of these liposomes. It was observed that the DMPC liposomes were more sensitive to light than the DSPC ones, which showed slower release rates. Both liposomes were more sensitive to visible light in the 400-700 nm range than to 365-nm UV light. The study also determined the optimal ratio of lipids to cholesterol to ZnPC (7:2:1) for liposome stability.

In the above described studies, the trigger directly causes a change in the carrier. However it is possible to use a trigger to cause a change in the environment that leads to a change in the carrier, upon which the release is observed. For example, when the trigger is light, its energy can be changed into other forms, e.g. heat. Since thermosensitive liposomes are affected by hyperthermia, researchers investigated the use of materials that can be heated when subjected to light, such as gold. In the work of Paasonen *et al.* [141], gold nanoparticles were loaded into TSL liposomes or attached to their surfaces, and then irradiated with UV light. It was observed that the UV light specifically triggered the release from these liposomes, while traditional liposomes were unaffected. The hypothesis that gold particles have the ability to absorb light energy and change it into heat, which is transferred to the liposomal lipids causing a phase transition, was further studied by Mady and co-workers [142] who later performed the biophysical characterization of these liposomes. If the temperature can be raised high enough to cause the lipid bilayer to undergo a phase transition from a gel phase to a rippled phase and then to a fluid phase, then release is achieved. By controlling the amount of gold particles present and the illumination intensity of the UV light, a controlled release can be achieved. The group of Paasonen also studied the

effect of these liposomes in cell cultures [143]. Gold nanoparticle-loaded liposomes encapsulating calcein were UV-triggered after cell internalization and the results showed that the cell viability was not decreased, which suggests that this system can be applied *in vivo*.

Most of the studies described so far use UV or near-UV light, which poses a problem when extrapolating them to potential clinical uses. UV radiation is phototoxic and may affect the stability of biological systems, for example by generating reactive oxygen species. In this sense, the use of infra-red (IR) or near-IR to trigger release from photosensitive liposomes, would provide a safer method. Additionally, IR or near-IR light has a deeper penetration into tissues [144]. Recently, Carter and co-workers [145] described liposomes containing porphyrin-phospholipid as a photosensitizer, characterized them, and studied their effect *in vitro*, in cell cultures, and *in vivo*, in mice xenografts. Permeabilization was achieved by irradiation with near-IR 658 nm laser light, and it was found to be dependent on the percentage of photosensitizer, irradiation intensity and exposure. The results obtained *in vitro* and *in vivo* when using these liposomes loaded with Dox were very promising, which makes this DDS a candidate for anticancer therapy. In summary, light can be used as a stimulus to directly or indirectly trigger release from photosensitive liposomes. However, the modification of the liposomes is the major accomplishment in this field. For more detailed information on the different mechanisms by which photosensitive liposomes can be triggered and how the liposomal composition affects the release [146], the reader is encouraged to read more about photopolymerization [133, 146, 147], photosensitization [134, 137, 138, 148], photo-isomerization [133, 146, 149], photo-oxidation [133, 136, 146, 147], or the degradation of photo cleavable lipids [133, 150].

3.1.5. Magnetoliposomes

The use of magnetic fields as a triggering technique, by which a controlled release can be induced, was already mentioned in previous sections. Magnetic materials were first used for hyperthermia, as initially proposed by Gilchrist *et al.* [79]. They proved to be the ideal hyperthermia-inducing systems since they are non-invasive, tissue-specific and capable of precise, localized, high-intensity heating of deep tissues (reviewed in [55]).

Drug delivery driven by magnetic fields was first proposed by Freeman and co-workers [151]. As discussed in Section 3.1.1, the first attempts on the use of magnetic fields as a release trigger was as a heating mechanism that could be combined with TSLs into one DDS. A local high frequency AMF can be used at very high intensities to induce hyperthermia at the tumor site, thus causing drug release from the TSLs. However, at such intensities of magnetic fields, it is hard to control the amount of energy that is absorbed and converted into heat in the body; hence excessive exposure could lead to second or third order burns [152]. Furthermore, hyperthermia-induced by AC magnetic fields has several limitations, as reviewed in [153]. To avoid the harmful side effects, a group of scientist worked on the development of magnetoliposomes (MLs), which combines liposomes as drug carriers and magnetic fields as a trigger. In this case, the magnetic fields are not used to induce hyperthermia that leads to drug release from TSLs, but they rather directly interact with the chemically-modified liposomes specifically made to be sensitive to a certain parameter of the magnetic field.

Magnetoliposomes have been defined as liposomes that contain super paramagnetic nanoparticles in their composition. A super paramagnetic nanoparticle is one that interacts with magnetic fields and can absorb most of the field's energy, quickly converting it to heat [154, 155]. Consequently, when such particles are added to liposomes and are placed in the radiation field of an AMF, their temperature increases, leading to a localized hyperthermia that affects the liposomes only. This DDS has several advantages due to its biocompatibility, chemical functionality and the fact that it can combine hyperthermia with drug delivery in the treatment of tumors [81]. The success of the MLs opened the field for researching magnetic nanomaterials that can be used along with magnetic field to cause hyperthermia, as reviewed in detail by Kumar *et al.* [48]. It is worth mentioning that the most widely used magnetic nanomaterial in MLs is the superparamagnetic iron oxide (Fe_3O_4), which produces the best release results when combined with AMF [156], [157]

In a recent review, Soenen and co-workers [158] clarified the ambiguity that is sometimes found in the literature concerning types of MLs. MLs may be considered as an individual magnetic nanoparticle (usually iron oxide with a diameter of about 15 nm) surrounded by a phospholipid bilayer and, in this case, they cannot encapsulate any substance since their core is the magnetic nanoparticle itself. The same name is used to designate large unilamellar vesicles encapsulating several magnetic nanoparticles in

their aqueous cores, which can also be used to encapsulate drugs. The last category is what will be reviewed here.

In the work of Babincova *et al.* [80], large unilamellar Dox MLs encapsulating stabilized colloidal gamma-ferric oxide, were tested for the possibility of inducing a controlled release by using an AMF as the trigger. The results showed that, by subjecting the MLs to this field with a frequency of 3.5 MHz and an induction of 1.5 mT for a few minutes, the temperature of the solution was raised to around 42°C, which was the transition temperature of the lipids used to synthesize the MLs. At this temperature, a noticeable drug release was observed which indicated the success of the experiment.

Tai and co-workers [82] used TSLs with carboxyfluorescein co-encapsulated with iron oxide nanoparticles and monitored the drug release in solution, in an *in vitro* gel phantom, and *in vivo*, in rat skeletal muscle. The application of an AMF triggered the drug release from the TSLs, and the *in vivo* experiments confirmed that the method is minimally toxic and relatively safe. The work of Pradhan *et al.* [81] demonstrated a very interesting synergism between biological and magnetic targeting, by synthesizing folate receptor-targeted thermosensitive MLs for use in hyperthermia chemotherapy. The liposome formulation was DPPC to cholesterol to DSPE-PEG2000 to folate (80:20:4.5:0.5 molar ratio) and a commercial aqueous solution of iron oxide magnetic nanoparticles was co-encapsulated with Dox. Using a permanent magnetic field, these MLs were targeted to KB and HeLa tumor cell lines, and led to increased cytotoxicity when compared to Dox encapsulated in the regular stealth liposomes, folate-targeted regular liposomes and free Dox. The cytotoxicity was enhanced due to magnetically-induced hyperthermia (42.5 °C and 43.5 °C).

Amstad and co-workers [44] designed stealth MLs containing the super paramagnetic nanoparticle iron oxide incorporated in the membranes. These particles (5 nm diameter) were individually stabilized with palmityl-nitro DOPA and mixed with DSPC and PEG to produce stable MLs with a T_m of around 54.6 °C. Release was observed when a sample of these liposomes, encapsulating calcein, was subjected to a 230-kHz AMF for 25 min period divided into 5 sessions. It was hypothesized that, when the iron oxide nanoparticles were subjected to the AMF, they absorbed the energy and converted it into heat that was dissipated directly into the lipid bilayer of the liposome causing the local temperature to increase to $T_m \geq 54.6$ °C. It was also observed that the

liposomal structure was maintained during exposure to the AMF, suggesting that the calcein was released due to transient changes in the membrane permeability and not due to rupture or fusion of the liposomes. This allowed control of the space and time of the released dose, making this a possible DDS to be used *in vivo*.

So, we can conclude that, in the future, AMF might have the potential to be a good triggering means by which drug release can be controlled either through direct interaction with the liposomes or, as is the case with light, by using it to induce hyperthermia at the location where TSLs are present. Furthermore, with more and more research in the area of magnetism, new magnetoliposomes can be developed that can be easily triggered and targeted. There are many properties of the ferromagnetic material that can be made use of especially in tracking and targeting. For example, a magnetic can be placed close to the location of the tumor once the liposomes are administered. This magnet can be kept there for some time in order to facilitate passive diffusion of the magneto liposomes to the tumor site. It can also enhance drug uptake by cancer as it will accumulate the liposomes close to the surface of the cells allowing for a more efficient key and lock binding between the ligands and the receptors. Moreover, fluorescent material can be attached to the paramagnetic materials making up the liposomes or those found in the loaded drug. This can help in tracking the location of the liposomes in the body as well as serve as a measure for the drug release. The technology is still young and much can be done in this field especially with the new substances being developed currently in labs.

Thus far, the major triggering means used to induce drug release from liposomes, except for US, were discussed, focusing on defining the terms and describing the mechanism by which each trigger can be used. Numerous studies have been done for each triggering mechanism, and many types of liposomal compositions were developed in order to create successful DDSs, since the liposomes have to be modified to be responsive to a specific trigger. This modification can be done through the addition of certain polymers, inclusion of superparamagnetic nanoparticles, introduction of certain lipids or peptides, addition of amphiphilic molecules into the composition, or chemical modification of certain chemical bonds to make them sensitive to a trigger. As for the trigger, the objective is always to cause disruption to the liposomal membrane allowing the release of the encapsulated drugs. By combining

the proper trigger with the proper carrier, side effects associated with chemotherapeutic agents can be avoided and their effectiveness in cancer treatment can be enhanced.

It is important to notice that, throughout the literature, several formulations and protocols have been described, to create liposomes that are sensitive to a certain trigger. It is also evident that liposomes with different chemical compositions can still be sensitive to the same trigger, yet differences between them remain based on their release efficiency. For example, there are many types of copolymers that can be added to liposomes to make them sensitive to the pH level; the way they release is the same but the amount of the drug they can encapsulate and then release when triggered, may differ. The aim of this part of the thesis was not to include all types of liposomal carriers but rather focus on the process of interaction between them and the specific triggering means. In the next section, a complete review on US as a trigger is provided, with a discussion on US physics that will help elucidate the ways by which it can be used to control drug release from liposomes [8].

CHAPTER 4: Ultrasound

In recent years, US has been researched as being a potential triggering technique that can be used in DDS due to its safety and low cost. Nowadays US has many applications in the medical field, but perhaps the best known is its use as an imaging technique (including the imaging of embryos). This indicates how safe and recommended US is as a means of diagnostics and therapy [159-164]. In this section, a detailed investigation of US physics is addressed that serves as the foundation for understanding the mechanism by which it is used to trigger drug release in drug delivery applications.

4.1. Physics of ultrasound

Ultrasound consists of sound waves (pressure waves) with a frequency higher than 20 kHz. As a comparison, sound waves within the human hearing range have frequencies between 40 Hz to 20 kHz [165-169]. The sound wave is a physical wave that needs a medium to travel through, unlike light or electromagnetic waves. Sound waves propagate by means of energy transfer between molecules of the medium, which occur as the pressure changes from compression (high pressure) to rarefaction (low pressure). Ultrasound waves possess the properties of any wave, i.e., attenuation, reflection, refraction, amplification, absorption and scattering. Yet, US waves, also called acoustic waves, have the ability of propagating on the surface of matter without traveling through it [168-171].

Ultrasound waves consist of cycles of successive varying pressure values, similar to those shown in Figure 6. There are two main types of pressure wave propagation, namely transverse and longitudinal, as described in Figure 6. The upper image shows a longitudinal wave and the lower one a transverse wave. In longitudinal propagation, particles tend to move back and forth along with the direction of the wave. Therefore, if the wave is traveling from left to right on the x-axis, the particles themselves will be propagating parallel to the x-axis. On the other hand, in the case of the propagation of a transverse wave, also known as shear wave, the particles are stationary in the translational sense; however, they oscillate perpendicular to the propagation direction producing a wave behavior similar to that exhibited by sinusoidal waves [166, 170, 172].

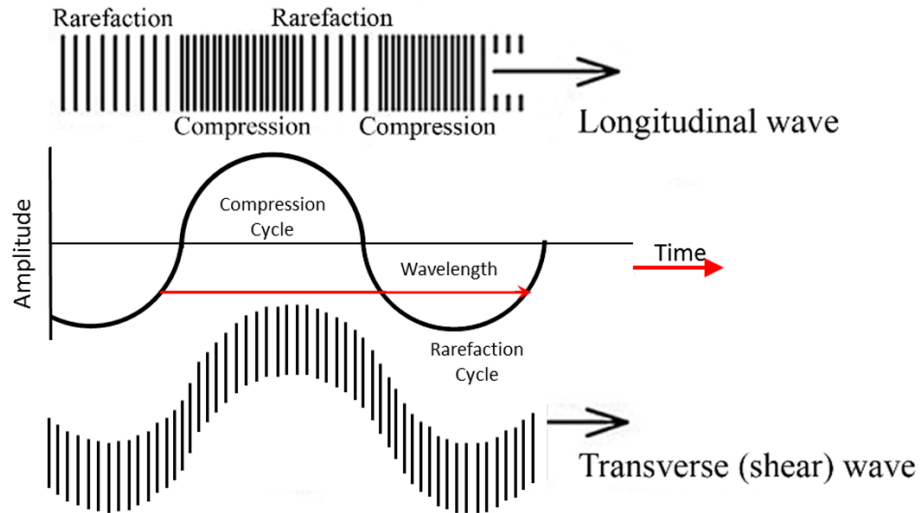


Figure 6. Nature of acoustic wave propagation: shear and longitudinal.

Usually the medium through which the propagation occurs is referred to as the fluid medium. Any fluid medium consists of a collection of particles that are always randomly floating and moving around the space. This motion is more restricted in the case of solids, it is moderate in liquids, and it is the least restricted in gases. The motion restriction is due to the density of the material: as the density increases, the number of molecules filling up a specific volume increases but the available space for each molecule to move decreases. Consequently, the molecules, in more dense materials, are closer to each other and can easily collide. Figure 7 shows the molecules as spheres distributed in the space. When no pressure is applied, there will be no pattern in the motion of the molecules, only random motion of the particles [173].

Once pressure is applied, the molecules are compressed together forming a band-like shape corresponding to the intensity of the pressure wave. The band of molecules will then be accelerated in the direction of the wave propagation, but as molecules come in contact with the next line of molecules, energy transfer occurs. Eventually, the initial band of molecules that were in direct contact with the pressure wave will lose the gained energy and will start to divert from each other. This state is referred to as the *rarefaction state* [174-176]. When a series of compression and rarefaction states are induced periodically into the fluid medium, a pressure wave can propagate smoothly as long as the fluid is clear of any obstacles. The region of compression corresponds to a region of high pressure, while the region of rarefaction corresponds to low pressure. It must be noted that only the wave propagates; particles just oscillate in place to allow this

propagation. The particles in the compressed regions are moving forwards, and those in rarefaction are moving backwards.

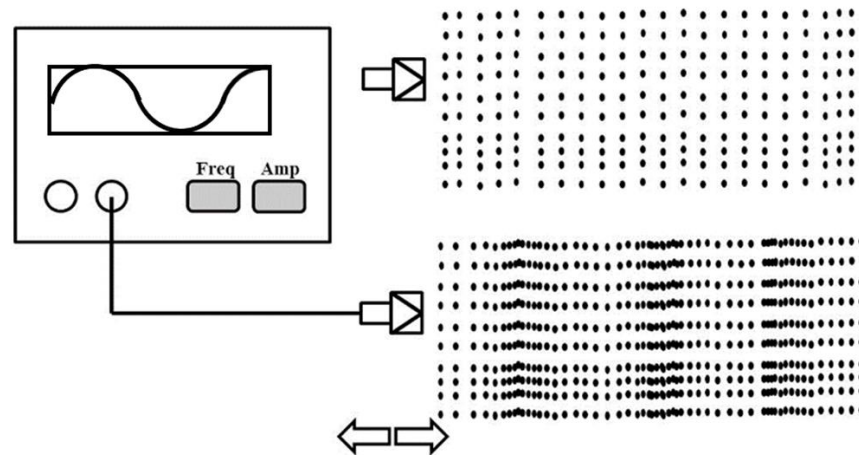


Figure 7. Image showing a successive cycles of high and low pressure areas formed due to the motion of a piston in a medium of particles.

Since solids have molecules that are tightly compacted, sound waves travel faster in solid media than in liquids and gases. In fact, air and vacuum are some of the worst sound conductors and the speed of sound in these media is considerably low compared to other media, for high frequency sound waves. In air, the molecules are distant from each other; hence, the particles of the medium take a long time to come close to each other, and the energy transfer rate is slower. Due to this slow motion of particles, the acoustic energy band that forms a compression region hardly forms, which in turn presents difficulties in the face of the acoustic wave propagation. For low frequencies, the scenario is different. As an example, the human voice propagates through the air, and can be clearly heard when people are talking. Hence, low frequency sound waves can travel through the air but they fade quickly due to losses caused by the nature of the medium [177, 178].

Acoustic waves are a form of pressure wave that propagate as described above. When the successive pressure variation is compared to a normal sinusoidal wave, the high pressure is equivalent to the upper peaks of the sinusoid, and the low pressure is equivalent to the lower peaks. Hence, speed, wavelength, frequency and amplitude of the pressure wave are parameters that can be used to characterize acoustic waves. Figure 8 shows an acoustic wave represented as a sinusoid with a wavelength (λ), a frequency

(1/T) and a speed which is the product of frequency and wavelength. In most soft tissues, the velocity of US is about 1540 m/sec [166, 167, 174, 179, 180].

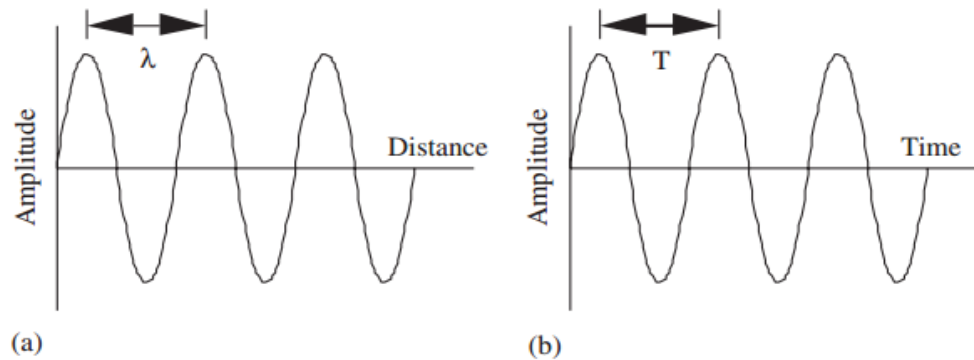


Figure 8. Representation of a sinusoidal wave. The wave is characterized by a certain wavelength λ and a frequency $1/T$

4.2. Ultrasound applications

Ultrasound waves are easily generated using a system that consists of an actuator that produces an alternating current at adjustable frequencies based on the application, and a wire that carries this AC current to a probe used as the terminal (from which the pressure waves are emitted [181]). Knowing the physics of US has helped widen the spectrum of applications. Frequency is one of the main controllable parameters that determines which application US can be used for [181, 182]. Table 1 shows the ranges of ultrasonic frequencies and their corresponding applications.

Frequencies of 1 MHz and greater are required to obtain ultrasound suitable for diagnostic imaging [183-185]. This is because, in human body imaging, ultrasound waves have to penetrate to a certain depth and reflect back while still having some of their initial power. So by adjusting the frequency, the proper depth can be reached based on the rule, the higher the frequency the lower the penetration depth described earlier in equation (2). Also, at higher frequencies, the wave's wavelength becomes shorter which allows for more precise and detailed images. But there is always a tradeoff between depth and details as there is a direct relation between the frequency and the wavelength as depicted in equation (3). Since the speed of ultrasound in human tissue is assumed to be constant, changing either of the two will lead to an opposite change in the other [183-187].

$$v = f * \lambda \tag{3}$$

Table 1. Ultrasound: range of frequencies and respective applications [188].

Frequency	Applications	Device	Description
30-150 kHz	Dentistry	Micro Probes	Debris removal
0.1-1 MHz	Kidney stone shattering	Lithotripter	Shattering of kidney stones through the absorption of ultrasound
0.5-1.5 MHz	Tissue ablation	High Intensity Focused Ultrasound (HIFU)	Heating of tissues to the point where cells start to die; intensities are high enough to cause the temperature to rise above 42°C
0.7-3 MHz	Physiotherapy	Normal Probes	Heating certain locations of the body to help clearing internal organs from unwanted cells, such as surface cancer cells; intensity used is moderate enough to heat up the surface of the skin and few mm in depth.
1-20 MHz	Organ imaging	Ultrasonic imaging	Lower frequencies in this region are used to capture images of deep organs such as liver and kidneys. Higher frequencies are used for imaging superficial areas such as muscles and brain. Intensities used are low just enough for a clear wave to be reflected back to the source.

By examining Table 1 carefully, it can be seen that applications have overlapping ultrasonic frequency ranges. Tissue ablation and organ imaging have an overlap in the range of 1-1.5 MHz. Yet, for imaging, the intensity of the US is very low, barely enough to allow the US to propagate through and reflect back with enough intensity that can be used to form the image. On the other hand, for tissue ablation, higher intensities are used leading to hyperthermia at the targeted area. Lower intensities cannot achieve the required increase in temperature. Thus, although the frequency ranges overlap, the application is determined by the intensity [173, 179, 182, 189-195].

Another controllable parameter is the mode of operation [191, 193, 196]. There are two main modes of operation: continuous mode or pulsed mode [197]. In continuous mode, the US wave is generated and applied continuously for a certain period of time. In the pulsed mode, the wave is generated in a cycle of *on* and *off* periods. The mode also plays a role in determining the application even if there is an overlap in the frequencies. For example, although there is an overlap in the frequency

ranges between kidney stone shattering and tissue ablation and both of them use US within the same intensity range, kidney stone shattering uses a pulsed mode to cause the breakdown of the stones while tissue ablation requires the application of US continuously for long periods, allowing for the tissue to overheat. Hence, these three controllable parameters are the key to understanding the ways by which US can be used in drug delivery and triggering release [197-201].

4.3. Ultrasound behavior in matter

Furthermore, using the wave properties of sound, the acoustic properties of a material, such as its acoustic impedance, can be determined. The *acoustic impedance* (Z), measured in rayls, of a material describes how a sound wave is affected by this material as it propagates through it, and determines the wave speed, attenuation, and reflections; factors that help when choosing the appropriate intensity and frequency of ultrasound waves that will be used to do a certain task [166, 202-206]. Thus, acoustic impedance is considered the most important parameter when analyzing an acoustic medium since it is a function of frequency, pressure and speed, as shown below:

$$Z = P/v = c * \rho_0 \quad (4)$$

where P is the *pressure* in Pascal, v is the *particle velocity*, c is the *speed of propagation*, and ρ_0 is the *density of the material*. It is wise to note here that there is a relation between the pressure P and the intensity of ultrasound that will be discussed shortly [184, 188].

Particle velocity refers to the oscillation speed of the particles as the wave passes through. If the propagation is assumed to be linear, the following relationships can be derived directly,

$$v = \frac{|P|}{|Z|} \quad (5)$$

$$\varepsilon = \frac{|P|}{\omega * |Z|} \quad (6)$$

$$\alpha = \omega * \frac{|P|}{|Z|} \quad (7)$$

where ε is the *amplitude displacement*, α is the *acceleration*, $\omega = 2\pi f$ is the *angular frequency*.

The amplitude displacement refers to the maximum distance that the particle subjected to the acoustic wave will travel from its initial position. This value is directly proportional to the pressure (intensity) of the wave and inversely proportional to its frequency. This is because the higher the pressure, the stronger the push that the particle exhibits. On the other hand, as the frequency increases, the impact time decreases which allows less time for the particle to travel away from its positions. On the other hand, acceleration refers to how quickly the speed of the particle increase as the wave passes. Initially, a particle in a medium is assumed to be stationary but when an acoustic wave passes through, it causes the particle to move at an increasing speed. The acceleration is proportional to both the intensity and the frequency for obvious reasons [166, 183, 186, 202, 207].

As mentioned previously, the acoustic impedance of a material is related to its acoustic behavior. For example, assume a piece of aluminum is subjected to a sound wave of 100 Pa pressure at 10 kHz frequency. The density of aluminum is known to be $2700 \text{ kg} * \text{m}^{-3}$ and the speed of sound in aluminum is 6400 m/s . Then using equations 3, 5 and 6,

$$Z = 2700 * 6400 = 1.73 * 10^7 \text{ rayls} \quad (8)$$

$$\varepsilon = \frac{100}{2 * \pi * 10^4 * 1.73 * 10^7} = 9.2 * 10^{-11} \text{ m} \quad (9)$$

$$\alpha = 2 * \pi * 10^4 * \frac{100}{1.73 * 10^7} = 0.37 \frac{\text{m}}{\text{s}^2} \quad (10)$$

What the above values suggest is that aluminum has an acoustic impedance of 17.3 Mrayls. Therefore, at a frequency of 10 kHz and pressure of 100 Pa, particles will be displaced a maximum distance of 0.92 pm and will be accelerated at an average of 0.37 m/s^2 . Those values are critical in characterizing the behavior of acoustic waves at the molecular level which reflects on the general parameters such as acoustic impedance, attenuation coefficient and others that are discussed shortly.

Another important aspect that must be analyzed and that helps in understanding the advantages and disadvantages of US in DDS is the reflection phenomenon, which occurs when a sound wave is translating at the boundary between two substances; each

of them has a parameter called the acoustic impedance, which is specific for it. Frequently, there is usually a mismatch between the impedances of any two contacting materials, which occurs at the boundary, and causes some of the wave to pass through, while the rest is reflected. The amount of reflection is determined by the *reflection coefficient*, which is, by definition, lower than one. This value indicates the percentage of the wave that will be reflected in terms of intensity. Let the impedance of the first material be Z_1 and that of the second be Z_2 . In the case of normal incidence, the *amplitude reflection coefficient*, R , can be derived as follows [170, 171, 173, 180]:

$$R = \frac{Z_2 - Z_1}{Z_2 + Z_1} \quad (11)$$

Using the amplitude reflection coefficient, the amount of energy, depicted in the intensity parameter, that will get through from one medium to the other can be approximated as a percentage by finding the *normal incidence intensity transmission coefficient* calculated as follows:

$$It = |1 - |R|^2| * 100\% \quad (12)$$

Besides the reflections that happen due to the mismatch in the impedance, impedance itself causes losses in the intensity of the passing wave. This loss is referred to as *attenuation due to absorption or energy change*, and it is another factor that governs the possibility of using US as a triggering means. When a wave passes through a medium, some of the transmitted energy changes into other forms, e.g. heat energy in the case of tissue ablation. This change will in turn lead to a loss in energy; hence, the amplitude of the pressure wave will decrease as the distance traveled through the medium increases. This can be modeled using equation (6). As can be observed, the attenuation is exponential and it differs from one medium to the other; hence, the *attenuation factor* β is specific to each medium [173],

$$I_2 = I_1 * \exp(-2\beta\Delta x) \quad (13)$$

where, I_2 is the intensity at x_2 , and I_1 is the intensity at x_1 , given that $\Delta x = x_2 - x_1$ where x is the position of the wave. To compare between two intensities in decibels, the

logarithmic scale is used. This is a measure of attenuation as the wave covers more distance in the medium. Thus when comparing the intensities and dividing by the distance, the *absorption coefficient* can be calculated as follows:

$$\gamma = \frac{10}{\Delta x} * \log_{10} \left(\frac{I_2}{I_1} \right) \quad (14)$$

The absorption is linearly proportional to the frequency, so at higher frequencies, absorption is higher; hence, the distance that the wave travels decreases. This distance is called the *depth of the signal in a medium*, and it is another factor that decides which frequency is to be used for which application. Since intensity is power per unit area, the absorption coefficient can be written in terms of power as well. Furthermore, energy is power multiplied by time so energy can be used also [184, 187]. Thus, the following relations can be derived:

$$I = \frac{Pm^2}{2\rho c} \quad (15)$$

$$\therefore \gamma = \frac{20}{\Delta x} * \log_{10} \left(\frac{Pm_2}{Pm_1} \right) \quad (16)$$

Furthermore, the absorption coefficient varies from one medium to the other, being lower in solids and higher in gases. The absorption coefficient and the depth of the signal are the two main factors that limit the applications of US in air. As mentioned earlier, air is one of the worst media for acoustic wave propagation in the case of high frequencies. If air is present in the medium of ultrasonic application, the system usually fails. Also, since air has very high acoustic impedance, there will always be a vast mismatch between it and any other medium, which causes the reflection of most of the wave. Table 2 presents a comparison between the attenuation due to absorption in water, sea water and air. The comparison also shows the effect on the attenuation level as the frequency increases.

Table 2. Acoustic absorption in fresh water, seawater, and air (at sea surface normal conditions) at 10 kHz and 1 MHz. From [173].

	Water	Air
<i>10 kHz</i>		
α_{ab} (dB m ⁻¹)	2x10 ⁻⁵	1x10 ⁻¹
e-folding distance for energy	250 km	50 m
<i>1 MHz</i>		
α_{ab} (dB m ⁻¹)	2x10 ⁻¹	1x10 ³
e-folding distance for energy	25 m	5 mm

α_{ab} is the attenuation coefficient in dB/m, e-folding distance is the distance needed for the wave to get attenuated by a factor of $e \sim 2.718$

As the frequency increases, the penetration depth decreases because the energy from the acoustic wave is more easily absorbed at higher frequencies. Also, depending on the type of medium, the amount of absorption can be determined. Table 3 shows the relation between the attenuation coefficient and frequency.

Table 3. Average attenuation coefficients in tissue (from [208]).

Frequency (MHz)	Average attenuation coefficient for soft tissue (dB/cm)	Intensity reduction in 1 cm path (%)	Intensity reduction in 10 cm path (%)
2.0	1.0	21	90
3.5	1.8	34	98
5.0	2.5	44	99.7
7.5	3.8	58	99.98
10.0	5.0	68	99.999

The attenuation coefficient and the acoustic impedance are important when dealing with the human body and analyzing how it interacts with US. The human body consists of stacked layers of tissues - skin, fat, muscle and bones, each one with its own acoustic impedance (Table 4). Hence, an acoustic wave passing through these layers will exhibit attenuations and reflections as it propagates, as discussed earlier. This is critical because the attenuation, which is usually due to absorption, will cause the tissues to heat up, as the absorbed energy is converted into thermal energy. This is the basis of several of the current applications of US. The accurate knowledge of the proper values is critical to avoid overheating and damaging the skin. Also, due to the mismatches, which are small, some of the wave is reflected. These reflections work as the basis for the imaging of human organs. The knowledge of the mismatches helps in calculating the proper frequency and intensity for the imaging process. It is worth noting that there is a small mismatch in the acoustic impedance of the skin, muscle and

fat, but the mismatch in bones is enormous. This is because bones are considered solids, while the other tissues are considered liquid as they contain a high percentage of water.

Table 4. Attenuation of human tissue at 1 MHz. Adapted from [208, 209].

Human tissue	Attenuation (dB/cm)
Blood	0.18
Fat	0.6
Kidney	1.0
Muscle (across fibers)	3.3
Muscle (along fibers)	1.2
Brain	0.85
Liver	0.9
Lung	40.0
Skull	20.0
Lens	2.0
Aqueous humor	0.022
Vitreous humor	0.13

Furthermore, due to the layered nature of the human body, it can be modeled as layers of different material each with its specific acoustic impedance, Figure 9. When the acoustic wave is propagating between the layers, as it reaches the boundaries, some of it will reflect back and the rest will pass to the next layer. Then this part that was able to go through will face another boundary and some of it will pass and the rest will be reflected within layer 2. However, if this reflected part survives until it travels back to the boundary between the second and the first layer, some of it will get reflected again and so on. Furthermore, as the wave passes through, there will be attenuation in every layer. Adding all the attenuations together, probably less than 99% of the wave would survive to reach the bones. Knowing those facts, it is clear that the higher the frequency, the lesser the depth that the acoustic wave can travel in the human body as the attenuation is tied to frequency and attenuation is higher in more dense material such as muscles. Consequently, to be able to reach further locations in the human body, higher pressure amplitudes (intensities) should be used. Nonetheless, increasing intensity come with the cost of the possibility of damaging the human body either because of overheating (hyperthermia) or due to cavitation (discussed shortly).

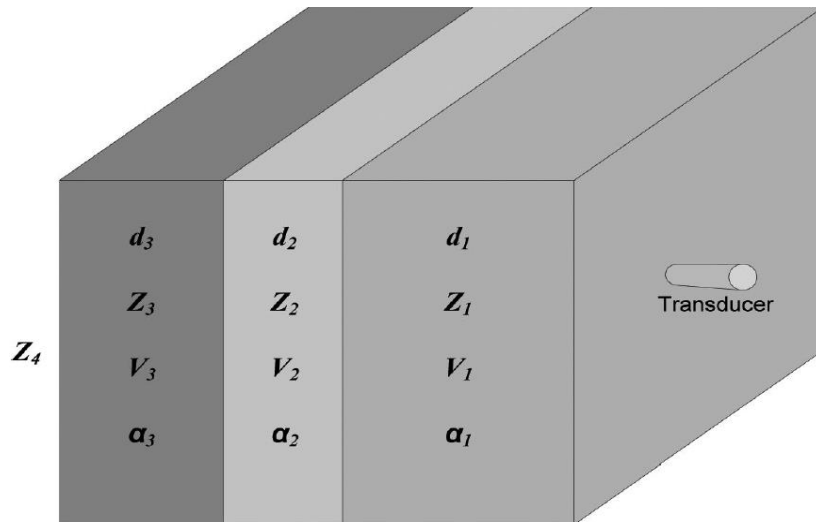


Figure 9. Layered model of the human body simplified into three main layers. The first layer is the skin, second is the muscle and fat, and the third is the bones

Assuming the scenario shown in Figure 9 where the human body is modeled as only three stacked layers: skin, fat and muscles. The wave reflections can be clearly defined. Using an ultrasonic transducer, a normal incident acoustic wave is induced into the first layer from the right. This normal incident wave will be divided into three components: the normal incident component, the reflected component and the transmitted component (Figure 10).

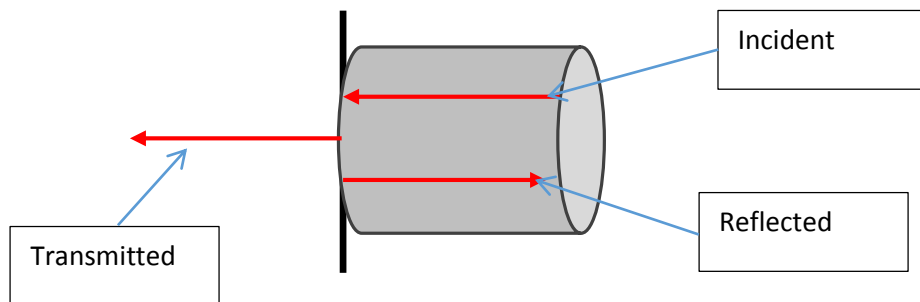


Figure 10. Wave propagation behavior at boundaries between layers of different acoustic impedances

Now, the same analysis can be carried out for the transmitted component from the first interface between the transducer and the first layer. This transmitted component will propagate through the first layer until it reaches the boundary of the second layer. Once at the boundary, it will split into three components as well: transmitted, reflected and incident. Then the reflected component will travel back through layer one towards the transducer. Once this component reaches the boundary between the transducer and the first layer, it will split again into three components and the process will keep going in each layer until the energy completely vanishes. This phenomenon is known as the

reflections due to mismatched impedances which causes a lot of losses to the original signal [210].

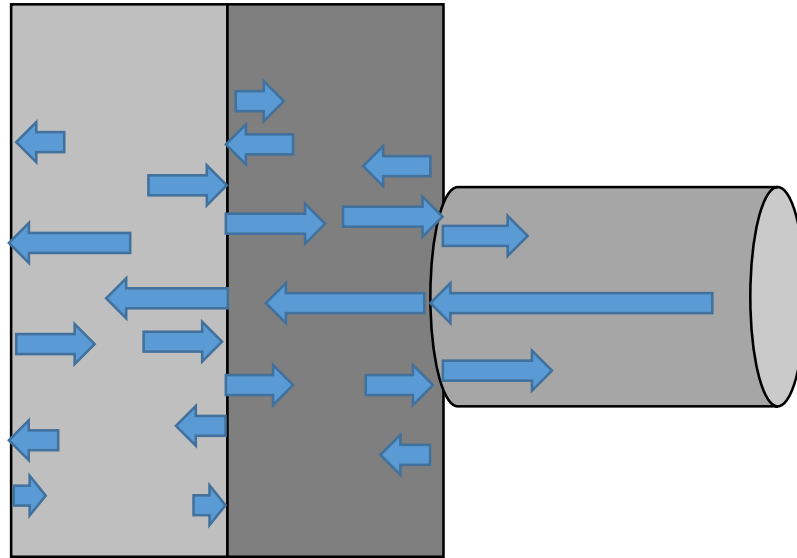


Figure 11. Ultrasound wave behavior in a multilayer medium

Using the analysis for the reflection coefficients, attenuation and the impedances of the different layers of the body, calculated values can be found for the reflected and transmitted waves at each boundary hence allowing for the possibility of designing the proper transducer that can be used to achieve a certain intensity at a specific depth.

4.4. Transducer design

4.4.1 Concept of Piezoelectricity

The word piezo in old Greek means pressure; hence, the term piezoelectric is used to describe the phenomenon in which pressure can be converted into electricity. Also, the inverse process is possible where electricity can be changed into pressure waves in the form of sound wave. Such a conversion process would not have been possible without the discovery of piezoelectric materials in the 1880s. The first discovery that led to the emergence of this field was the quartz crystal which was discovered by J. and P. Curie in France in the beginning of 1880.

Silicon dioxide which later was given the name quartz is a naturally occurring piezoelectric material which has the ability to convert deformations due to exerted force into electricity. Quartz is considered the best natural piezoelectric known to humanity. It can be found in the form of rock crystals or can be extracted from desert sand. What

makes it appealing is that it is easily fabricated into solid crystals. Those crystals conserve the original properties of the silicon dioxide and they are easy to cut to suit specific applications. They are resistant to chemical agents and they tolerate very high temperatures. Last but not least, they have low electrical and mechanical losses which make them ideal for ultrasonic applications.

Nonetheless, there are other fabricated materials that exhibit the piezoelectricity phenomenon most of which are ferroelectric. Ferroelectric materials are those which have naturally-occurring internal dielectric moment that allows them to polarize when an electric field is applied on them. Those materials are not polarized naturally as long as they are kept at a temperature below the Curie temperature. Once they are subjected to elevated temperatures, they lose their ferroelectric property. Nonetheless, as long as they are functional, they tend to have very high electric constants or electric permittivity which makes them strong piezoelectric material.

There are a lot of such ferroelectric material but the most well-known is lead zirconate titanate ($\text{Pb}(\text{Zr},\text{Ti})\text{O}_3$) which is known as PZT. Currently there are some good newly emerging piezoelectric materials such as polyvinylidene fluoride (PVDF) which is a polymer, but they need further enhancement before they replace PZT. However, currently, the dominating material is PZT, which is made into powder that can be placed between metal plates to form a transducer as shown in Figure 12 below.

PZT has the ability to work as a two way converter where it can convert mechanical energy from pressure to voltage or the other way around. If a sinusoidal signal is applied at the terminals of the PZT towards the metal plates, the whole transducer starts to vibrate. The vibration of the PZT comes in the form of compression and stretching. When the input voltage is in the negative cycle, the PZT is stretched radially outwards in the x direction. When the input voltage is in the positive cycle, the PZT compresses inward also in the x direction. As this in and out motion repeats, the air molecules at the surface of the transducer, close to the metal plates, start to vibrate along with the transducer vibration. From the earlier discussion on waves, such air molecule vibration creates a region of successive compressions and rarefactions which allows for a pressure wave to propagate. Hence, using PZT along with an oscillating input, an acoustic wave can be produced at the frequency of the input oscillator. Nonetheless, the physical dimensions of the transducer also affect the fundamental

frequency as well as the intensity that the transducer can produce, as will be discussed shortly.

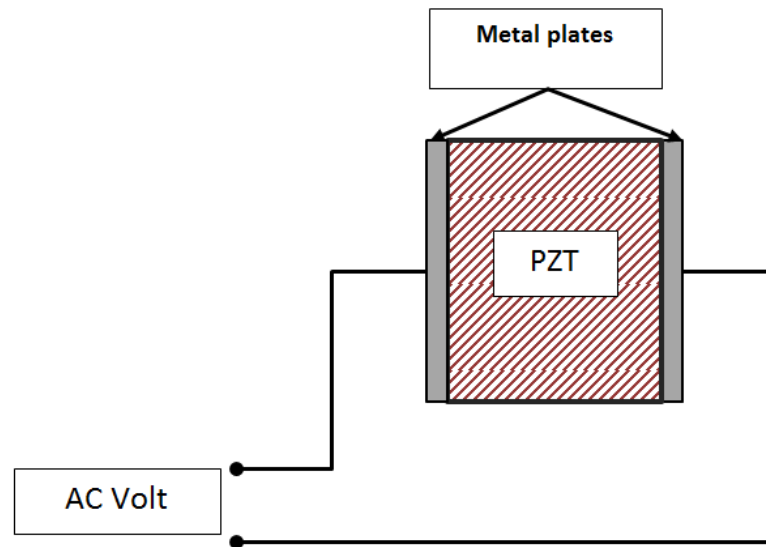


Figure 12. PZT ultrasound system showing the PZT powder placed between two metal plates

4.4.2. Piezoelectric material properties

When PZT is pressed on by an external force, the atoms polarize producing a capacitive effect that leads to the induction of electric charges into the lead wires which gives rise to AC voltage. The induced charges can be quantified by what is known as the charge density or dielectric displacement D .

$$D = e * S \quad (17)$$

where S is the strain due to the applied force.

The inverse effect of piezoelectricity deals with the PZT when a voltage is applied on it and pressure waves are produced from it. When an electric field is applied onto PZT, the internal atoms tend to polarize which allows the electric field E to pass through. This is because all the moments get aligned in the direction of the field which produces a natural given elastic stress that is quantified as:

$$\sigma = -e * E \quad (18)$$

where e is common in the two equations and it is the piezoelectric constant of the PZT.

As can be seen from the above two equations, they are linear and both depend on e which is fixed for every piezoelectric material; however, those equations assume that the material is either very elastic or very stiff. This is because, if the material is very elastic, no deformation can happen that can produce electricity so the material works only in the reverse mode of piezoelectricity. If the material is assumed to be very rigid, then hardly any electric field will be able to cause it to vibrate. The material in this case will only work if a certain amount of pressure is applied on it. In reality, a PZT material is both rigid and elastic to a certain extent which is what defines its properties. Hence, if the charges produced D or the elastic stress σ are to be quantified, additional terms must be included as shown in the below equations [211-213].

$$D = e * S + \epsilon s * E \quad (19)$$

$$\sigma = -e * E + KE * S \quad (20)$$

where, ϵs is the dielectric constant and KE is the elastic constant .

As seen from the modified equations, both are dependent on strain as well as electric field which to a great extent approximates the actual behavior of a PZT material. However, there are some extreme conditions that governs the values of the constants which are: when there is no constraint on the thickness of the PZT layer i.e. $\sigma = 0$ and when the electrodes connected to the metal plates are electrically shorted i.e. $D = 0$. By solving for the constants using those conditions, it can be shown that:

$$\epsilon s = \epsilon \sigma * (1 - K^2) \quad (21)$$

where, $\epsilon \sigma = \epsilon s + \frac{e^2}{KE}$ is the dielectric constant at $\sigma = 0$ and $K^2 = \frac{e^2}{KE * \epsilon \sigma}$ is called the coupling factor.

Similarly,

$$KE = KD(1 - K^2) \quad (22)$$

where, $KD = KE + \frac{e^2}{\epsilon s}$ is the elastic constant at $D = 0$ and $K^2 = \frac{e^2}{KD * \epsilon s}$ is the coupling factor.

Furthermore, by analyzing the wave equation combined with the above equations on the electro-mechanical characteristics of the PZT, it can be shown that the velocity of the sound can be calculated as follows [211, 214]:

$$c = \sqrt{\left(\frac{KD}{\rho}\right)} = \sqrt{\frac{KE}{\rho*(1-K^2)}} \quad (23)$$

With all the above analysis, it is clear that the design of an ultrasonic transducer is a quite complex process that requires the considerations of various factors. To further simplify the concept of a PZT transducer design, it is possible to model it as a transmission line as shown in Figure 13.

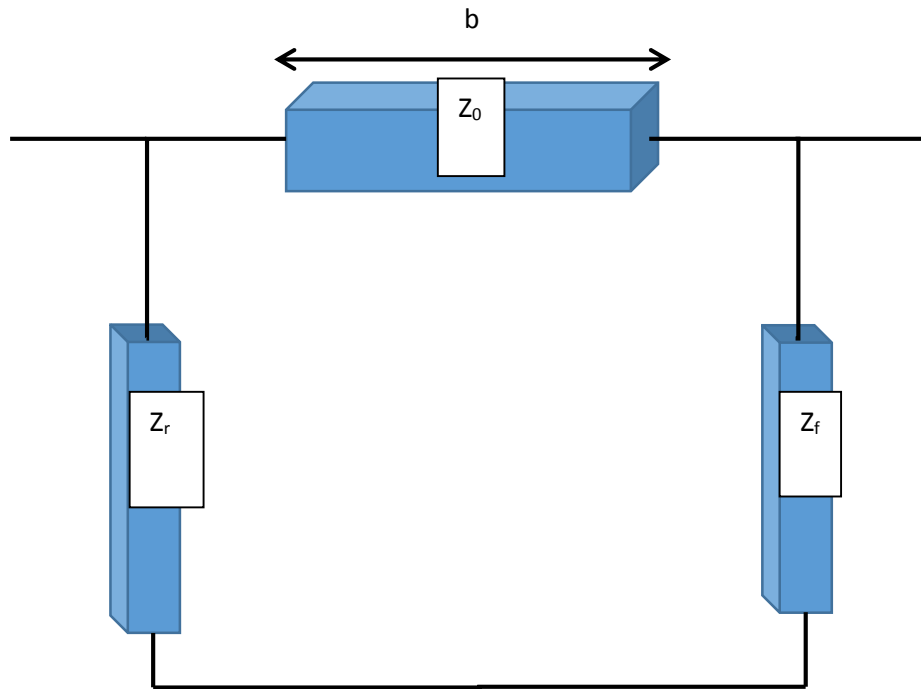


Figure 13. Transmission line model for Ultrasound PZT probe

Let Z_0 be the characteristics impedance of the PZT, Z_r and Z_f be the impedances of the rear and front metal plates. When the rear plate is excited with an oscillating input, the PZT is excited as well since they are both connected together directly. However, due to the coupling factors discussed earlier, the excitation amplitude is not completely conveyed from the plate to the PZT. Hence, each will have a certain excitation amplitude. The difference between those amplitudes is due to the differences in their impedances and can be calculated as follows.

$$\sigma e(t) = Pr(t) - Po(t) \quad (24)$$

Further, assume the following analogies:

- Pressure = voltage
- Impedance = resistance
- Velocity = current

Using the above analogy, almost all electricity laws apply such as ohms law.

Therefore, the velocity of the sound wave can be derived as follows:

$$Vr = \frac{Pr}{Zr} \quad (25)$$

Then,

$$Pr(t) = \frac{Zr * \sigma e(t)}{Zo + Zr} , \quad Po(t) = \frac{-Zo * \sigma e(t)}{Zo + Zr} \quad (26)$$

However, a similar simple analysis cannot be done for the front side of the transducer. This is because; there are other factors such as refractions and reflections that affect the output amplitude. Unlike the rear-PZT junction, the front-PZT junction will suffer from heavy attenuation and randomness caused by the composition of the PZT material itself. The closest model where only reflections are accounted for can be calculated using the following expression.

$$Pf(t) = Pr(t) + T * [Po(t - \tau) + R * Po(t - 2\tau) + R^2 * Po(t - 3\tau) + \dots] \quad (27)$$

where,

$$R = \frac{Zf - Zo}{Zf + Zo} , \quad T = 1 - |R| , \quad \tau = \frac{b}{c} \quad (28)$$

Moreover, the pressure amplitude depends, not only on the characteristics of the PZT and the metal plates, but also on the excitation frequency. For every PZT, there is a resonance frequency at which the maximum output pressure (intensity) can be achieved. So, by modifying the above equation for the radiated pressure from the front plate, the following is a more precise representation:

$$Pf = \frac{\sigma o}{1 - i * \left(\frac{Zo}{Zr}\right) * \cot\left(w * \frac{t}{2}\right)} \quad (29)$$

where,

$$\sigma_0 = -\frac{eV}{b} \quad (30)$$

By finding the roots of the denominator of the transfer function, it can be found that sharp resonance happens at a fundamental frequency that has a wavelength equal to half the thickness of the PZT core [212, 215]. Also, other peaks happen at the multiples of this frequency which are called its harmonics. This relation is summarized in the following equation:

$$\lambda = \frac{b}{n-0.5} \quad , \quad n = 1,2,3, \dots \quad (31)$$

Also the bandwidth of those peaks can be calculated as a function of the characteristic impedances, physical dimensions and the speed of sound as follows:

$$BW = 2 * \frac{cd}{\pi * b} \left(\frac{Z_r}{Z_0} \right) \quad (32)$$

To eliminate the problem with the resonance and its harmonics, matching impedances can be used in the packing material and a matching impedance layer can be used at the outer surface of the transducer to reduce internal reflections when the transducer is used against a none-matching impedance surface. The matching layer in the front side of the transducer is from where the wave is transmitted. This is a crucial part in the design of any transducer as it increases the efficiency of it by reducing the losses due to impedance mismatch. However, for the optimum performance, the transducer should be design with a matching layer that matches the impedance of the medium in which the transducer will be used. This information should be provided by the user to the manufacturer as a part of the specifications. Overall, a transducer is usually composed of a connector that is attached to a housing package. Inside the housing, the electrical connection is extended from the connector to the rear plate of the transducer. However, the rear side is attached to a backing material that absorbs internal reflections and lowers the loss in the radiated amplitude due to harmonics. On the front end of the transducer, the outer surface of the housing is composed of a thin layer (quarter the wavelength) of a material (impedance $Z_m = \sqrt{Z_f * Z_0}$) matching to the external medium to lower the reflection loss. The setup of most transducers looks similar to the one shown below in Figure 14.

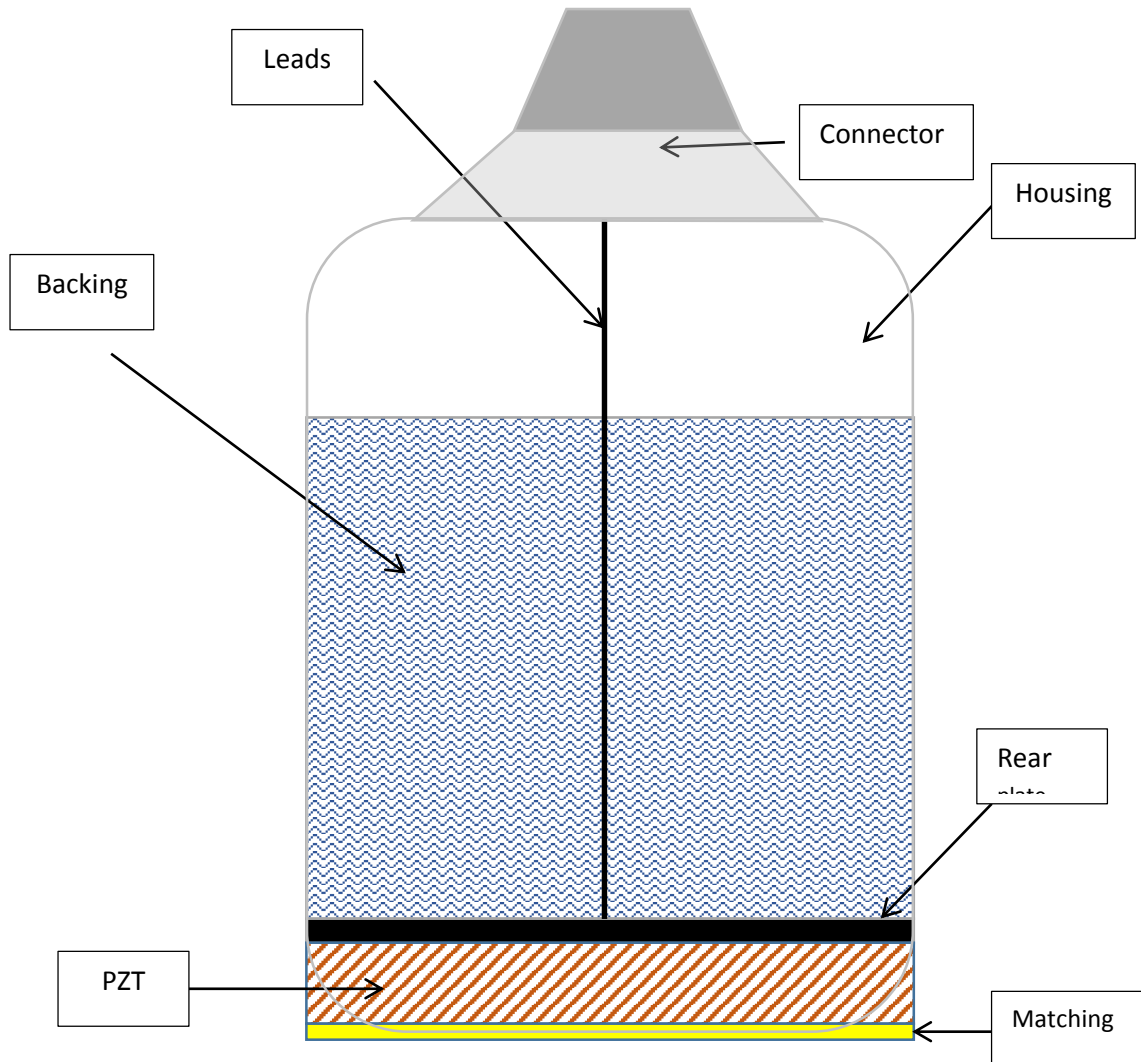


Figure 14. Circular Disk Ultrasound Probe. All the main components such as the matching layer, the backing material, and the PZT powder compressed between the metals plates (front and rear) are shown.

4.4.3. Radiation Field of Piston Transducer

A transducer can be molded into different shapes and sizes. However, the most popular are the transducers with circular surfaces. In this work, the focus will be on this type of transducers. In this part, the radiation field of the circular (piston) transducer is discussed.

There are many factors that may influence the behavior of a transducer such as: composition material, mechanical construction and external mechanical and electrical load. The best model that approximates the radiating acoustic wave is a circular wave. Assume that the surface of a transducer is in fact made up of many infinitely small point

acoustic sources the analysis of which is best to start with to understand the general radiation field of the whole transducer.

Assume that a circular source is located in the x,y plane of the Cartesian coordinates (x,y,z) as shown in Figure 15. Also, assume that the velocity of the sound over this surface has a distribution of $V_o(x,y)$. Further, assume that the produced wave propagates in a spherical shape. So, by solving the wave equation for a spherical wave, the pressure can be calculated as follows:

$$P(r) = P_o * \frac{e^{i(k*r-w*t)}}{r} \quad (33)$$

Where,

$$r = \sqrt{x^2 + y^2 + Z^2} \quad (34)$$

$$P_o = - \frac{i(w*\rho*So)}{2*\pi} \quad (35)$$

Therefore, the above equation can be used to calculate the pressure at any point in the plane given that the initial pressure P_o , frequency ω and the characteristics of the transducers k are known. By assuming that the circular transducer can be divided into infinitely small point sources, then So (volume velocity) can be calculated as:

$$So = 4 * \pi * a^2 * Va \quad (36)$$

where a is the radius of the point source and Va is the velocity at that point source. Hence, in this model, the pressure of the whole circular disk can be assumed to be the summation of all the pressures produced from the point sources. For the most general case and as the size of the point sources goes to zero, the summation can be assumed to be an integral which is given as follows [216, 217]:

$$P(r') = - \int_A i(w * \rho * V_o(x, y)) * \frac{e^{i(K*r'-w*t)}}{2*\pi*r'} dA \quad (37)$$

where,

$$r' = \sqrt{(x - x')^2 + (y - y')^2 + (z)^2} \quad (38)$$

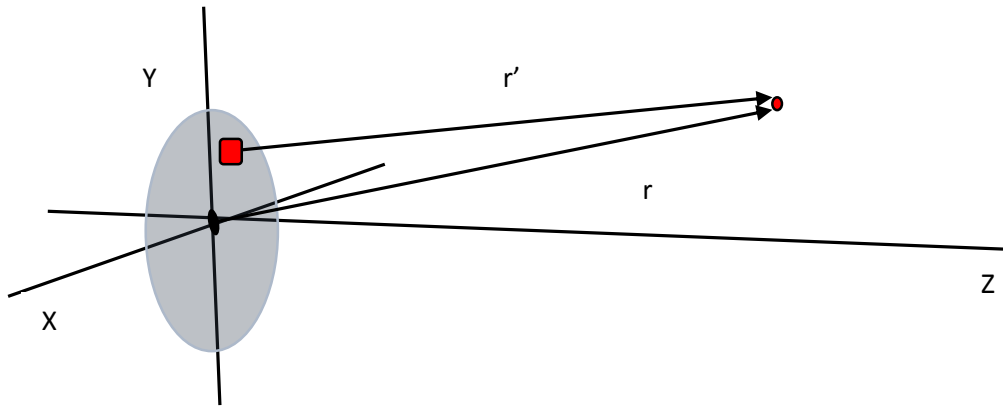


Figure 15. Division of the circular PZT disk into very small sub-disks and analysis of the US waves radiated from those points at a certain point in space distanced from the origin by “r”. The total US power density will be the summation of the radiations of the individual sub-disks.

Moreover, for every transducer, there are regions of radiation within which the radiation pattern of the generated waves behaves in a certain general manner. In the circular transducer discussed here, there are two main regions namely the near field and the far field and each has its own patterns.

- Near field (fresnel region)

The generated wave in this region assumes propagation like that of a plane wave.

- Far field (fraunhofer region)

The generated wave in this region is best approximated as a diverging spherical wave which is similar to the wave behavior of the point source discussed earlier. Therefore, all of the earlier discussion applies only when dealing with the circular transducer that is operated within its far field. However, an added term called directivity is included as a multiplication factor when calculating the pressure. Hence, the pressure equation becomes:

$$P(r, \theta) = P_0 * \frac{e^{i(k*r - w*t)}}{r} * D(\theta) \quad (39)$$

where,

$$D(\theta) = 2 * \frac{J_1(a*k*\sin(\theta))}{a*k*\sin(\theta)} \quad (40)$$

The added factor of directivity is very critical as it determines the direction at which most of the intensity will be radiated. As can be seen, the directivity is in fact a function of the physical dimensions of the transducers, its chemical composition and the half angle θ . A few examples of the directivity patterns are shown below in Figure 16 for different sizes and types of transducers. Also, the half angle is shown for each case. The half angle (angle of divergence) can be used as a measure for the directivity and it is calculated based on either the first main lobe or when the intensity falls by 3 dB.

$$a * k = \pi * \frac{d}{\lambda} \quad (41)$$

$$a * k * \sin(\theta) = \zeta \quad (42)$$

where ζ is the value at which the first lobe occurs which is usually 3.83 after normalization. The -3 dB is equivalent to $\zeta = 1.62$ which can be used as well.

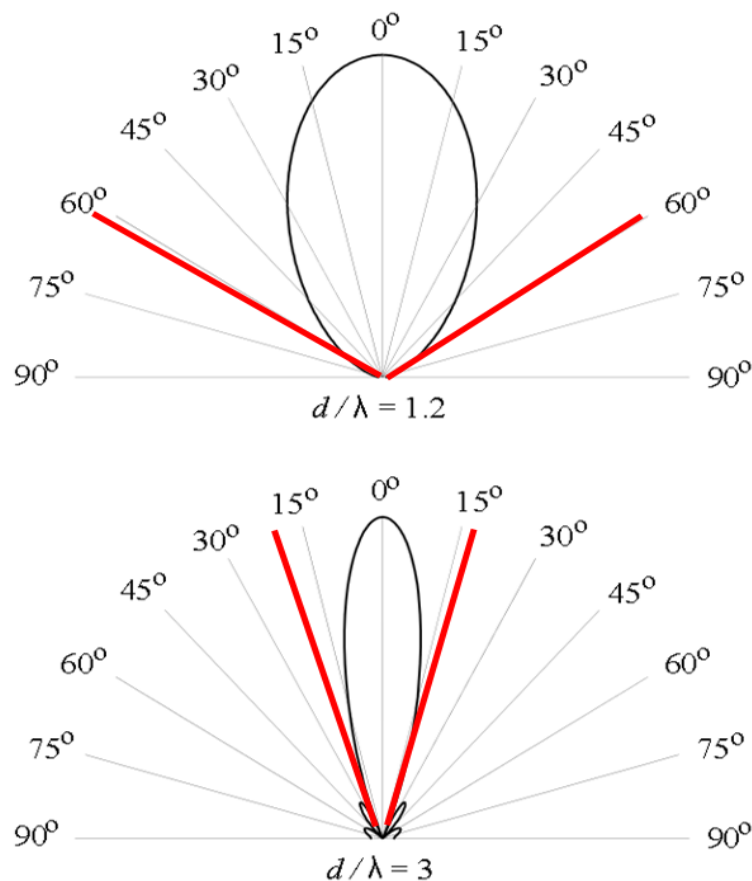


Figure 16. Radiation pattern of different probes at different half angles

Another critical point that should be considered when studying the field pattern of a transducer is to note the location of the near-field/ far-field transition. This point is usually referred to by the variable N which is proportional to the physical measurements of the transducer as well as its resonance frequency. It is worth mentioning that, unlike the pattern in the far-field, the pattern in the near field is random and is full of maxima and minima. In the near field, some regions will exhibit very high pressures and others will not produce any. Some books like to define the transition point N as where the maximum amplitude in the near field ends, however, with minimal analysis and equation manipulation, the results will converge into the following.

$$N = \frac{a^2}{\lambda} \quad (43)$$

4.4.4. Unfocused circular transducer

This discussion leads to one of the most widely used transducers which was one of the transducers that were used in this work which is circular unfocused transducer. The radiation behavior of these transducers in the near field is like a well collimated beam with very minor convergence until the transition point. However, in the far field, the diffraction losses increases as the divergence of the wave becomes severe and the propagation turns into a spherical pattern. Also, the amplitude becomes inversely proportional to the distance from the transducer. In the early 1950s, a scientist named Lommel was the first to do work on the calculation of the diffraction of the ultrasonic wave. Later on, a diffraction correction formula was derived based on Lommel's work which is calculated as follows:

$$DL(s) = 1 - e^{-i*2*\frac{\pi}{s}} * \left[J_0 \left(2 * \frac{\pi}{s} \right) + iJ_1 \left(2 * \frac{\pi}{s} \right) \right] \quad (44)$$

where J_0 and J_1 are the zero and first order Bessel functions respectively and s is the normalized distance from the transducer.

This divergence correction formula is what helped in completing the picture of the radiation pattern of a circular transducer. However, those are all approximations. Furthermore, it is assumed that the beam does not converge or diverge in the near field up until the transition point. This assumption, when comparing the resulting pattern to the actual, cost a 3 dB loss in the intensity at the transition point as shown in Figure 17. The actual field is shown in red where it converges until the transition point and then it

starts to diverge. The dashed field is the calculated one. As can be seen, the calculated follows the actual in the overall shape; however, it fails to show the slight convergence of the beam in the near field. This is expected as the modeling equation fails to include the nature of the medium along which the wave propagates.

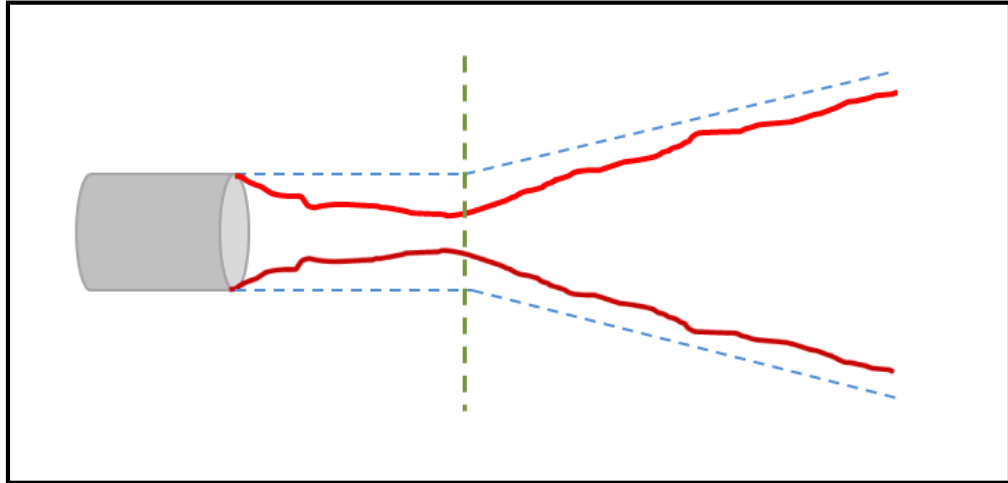


Figure 17. The actual field pattern of the circular disk transducer versus that of the theoretical one, plus the transition point after which the wave can be regarded as a plane wave.

Since intensity is power divided by unit area, the maximum intensity of an unfocused transducer should happen somewhere close to the transition point as it has the smallest diameter. Thus, when designing a transducer, the transition point is considered as the critical point to set the upper bound on the performance of the transducer. Further, experiments showed that there is an inverse relation between the lommel diffraction correction and the frequency. So, as the frequency increases, the diffraction correction decreases, yet this relation is not present in the current formula of the $DI(s)$ stated earlier.

4.4.5. Focused circular transducer

Another type of US transducer is referred to as focused transducers. From the name, it indicates the nature of the output wave where it can be designed to be focused onto a single point in space. The buildup of the transducer remains the same, but to achieve the focusing feature, three methods can be used. The first method is by using a concave transmitting PZT layer that works as a dish-like antenna. The second method involves the use of a focusing lens capable of converging US waves based on its location from the normal flat transducer. The third method is by designing the transducer from an array of transducers termed as phase array transducer. In this

section, a brief description of the first focusing method is presented as the focused transducer used in this thesis was based on that method.

The transducer of this type usually has a concave like transmitting end as shown in Figure 18. This concave shape helps in defining the radiation pattern of the transducer and depending on the diameter of the PZT, the concavity of the transducer, and the resonance frequency at which it operates, the focal point position is determined.

For example, assuming the position of the focal point does not matter, for the same transducer with the same dimensions, the higher the frequency, the more focused the wave can be. This is due to the fact that, at higher frequencies, the wavelength decreases which makes it possible for the wave to be focuses onto a smaller focal point. Assuming the focused wave will have a triangular like shape, the higher the frequency, the narrower the focal point can get as shown in Figure 18. On the other hand, the dimensions of the transducer can be designed to get a certain focal size at a certain distance for a certain resonance frequency by simply understanding how the wave behaves in different media.

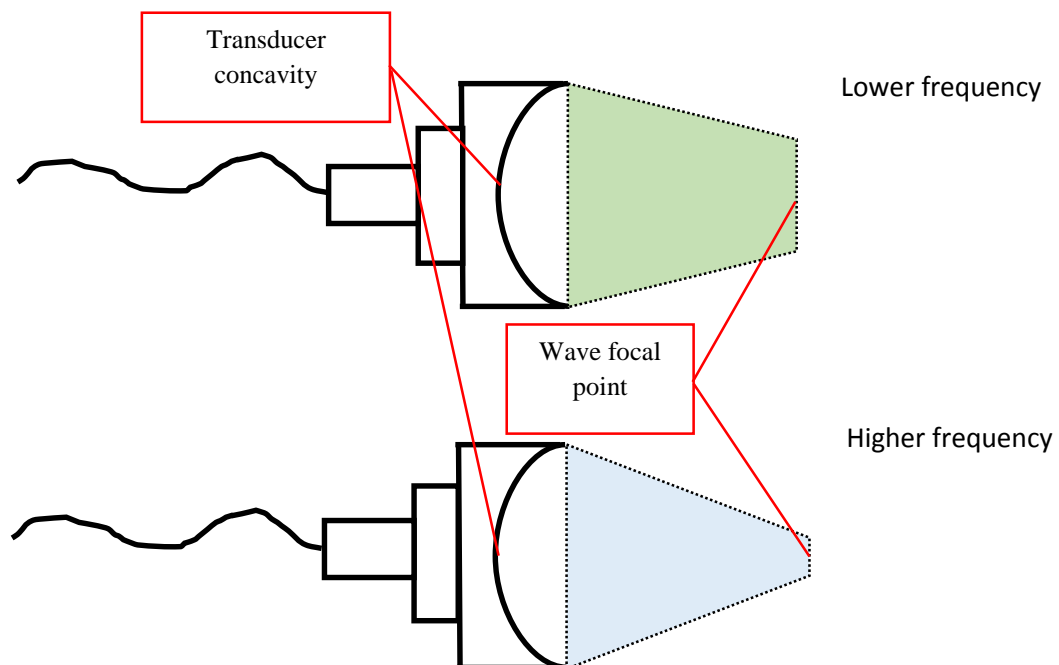


Figure 18. The focused ultrasound probe and the corresponding radiated wave, plus the effect of increasing the frequency on the size of the focal point and its distance from the center of the probe.

In this work, the ultrasonic transducers used are of two types. Some are focused ultrasonic transducers with resonance frequencies of 1 MHz and 3 MHz. They were

bought from Precision Acoustic, London, England. The others were unfocused and were already available in the university from Optel inc, Poland. They have resonance frequencies of 5 MHz and 10 MHz. All transducers had a circular surface and worked in a continuous wave excitation mode. For further details of the equipment used, see Appendix A.

So, by now, most of the basics needed to understand how ultrasound behaves in the human body have been covered. This information is critical for the understanding of the next part of this work which deals with mechanisms by which ultrasound is used to cause drug release from liposomes. The mechanisms are explained in detail with reference to the physics portion of ultrasound discussed so far.

CHAPTER 5: Ultrasound in Drug Delivery

5.1. Interaction of ultrasound with liposomes

Ultrasound, a potential trigger for drug release from nanocarriers, is gaining significant attention in creating successful DDSs. Nonetheless, similar to other triggering means, the drug carriers must be modified to become more responsive to acoustic waves. Liposomes modified to increase their acoustic sensitivity are referred to as echogenic or acoustically activated liposomes (AALs). The modifications depend on several US parameters, including intensity and frequency of the triggering acoustic wave, and are aimed to obtain the most efficient release. For example, high intensity US at a low frequency causes an increase in the temperature of the medium, hence, liposomes triggered using this technique are synthesized/designed to respond to hyperthermia. This section introduces several types of echogenic liposomes and the mechanisms by which US induces drug release. By understanding the different ways US interacts with a liposome and the advantages and disadvantages of each, new, and possibly better, liposomal chemical formulations can be developed, leading to better DDSs.

5.1.1. Hyperthermia

Liposomes are made up of a lipid bilayer which, similar to cell membranes, gives them an acoustic impedance, close to that of muscle tissues. This impedance means that, as the acoustic wave passes through the liposomes, there will be some energy dissipation absorbed by the liposome. This energy is converted into heat, which raises the temperature of the lipids. If the liposome is designed with a specific transition temperature (e.g. the TSL discussed earlier) hyperthermia can be used to achieve this temperature, causing the lipid bilayer to transition from the LO state to the SO state, introducing pores within the shell, which in turn allows for the release of therapeutic agents. Hyperthermia, as stated in the work of Schroder *et al.* [24], can be achieved using HIFU at frequencies higher than 0.5 MHz, with intensities that can reach up to several hundreds W/cm^2 .

The intensity of an acoustic wave is defined in terms of power over unit area. The intensity is affected by the amplitude of the wave (i.e., the larger the amplitude of the generated wave, the higher the intensity) and also by the size of the area that it is

directed at. Hence, for hyperthermia applications, HIFU is used, since the ultrasonic wave is focused onto a small area at large amplitudes, thus very high-power-to-area ratios can be achieved. Nonetheless, not all ultrasonic waves can be focused. There are two factors, namely the *diffraction correction factor* and the *directivity of the beam*, which govern the process of focusing a beam [165-167, 170, 171, 179]. Since both factors are dependent on the physical parameters of the transducer, which in turn are dependent on the resonance frequency, it was observed that higher frequencies are more easily focused than lower ones.

When using HIFU with TSL, and depending on the size of the liposomes, power and frequency can be optimized to yield the required intensity at the desired location and the needed depth within the body. The lower the frequency, the lower the intensity needed to achieve the targeted hyperthermia, since low frequency US (LFUS) can penetrate further, hence allowing more energy to be absorbed by the liposomes and the human cellular structure at the tumor site. On the other hand, at higher frequencies, higher intensities are needed to reach the tumor site and achieve the required hyperthermia [50, 51, 58, 70, 218, 219]. Hence, similar energy absorptions can be achieved when using low intensity at lower frequencies, and high intensity at higher frequencies; however, there is always the tradeoff of causing damage to the healthy tissue being irradiated. For example, if the decision was to use high frequency at high intensity, the outer layers of the body will be subjected to extremely elevated temperatures as the US will lose energy quicker and at shallower depths. On the other hand, lower intensities can penetrate further avoiding over heating of the outer layers of the body, but this might be at the expense of a more dispersed (unfocused) beam of US. Therefore, there is a need to optimize frequency and power density when US is used to induce hyperthermia. Such optimization has been adequately addressed in the literature [220-223]. Hence, although hyperthermia can be easily introduced using lower frequencies at lower intensities, this frequency range is hardly focused, which makes it difficult to attain the required intensity at the target point. Further, medical US is within the range of 1 to 15 MHz, since US of lower frequencies interact more efficiently with the body tissues, and can cause severe hyperthermia that damages healthy tissues [179, 224]

Another factor when optimizing the use of HIFU is the skin depth, which determines the penetration depth of the acoustic wave into the body. This is critical in

the case of deeply localized tumors, since losses due to penetration have to be taken into consideration if a certain intensity is required at a deeper level in the human body [58, 225]. For example, if an intensity of 10 W/cm^2 is required at a depth of 5 cm into the human body, the applied acoustic HIFU wave should have a higher intensity to account for the losses as the wave propagates into the body. As discussed earlier, the losses may arise due to reflections caused by impedance mismatches between the different layers in the body, and also due to the absorption of some of the energy by the cells. Both factors are dependent on the frequency of the wave: the higher the frequency, the higher the losses and the lower the penetration ability. The proper frequency should be chosen carefully so that the required intensity can be reached at the desired site without greatly increasing the intensity at the surface, since this could lead to tissue damage of the skin and other structures.

Besides being used as a trigger for drug release from TSL, hyperthermia induced by HIFU can also be used as a direct means to induce the death of cancer cells. Cancer cells subjected to temperatures above 42°C die; hence, if the cancer is superficial or directly on the skin, it can be treated by HIFU without the need for chemotherapy [226-228].

5.1.2. Cavitation

Another form of ultrasonic triggered release depends on cavitation. Cavitation is a natural phenomenon that occurs when a wave is incident on a bubble filled with a liquid that has the same resonance frequency as that of the incident wave [229]. In this case, the bubble will start to oscillate at its resonant frequency. This is a well-known phenomenon since everything has a resonant frequency of its own. For example, in 1940, Tacoma Narrows Bridge, in Washington, USA, collapsed when the passing winds caused it to resonate at its resonance frequency [230]. At this frequency, the particles tend to vibrate in a harmonious way. For example, if the vibrations were to the right, all the particles of the bridge would be moving to the right. If the vibrations were to the left, all the particles would be moving to the left. When the amplitude of the vibration was high enough, all the particles were vigorously swinging to one side or the other, and the vibration could no longer be sustained by the bridge, which caused its collapse. The same concept applies to the cavitation of a microbubble. If an acoustic wave is applied at the resonance frequency of the bubble, it will start to oscillate along with the

wave. When the wave is in the low pressure stage, the bubble will be stretched, and, as the wave cycle goes from low pressure to high pressure, the bubble will start to compress gradually until it reaches the peak of compression, which corresponds to the maximum peak of the pressure wave. Microbubbles have certain tolerance points after which they can no longer get compressed or stretched based on the encapsulated gas. When the applied wave reaches peak pressures higher than the tolerance point, the microbubbles will not be able to oscillate and will burst, generating an intense shock wave that can shear open nearby cells. Also, this collapse is accompanied by the generation of very high temperatures, which can reach up to thousands of Kelvins [231]. While the bubble is oscillating with the wave, the cavitation is referred to as *stable cavitation*, while in the case of a bursting bubble, it is referred to as *inertial or transient cavitation* [232, 233].

In drug delivery, the transient cavitation phenomenon is of interest, since if the liposomes are close to microbubbles that undergo transient cavitation, the shock wave produced may cause the liposomal membrane to open thus allowing for the drug to diffuse out of the nanocarrier (Figure 19). Also, if the bubble is close to the tumor site, the shock wave as well as microjets of liquid can lead to the disruption of the cell membranes, allowing the released drugs to enter and accumulate into the cells. This greatly enhances the performance of a DDS. These shooting jets occur when one side of a bubble is close to a cell or tissue. In this case, the burst bubble causes liquid jets rather than shock waves [234]. This type of collapse, called asymmetrical collapse, only occurs when the motion of the bubble is restricted from only one side, while the other side is free to oscillate. The collapse happens on the free side and propagates towards the inner side giving rise to a directed shock wave, which, unlike the normal shock wave which propagates spherically with the center being the collapsed bubble, propagates along a straight line. Thus, all the energy is directed towards one point, in other words focused on the desired location [235]. If these liquid jets are directed towards a cell or tissue, they can cause extensive damage. Therefore, a combination of both types of bubble collapse leads to an enhanced DDS [236].

In summary, the cavitation-induced release from the liposomes is triggered due to either the shear wave produced from the collapse, directed or not, and/or due to the elevated temperatures that are generated in the process.

As discussed earlier, carriers designed to be triggered by this method are usually either dependent on naturally occurring bubbles in the vicinity of the targeted site, or make use of manually introduced microbubbles in the vicinity of the tumor. Otherwise, they must be loaded with nano-bubbles that can oscillate and cause cavitation. The problem with the first method is the fact that the sizes of naturally-occurring bubbles are difficult to know except through sophisticated means, e.g. imaging. This presents a constraint on the choice of the frequency as the resonance frequency of a bubble is dependent on its size. If the size is unknown, the only way to cause cavitation is through trial and error, hence different frequencies and power intensities have to be used until transient cavitation is achieved. Higher intensity means higher risk of causing damaging hyperthermia and this is undesirable. This tradeoff between complexity and side effects calls for a controlled size of microbubbles used to induce cavitation. Thus, researchers created microbubbles of a fixed size and introduced them into the tumor site [237]. Since the size of these microbubbles is known, their resonance frequency can be calculated; hence, transient cavitation and drug release can be controlled. In the case of AALs, these are best triggered using low frequency and intensity US. At low frequencies, in the range of 20 to 500 kHz, small intensities in the range 0.5-10 W/cm² can be used; the higher the frequency used, the higher the intensity needed, which leads to the use of HIFU [238].

There are two methods by which bubbles can be manually introduced. They can be either encapsulated inside the liposomes, along with the drugs, or they may be placed in the membrane, sandwiched between the lipid bilayer, as described by Huang and MacDonald [40, 239]. Figure 20 clearly shows the location of the bubble in the membrane as well as the place of the loaded drug. Using this AAL, transient cavitation can be induced and the drug can be released easily into the surroundings. These carriers can be further enhanced to make them actively targeted, so they can be directed to cancer cells and the release can be triggered directly into the cytosol.

However, the smaller the bubble the higher its resonance frequency and the higher the intensity it needs to undergo transient cavitation. This is because, as the frequency increases, larger bubbles tend to be less sensitive to the acoustic wave and may not even oscillate. The only bubbles that would oscillate are those with very small diameters. A governing factor that measures the possibility that transient cavitation will occur is called the *mechanical index*, which is calculated as follows,

$$MI = \frac{P_{neg}}{f^{0.5}} \quad (45)$$

where P_{neg} is the peak negative pressure of the acoustic wave (in MPa) and f is the frequency (in MHz). As shown in this equation, the mechanical index is a function of both the frequency and the pressure amplitude of the incident acoustic wave, thus as the frequency increases, the MI decreases which mean that the possibility of cavitation decreases. To counteract the effect of increasing the frequency, the intensity should increase extensively. For cavitation to be probable, the MI should be 0.7 or higher [240, 241]. At lower frequencies this can be easily achieved by using very low intensities.

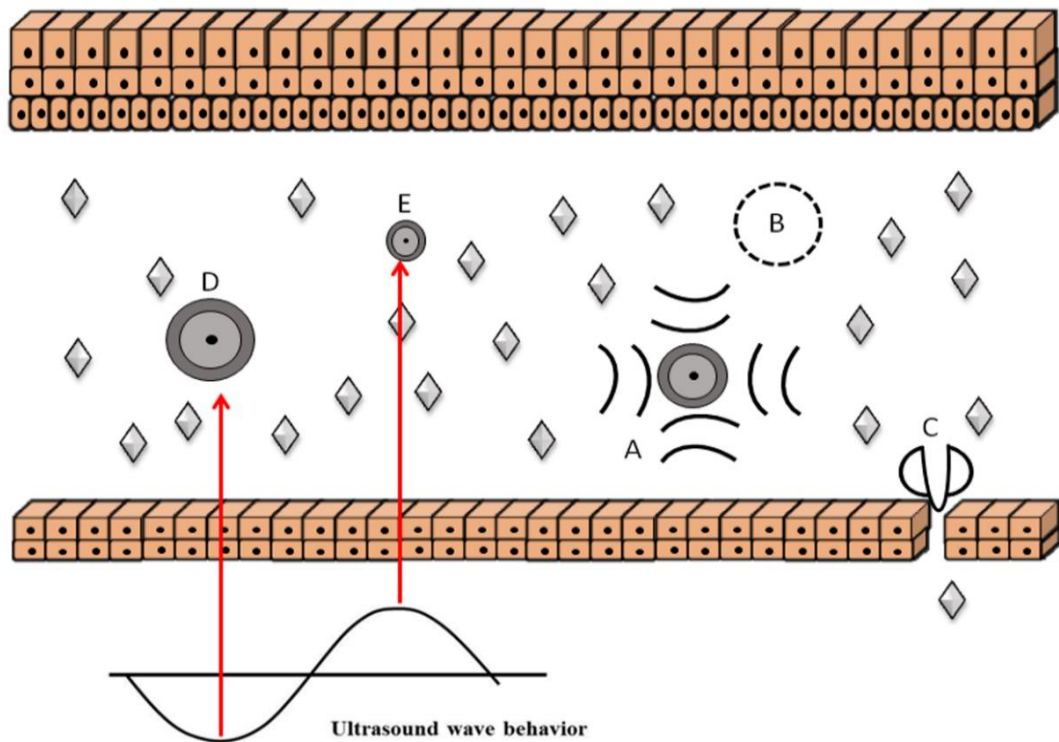


Figure 19. Different types of cavitation processes. Microbubble (A) is undergoing stable cavitation, Microbubble (B) is undergoing collapse cavitation. Microbubble (C) suffered an asymmetric collapse. Bubbles (D) and (E) illustrate the effect of the compression and rarefaction.

Optical and acoustic methods were used to track the destruction that takes place when an acoustic wave is directed towards phospholipid-shelled microbubbles. Experiments showed that the bubbles are destroyed by either one of two main mechanisms: acoustic dissolution at low acoustic pressure, or fragmentation of the parent bubble into two or more daughter bubbles at high pressure. Once the US is applied, the gas inside the microbubbles starts to oscillate causing the whole bubble to oscillate. If the oscillation is stable, currents are formed in the aqueous environment around the bubble. The work done by Mehier-Humbert and co-workers [242] showed

that at a frequency of 2.25 MHz, small bubbles start to oscillate. As the intensity increases, the bubbles undergo transient cavitation which causes some damage to the surroundings. Yet, these experiments were done *in vitro* and the pressure used at this frequency was 300 kPa. The MI for these parameters is around 0.2 which is less than the 0.7 threshold. Further research was done at a frequency of 1 MHz and a pressure of 1.3 MPa, yielding a MI of 1.3. Although transient cavitation is possible at this MI, damage in this case was lower and low bubble collapse could be observed, with some bubbles expanding from 2 μm to approximately 20 μm , when simulation experiments set the limit at a maximum expansion of 55 μm . These puzzling results were further analyzed by Oerlemans *et al.* [243] who suggested a different mechanism for the observed damage when high frequency US (HFUS) was used, as discussed in the next section.

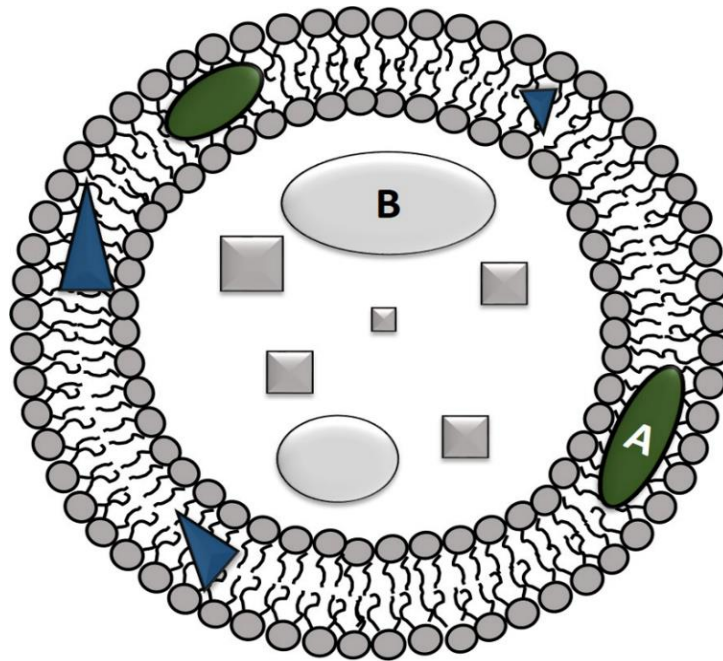


Figure 20. Liposomes loaded with microbubbles.

5.1.3. Collisional mechanism

In 2013, a paper published by Oerlemans and co-workers [243] suggested a different mechanism for HIFU-induced drug release from nanocarriers. Experiments were conducted using TSL and non-TSL (NTSL) carriers, to exclude hyperthermia as the main mechanism of release. The sizes of the liposomes were between 97 to 139 nm, and the chemical composition of the TSL made its T_m around 42 $^{\circ}\text{C}$. Each type of liposome was loaded with a lipophilic compound (Nile red) and with a hydrophilic

compound (Fluorescein), and both carriers were then subjected to a continuous wave of HIFU. When TSL were subjected to the HIFU waves for 15 min, their temperature rose above the T_m and 80% release of the content was observed. However, in the case of the NTSL there was no release under the same conditions. Further, both carriers were then subjected to PW- HIFU (Pulsed Wave- High Intensity US) with an intensity of 20 W for 16 min. This failed to increase the temperature above the T_m , yet a release of about 85% was observed for the TSL and a slight release of about 27% was observed for the NTSL. These results suggested that when HIFU is used, hyperthermia is not the main mechanism for release. The second part of the experiment was designed to eliminate cavitation as the main release mechanism. Designed microbubbles were introduced into the vicinity of the liposomes before PW-HIFU was applied, and the release levels observed were similar to controls where PW-HIFU was applied in the absence of external microbubbles. This suggested that, although the MI was high enough to cause transient cavitation, this was not the main mechanism behind the observed release. The researchers proposed that the shear force exerted by the acoustic wave forces the liposomes to move at very high speeds and collide with each other and/or with the walls of the testing chamber. The results were similar for the release of the hydrophobic and hydrophilic compounds.

5.1.4. Acoustic droplet vaporization

The last mechanism by which US can interact with carriers to cause release is referred to as acoustic droplet vaporization (ADV) and is based on the expansion of nanoemulsions as the surrounding pressure changes. This mechanism applies to the previously described eLiposomes. This triggering method makes use of the restricted volume of liposomes, (i.e., once they are formed, expansion is allowed but cannot exceed a certain limit without destabilizing the liposomal membrane and eventually causes their rupture). The PCF₆ and PCF₅ nanoemulsions have high internal pressure; hence when the surrounding pressure falls below their internal pressure the emulsions are allowed to expand which in turn increases the volume of the liposomes forcing some tension on the shell. This tension may lead to the formation of pores that will allow the drug to be released. Sometimes, the liposomes can be completely ruptured if the volume of the emulsion increases beyond the threshold point that the liposome can tolerate. The tolerance of a liposome is determined by its chemical composition, with expansion

tolerances ranging from 2% to 4% [37, 38, 244, 245]. Ultrasound can be used as a trigger to change pressure, since it is a pressure wave made up of a periodic series of low and high pressures.

Lin and co-workers [39] used HIFU to trigger the release from eLiposomes containing PCF₅ nanoemulsions and loaded with Dox, a carrier named eLipoDox. The exposure to HFUS (1 and 3 MHz) at low intensities of 1 to 5 W/cm² caused release, which was, in all cases, lower than that observed for 20-kHz LFUS. The release with HIFU was relatively low, about 10% after 2 seconds of insonation, increasing to only 15% after 30 seconds. For these shorter times, no temperature increase was observed, for either frequency, nor for the power densities used, which indicated a mechanical action on the liposomes. For higher insonation times, up to 5 minutes, the temperature rise for both frequencies at a power density of 5 W/cm², is significant, and release is increased (50% for 1 MHz and 60% for 3 MHz) due to the PFC₅ phase transitioning to vapor. eLiposomes are promising nanocarriers that can easily be triggered using US, yet the technology is still new. Hence more research is needed to optimize their use in US drug delivery.

5.2 Relevant research

In this section we summarize several recent *in vitro* and *in vivo* studies performed in acoustically enhanced chemotherapeutic delivery from liposomes.

In 2003, a study by Lin and Thomas [246] used stealth PEGylated liposomes encapsulating calcein to study the effect of sonication at 20-kHz US (LFUS), on drug release. The reported results showed an increase in calcein release which was attributed to the echogenic nature of the PEGylated liposomes, whereby US enhances the permeability of the nanovehicles.

A year later, a method was described to prepare AALs, and their hydrophilic encapsulation capacity and their sensitivity to US were investigated [40]. Release was achieved using 1-MHz US at 2 W/cm² for 10 s, and the authors concluded that this was a promising DDS.

Yuh and co-workers [247] conducted an *in vivo* study using pulsed-HIFU in a mice model inoculated with SCC7, a murine squamous cell carcinoma cell line. A group of mice were treated with liposome-encapsulated Dox alone, while another group was treated with same formulation in conjunction with pulsed HIFU. The results showed

that the mean Dox concentration in the tumors treated with HIFU was 124% higher than when the mice did not receive US treatment, supporting the possible effectiveness of this DDS in cancer treatment.

In 2007, a study examined the effect of pulsed-HIFU on low-TSL and Dox release was monitored *in vitro* and *in vivo* [248]. *In vitro* results showed a triggered 50% release of Dox from the low-TSL, but not from regular (non-temperature sensitive) liposomes. *In vivo* studies using a murine adenocarcinoma model, showed that the combination of the TSL with noninvasive and nondestructive pulsed-HIFU resulted in a rapid release of Dox and was correlated with a significant reduction in the tumor growth rate.

In the same year, Schroeder and co-workers [249] published the results of a study that involved LFUS and sterically-stabilized liposomes (SSL) to control the release of different payloads of drugs from three different liposomal formulations, with a similar size. The three types of liposomes were exposed to a short period of LFUS after which around 80% of their contents were released. The release amount was a function of the US amplitude and exposure time, and it was attributed to the formation of transient pores on the surface of the liposomes through which the drug was allowed to diffuse.

In 2009, the same group reported the results of an *in vivo* study that inspected the possibility of controlling drug release of cisplatin from nano-SSL (nSSL) using LFUS in mice-bearing murine lymphoma tumors [250]. The results showed that the group treated with nSSL and LFUS had superior therapeutic results compared to the groups where free cisplatin with or without LFUS were used, or when the tumor was treated with liposomes containing cisplatin without the use of LFUS. Additionally, the same study reported that the therapeutic efficiency of cisplatin was increased when the LFUS was used to induce the localized release of the liposomal drug in C26 colon adenocarcinomas developed in the footpad of BALB/c mice.

On the other hand, in 2010 a study was published on the use of 1.1-MHz HIFU to trigger the release of fluorescent materials (FITC) from liposomes ranging in size from 150 to 200 nm in diameter [220]. The results showed that a release of 21.2% was achieved after 10s and around a 70% release was observed after 60s of exposure to continuous wave US. Transmission electron microscopy showed that the large

liposomes (> 100 nm) were ruptured, while smaller ones (< 100 nm) showed pores in their membrane.

In 2011, the group of Pitt *et al.* [251] published the preliminary results achieved when combining the use of liposomes loaded with therapeutic drug and low frequency/low intensity US on tumors. The *in vivo* study used BDIX rats inoculated with rat colonic carcinoma DHD/K12 cells. The tumors were treated with Dox-loaded liposomes subjected to 20-kHz US for 15 minutes. The treatment was continued for 4 weeks. The results showed a statistically significant drug efficacy when the animals were subjected to US waves compared to the control case which involved the treatment of the rats with the same liposomes but without insonation.

In 2013, another *in vivo* study examined the use of liposomes synthesized using DOPE in treating mice inoculated with human prostate tumor cells (22Rv1). The tumor site was sonicated with a 1.1 MHz US wave. The results showed an enhancement in the release and the cellular uptake from these novel DOPE carriers compared to liposomes synthesized using hydrogenated soy phosphatidylcholine (HSPC) [252].

A recent study by Ninomiya and co-workers [253], presented a DDS consisting of liposomes modified with poly(NIPMAM-co-NIPAM), a temperature sensitive polymer, exposed to 1-MHz US with a power density of 0.5 W/cm². After 120 seconds, the release of encapsulated calcein was observed. A similar release was detected when the liposomes were incubated at 42 °C for 15 minutes. The study also involved *in vitro* experiments with the liver carcinoma cell line HepG2, using the same liposomes loaded with Dox. The cells were sonicated with 1- MHz US, 0.5 W/cm² for 30 sec, and 6 h after the exposure the cell viability was 60%, significantly lower than in any of the controls (Dox thermosensitive liposomes with no US, Dox-loaded regular liposomes).

Rizzitelli and co-workers [254] also used pulsed high-frequency 3-MHz US, but it was non-focused, to develop an MRI-guided protocol to observe the release of a paramagnetic agent from liposomes. The protocol was validated *in vivo* on mice inoculated with a B16 melanoma cell line, and it was observed that after 2 min insonation the MRI signal was enhanced by 35%, confirming the release of the encapsulated paramagnetic molecule.

Further research and *in vivo* experiments were conducted and almost all results were positive and showed the effectiveness of combining US with drug carriers. By

doing so, the side effects of the therapeutic agents are extensively avoided while the efficiency of the treatment is enhanced.

It is worth mentioning that, from the review done in this work, it was noticed that LFUS has an advantage over HFUS in terms of rate of release from normal liposomes and TSLs especially for *in vivo* applications. This is explained by the physics of US. As the frequency increases, the absorption rate of the energy increases which presents a challenge if HFUS is to be used to cause release from deep sites in the body. Consequently, to penetrate deeper into the body at high frequencies, the intensity has to be increased to levels that might be damaging to the human body. The next section reviews the advantages and the disadvantages of the different types of US in DDSs.

5.3. Advantages and shortcomings of US as a trigger in DDSs

The main goal of the trigger in a DDS is to be able to reach the tumor site regardless of its location in the body while being as localized as possible. As described earlier, US used in triggering drug release can be of a low or high frequency nature, and both have advantages and disadvantages.

An important advantage of LFUS is its higher penetration ability compared to that of US at higher frequencies. This penetration ability is a derivative of the absorption constant of the medium at different frequencies and is usually referred to as the skin depth, which can be calculated using equation (2), which shows an inverse relation between the penetration depth and the frequency. Hence, as the frequency increases, the penetration depth decreases. Furthermore, most of the echogenic liposomes were shown to be more sensitive to LFUS as the waves have the ability to produce much more energy compared to higher frequency. Also, at lower frequencies, there is a higher chance of interaction between US and available microbubbles. This is because most of those bubbles have diameters in the range of micrometers which is very close to the wavelength of the US wave at lower ranges of frequencies. On the other hand, high frequencies of US are easily focused either using a lens-like structure or by simply designing a focused probe. This helps in the treatment of cancer using DDS as the insonation is required to be localized.

However, according to the literature, US can actually induce cell death as its intensity increases. For example, Wang and co-workers [255] studied the bioeffects of increasing intensities of 1.1-MHz US on the myelogenous leukemia cell line K562. It

was observed that at intensities of 1 and 2.1 W/cm², cell death increased to around 14 % and 40.7 %, respectively. The aim of the study was to find the intensity at which US will induce cell death, and it could be concluded that US can indeed cause harm to human healthy tissues. Furthermore, HIFU has been recently used as a radiation therapy against prostate cancer; nonetheless, it was shown to be associated with some side effects such as urine leakage and possible infections in the prostate area [256].

The literature reports several studies that utilized US to increase the local tissue temperature and kill cells via hyperthermia. However, the human body is not a smooth structure. It is composed of layers, solid structures and fluids, which complicates therapeutic procedures. Fluids are usually filled with gas bubbles through which US propagation, and hence penetration is restricted. The case is the same with solid tumors. This non-smooth nature of human tissue presents a challenge when a certain depth is to be heated to a certain temperature. Reflections, attenuation and absorption occur in order to heat the tissues at a certain depth, US intensity is sometimes increased to overcome any obstacles, and this may lead to over-heating the more superficial tissues. For example, Hayes and co-workers [257] observed that 3- MHz US can heat 0.5 cm deeper in the tissue than previously reported, which supports the inaccuracies that might happen when dealing with US.

Until recently, US was thought to be harmless to human tissues, but in the last few years, more incidents of unwanted side effects have been reported. For example, in 2006, an article published in *Midwifery Today* [258], discussed the possibility that US imaging during pregnancy may actually affect embryo development, due to hyperthermia. A study by Ang and co-workers reported in *PNAS* [259] showed that neural migration in mice embryos is affected by exposure to US waves.

These examples, definitely call for further research to make sure that the ultrasonic parameters (including frequency, power intensity and pulse length) used are harmless to healthy tissue.

5.4. Liposomes and ultrasound: clinical uses

Many liposomal drugs have been approved for clinical use, and several others are undergoing clinical trials. However, to the best of our knowledge, no clinical trials are being conducted to test the combined effects of liposomes and US in cancer chemotherapy, yet. A phase II clinical trial named *MRI Guided High Intensity Focused*

Ultrasound (HIFU) and ThermoDox for Palliation of Painful Bone Metastases, has finished recruiting participants but has not yet begun (<http://clinicaltrials.gov/ct2/show/study/NCT01640847>).

The aim of the study is to evaluate whether the combination of HIFU with ThermoDox® (Dox encapsulated in lysolipid thermosensitive liposomes) can effectively and safely reduce the pain of patients with bone metastases. Another study conducted at the University of Oxford aims at studying the targeted delivery of ThermoDox® by mild hyperthermia induced by HIFU, in patients with liver metastases from lung, breast or colorectal primary tumors (<https://clinicaltrials.gov/ct2/show/NCT02181075>). This trial is currently recruiting participants.

Some examples of liposomal-based drugs used for cancer therapy that have been approved for clinical use or are undergoing clinical trials will now be discussed.

The first liposomal formulation that was approved for clinical use in Europe in 1990 (and in 1997, in the USA) was AmBisome [239, 260, 261]. One of the best known liposomal formulations that was FDA-approved in 1995, for the treatment of Kaposi's sarcoma found in AIDS victims, is Doxil/Caelyx [239, 260, 261]. Doxil consists of PEG-stabilized liposome-encapsulated Dox and is currently used for the treatment of patients with progressing ovarian cancer and patients with multiple myeloma [260, 262, 263]. Several other liposomal formulations were approved for clinical use, such as DaunoXome (liposome-encapsulated daunorubicin, used for the treatment of Kaposi's sarcoma, FDA-approved in 1996), Myocet (non-PEGylated liposome-encapsulated Dox, used for the treatment of breast cancer, approved in 2000 in Europe and Canada, and undergoing clinical trials in the USA), and DepoCyt (liposome-encapsulated cytosine arabinoside, used for the treatment of lymphoma complications, FDA-approved in 1999) [264]. More recently, the FDA also approved a drug called Marqibo (vincristine sulfate liposome injection) to treat patients with a rare type of lymphoblastic leukemia [262]. The first commercially available liposomal formulation of paclitaxel, called Lipusu®, has been approved in China for the treatment of ovarian, breast, gastric and head and neck cancers [265].

Several liposomal formulations are currently undergoing clinical trials in the USA, for example: Onco-TCS, liposomal cytarabine, for the treatment of non-Hodgkin lymphoma (phase I/II trial); SPI-77, stealth liposomal cisplatin, for the treatment of

head and neck, and lung cancers (phase III trials); and Lipoplatin, liposomal cisplatin, for the treatment of pancreatic, head and neck, and breast cancers (phase III trials) [264]. Paclitaxel formulations undergoing clinical trials have recently been reviewed by Koudelka and Turanek [265] and Nehate *et al.* [266]. Babu and co-workers recently reviewed the state of ongoing or completed clinical trials using liposomal formulations [262]. Comprehensive information about clinical trials can be retrieved from the US National Institutes of Health website (<http://clinicaltrials.gov/>).

CHAPTER 6: Experimental Work

6.1. Experimental Setup

In this work, the knowledge developed after doing an intensive literature survey on the topic of drug delivery is used to set up an experimental procedure to test newly developed liposomal carriers against US with different intensities and frequencies. As discussed, a drug delivery system is composed of two main parts: the carrier and the triggering means. The final objective of the whole project is to design liposomes that are actively targeted and triggered. Those liposomes should be capable of circulating in the body for a long period and accumulate at the targeted site through passive means such as the enhanced permeation and retention effect (EPR). Then, once the liposomes are close to the tumor cells, the active targeting stage starts where in the liposomes are modified with ligands that can successfully bind to cancer cells while avoiding binding to healthy cells. Once bounded to a cancer cell, the liposomes are then transported into the cell across the cell membrane through the process of endocytosis. After ensuring that almost all the liposomes are inside the tumor cells and only a few are still in the blood stream, the triggering stage with the aid of ultrasound is initiated. This system is described in Figure 21.

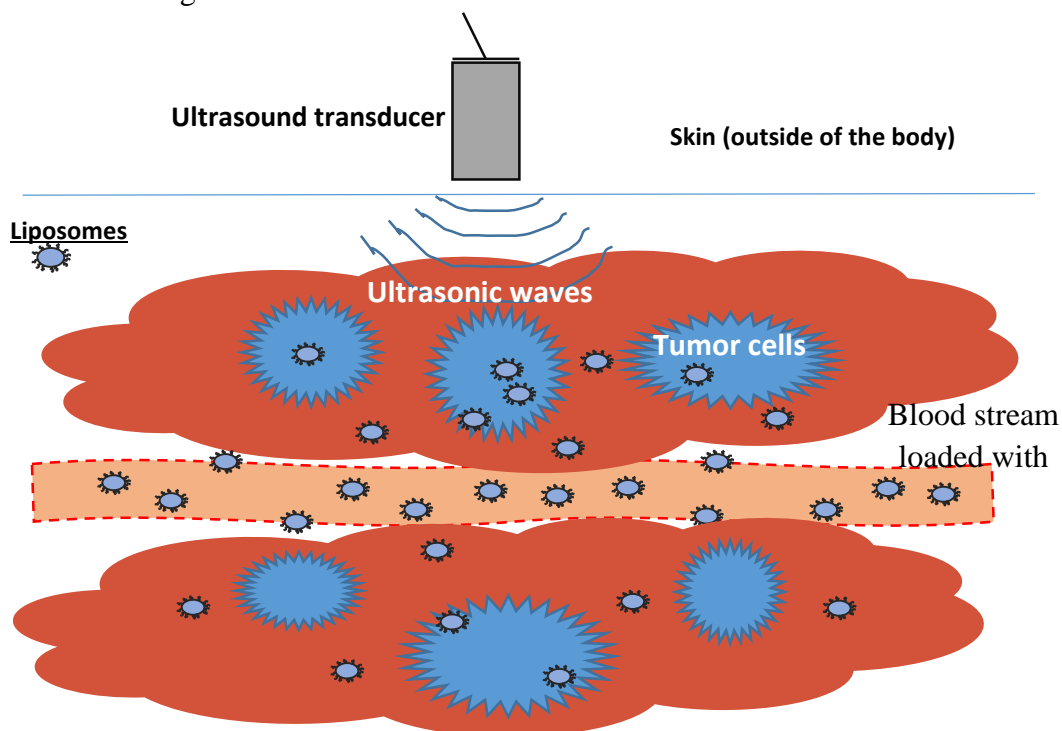


Figure 21. Complete drug delivery system explaining the objective of this work.

However, the objective of this thesis is to design a system that involves stabilized stealth liposomes loaded with the model drug calcein the release of which is to be induced using high frequency focused ultrasound in *in vitro* experiments. This is considered a step towards the final objective of the whole project. Ultrasound used for triggering drug release from liposomes can be of high or low frequency. Low frequency US is known to be effective in triggering the release; however, it is hardly focused, hence there is a need to test the possibility of using higher frequencies, easily focused, to function as the trigger. The following results includes drug release experiments done using 1 and 3 MHz focused US waves; however, due to equipment restrictions, the experiments had to be done in offline mode. The results also include experiments done using a 20 kHz US probe which can be used to conduct online experiments. The results serve as proof of the effectiveness of low frequency ultrasound in inducing release from acoustically activated liposomes in comparison with high frequency US. Furthermore, the results of the online experiments are also used for the next part of the thesis; the modeling and control part discussed in Chapters 7 and 8.

6.2. Expected results based on literature

Positive results are expected when using the 20 kHz frequency ultrasound to trigger drug release. It is expected that almost all the loaded drug should be released when using this frequency at low intensities and the rate of release shall increase as the intensity increases. According to the literature, low frequency ultrasound is expected to cause transient cavitation which is known to cause release from liposomes. However, since the chemical formulation of the liposomes used in this experiment is a bit different from the liposomes found in the literature, a release is expected but the percent release should be investigated and compared with the literature.

As for the higher frequency acoustic waves, according to the literature, no release is expected if low intensities are used with normal liposomes. The only documented release from similar liposomes happened when high intensity focused ultrasound (HIFU) was used. Hence, in this work, a HIFU transducer from Precision Acoustics is used to generate similar intensities as mentioned in the literature which are in the order of a few tens of Watts/cm². Nonetheless, the transducer can also deliver lower intensities which will allow for testing the liposomes at a wide range of power densities. The release, if any, that happens when using this range of frequencies is

postulated to be due to either hyperthermia or colloidal reasons, since the high frequency ultrasound, as discussed earlier, has a very low probability of inducing transient cavitation. Also, the pressure change expansion mechanism is not possible as the liposomes used do not contain the nano-emulsions required for it to happen. Furthermore, when HIFU is used, hyperthermia may be inevitable as high amounts of energy will be absorbed and converted into heat which makes it a possible reason for release. Yet, the liposomes used are not of the TSL type which, although hyperthermia is induced, may not cause the liposomes to release. The last option is the colloidal action that may occur when using high frequency ultrasound. The liposomes may be driven harshly into colliding with other liposomes or the sides of the cuvette causing them to rupture and release their content. So the main focus will be on investigating which is the most probable reason for the release.

6.3. Methods

The first part deals with creating the liposomal carrier the synthesize procedure of which was developed by the chemical engineering team of the research group. This procedure, described below, was adapted in this work to synthesize the required liposomal samples for the in vitro experiments

6.3.1 Synthesis of PEGylated liposomes

The PEGylated liposomes used in this work were prepared using the amphiphilic PEG derivative DOPE(1,2-dioleoyl-*sn*-glycero-3-phosphoethanolamine)-PEG-pNP, a group that allows the subsequent attachment of protein ligands to the liposomes. The first step in the procedure was the synthesis of (*para*-nitrophenylcarbonyl-PEG-(*para*-nitrophenylcarbonyl) (pNP-PEG-pNP), by reacting PEG with two molar equivalents of 4-nitrophenyl chloroformate (p-NPC) in the presence of dichloromethane and pyridine [267]. DOPE-PEG-pNP was synthesized by reacting the previously synthesized PEG-(pNP)₂ with one molar equivalent of 1,2-dioleoyl-*sn*-glycero-3-phosphoethanolamine (DOPE, Avanti Polar Lipids, Inc., Alabaster, AL, USA) in dry chloroform in the presence of triethylamine (TEA), in a protocol modified from that of Torchilin and co-workers. [268] The pNP-PEG-pNP was dissolved in 32.2 μmol of DOPE in chloroform, in a round bottom flask, followed by the addition of 80 μl of pure TEA (99% concentration), and 5 ml chloroform. The

mixture was incubated overnight at room temperature, with stirring, under an argon atmosphere. The chloroform was then removed in a rotary evaporator, and 2 ml of a 0.01 M HCl-0.15 M NaCl were added to hydrate the lipid residue. The solution was sonicated in a 40 kHz sonicating bath (Elma D-78224, Melrose Park, IL, USA), at full power for 10 min and the micelles were separated from the unbound PEG and released pNP, using Sephadex G-25 PD-10 desalting columns (GE Healthcare Life Sciences). The solution was evaporated in a rotary evaporator at high speeds under a vacuum for 2 h, and the DOPE-PEG-pNP was extracted 4 times with chloroform. The salt residues were precipitated on ice and removed by centrifugation and the DOPE-PEG-pNP was stored at -20°C as a chloroform solution, with a concentration of 8.4 mM.

The PEGylated liposomes were then prepared by reacting the DOPE-PEG-pNP with 1,2-dipalmitoyl-*sn*-glycero-3-phosphocholine (DPPC, Avanti Polar Lipids, Inc., Alabaster, AL, USA) and cholesterol (AlfaAesar, Ward Hill, MA, USA), using a molar ratio of 68:30:2 DPPC-Chol-(DOPE-PEG-pNP). The DOPE-PEG-pNP attaches to the liposome via its phospholipid residue and, as mentioned, the water-exposed pNP group can be used in a reaction to bind a variety of amino group-containing ligands and form stable and non-toxic bonds, making them a convenient tool for protein attachment to the distal ends of liposome-grafted PEG chains. [268] The liposomes were prepared by the lipid film hydration method. Upon evaporation of chloroform, the film was hydrated with a solution of calcein at a self-quenching concentration (~30 mM), with the pH adjusted to 5.2. The resulting solution was sonicated at 40 kHz at full power for 15 min, and extruded three times (10-times each) through 0.2 µm polycarbonate filters using the Avanti® mini-extruder (Avanti Polar Lipids, Inc., Alabaster, AL, USA). Afterwards the liposomes were resuspended in the buffer to be used in the release assays, and cleaned using Sephadex G-25 PD-10 desalting columns (GE Healthcare Life Sciences, Pittsburgh, PA, USA). The liposome solution was stored at 4°C until use.

6.3.2. Experimental procedure and result for the high frequency offline experiments

The sample is first diluted in a glass beaker which is fitted inside a cold water bath to control the temperature of the sample during the offline sonication. The beaker is placed such that its bottom is sufficiently immersed to cover the whole sample. Then, an aliquot of the diluted sample is placed into a cuvette that is placed in the fluorometer to measure the initial fluorescence (baseline, F_0) which corresponds to the amount of

calcein that failed to be encapsulated by any of the liposomes during the synthesis process. In electrical terms, this free calcein acts like a DC offset that has to be removed. Therefore, the measured fluorescence level at this setting will act as the baseline for later measurements. The fluorescence level is measured using a QuantaMaster 30 Fluorescence Spectrofluorometer (Photon Technology International, Birmingham, NJ, USA), where excitation and emission wavelengths are set at 494 nm and 515 nm respectively. The baseline serves as a normalization factor by which drug release is converted into percent release using equation (46). The baseline recording length is 20 seconds at a sampling frequency of 20 samples/seconds, and the average of these data points is set as (F_0). The aliquot is then returned to the sample so as to be sonicated.

$$\% \text{ Drug release} = \frac{F_t - F_0}{F_{max} - F_0} \times 100 \quad (46)$$

The next part of the experiment deals with inducing a release. The main technique that was used to trigger a drug release is through using ultrasonic waves at different frequencies and intensities directed towards the tumor site. Triggering is done using two frequencies: 1 and 3 MHz. Once a release is induced using either of the frequencies from the liposomes, the fluorescence level is measured again. If it increases, this indicates that the amount of free calcein increased which means that some of the liposomes were induced to release some of their content. After that, a detergent called titron x100 is added to the liposomal solution. This detergent has the ability of shattering the membrane of any healthy liposomes left in the solution which ensures that all the calcein is now released. The fluorescence level is measured again and this level serves as the 100% release.

The ultrasonic probe used to sonicate the samples at 1 MHz (with 5 different power densities) and 3 MHz (with 6 different power densities) was designed to specifications at American University of Sharjah (AUS), Sharjah, UAE and manufactured by (Precision Acoustics, Dorchester, UK). The probe is connected to an AC amplifier (High Voltage Amplifier WMA – 300, Falco Systems, Amsterdam, The Netherlands) which takes its input voltage from a function generator (AFG 310, Tektronix, Beaverton, OR, USA). The probe is fitted just below the surface of the water in the bath and aligned. The complete setup is shown in Figure 22.

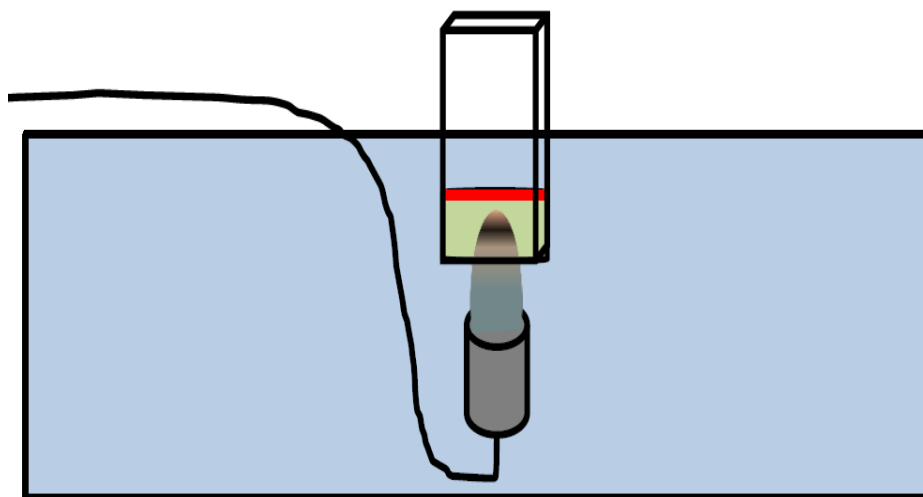


Figure 22. Experimental setup for sonication of the liposomes from down below

The sonication is then done in a continuous (continuous wave –CW) mood for a total sonication time of 60 min divided into 4 periods of 15 minutes each. After each sonication interval, the new fluorescence level (F_t) of an aliquot is measured and the aliquot is returned to the glass beaker to commence with the next sonication interval. At the end of the 60 min, 2% (w/v) Tx100 is added to the sample to lyse any remaining liposomes as described previously, and the percent release is calculated as described previously. A sample of the results collected is shown in Figure 23.

As can be seen from the sample results presented in figure 23, release is indeed induced and increases as the time of insonation increases. Hence, the experiment is a success and is repeated for confirmation and consistency. The experiment is repeated three times for each intensity and the average drug release is calculated then the release curve for each frequency at the different intensities is plotted as shown in Figure 24. Error bars for each measurement are also included in the graphs. The X-axis is the time and the Y-axis is the release in terms of percentage.

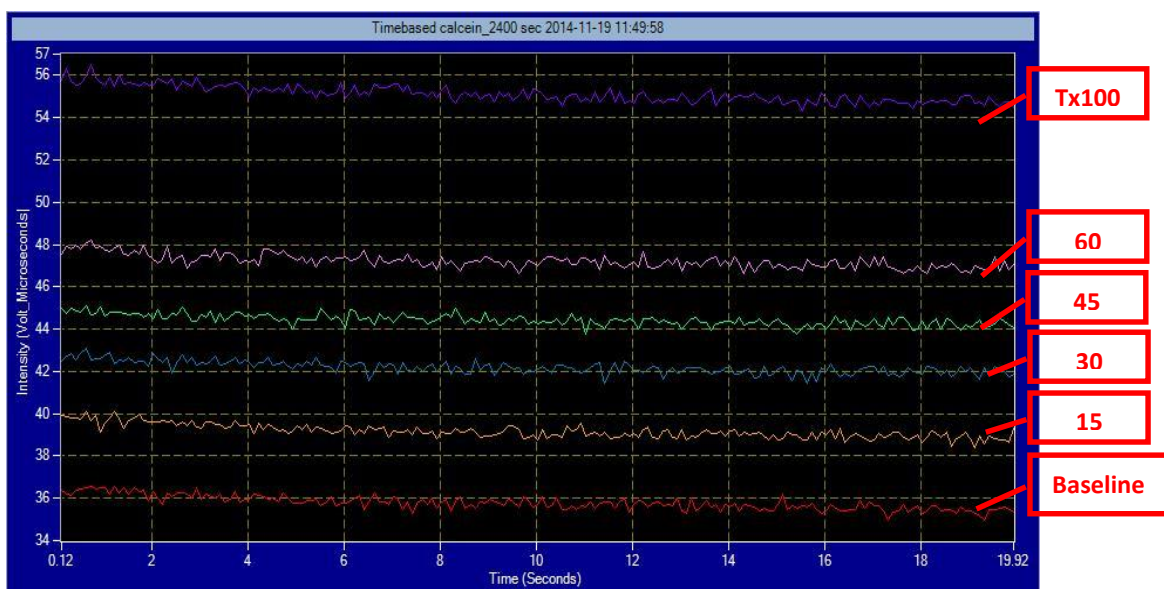


Figure 23. Sample results showing the fluorescence level against offline sonication for a period of 1 hour divided into 4 equal portions of 15 minutes each.

Table 5. Tabulated results of the sample given in Figure 23

Time	Average Fluorescence level
Baseline	36.08
15 minutes of sonication	39.24
30 minutes of sonication	42.13
45 minutes of sonication	44.39
60 minutes of sonication	47.43
Tx100 added	54.87

- % release = $\frac{\text{current release} - \text{baseline}}{\text{Tx100 release} - \text{baseline}} * 100$
 - For the 15 minutes: $\frac{39.24 - 36.08}{54.87 - 36.08} * 100 = 16.82\%$
 - For the 30 minutes: $\frac{42.13 - 36.08}{54.87 - 36.08} * 100 = 32.20\%$
 - For the 45 minutes: $\frac{44.39 - 36.08}{54.87 - 36.08} * 100 = 44.22\%$
 - For the 60 minutes: $\frac{47.43 - 36.08}{54.87 - 36.08} * 100 = 60.40\%$

Figure 24 clearly shows the non-linear, though proportional relation between the sonication intensity at 1 MHz and drug release. The figure shows the relation between the percent release and the power densities (10.5, 18.7, 27.6, 39.2 and 50.2 W/cm²). The results obtained at this frequency also show that as the power density increases, the rate of release as well as the amount of the encapsulated drug released increases. It is also observed that even with the slightest increase in power density, the release curve changes. The maximum release achieved after 60 min of sonication at 1 MHz was approximately 57%, when the highest power density was used (50.2 W/cm²). The differences in percentage release for the different power densities are significantly different for each time point where the Ttest showed that $p < 0.05$.

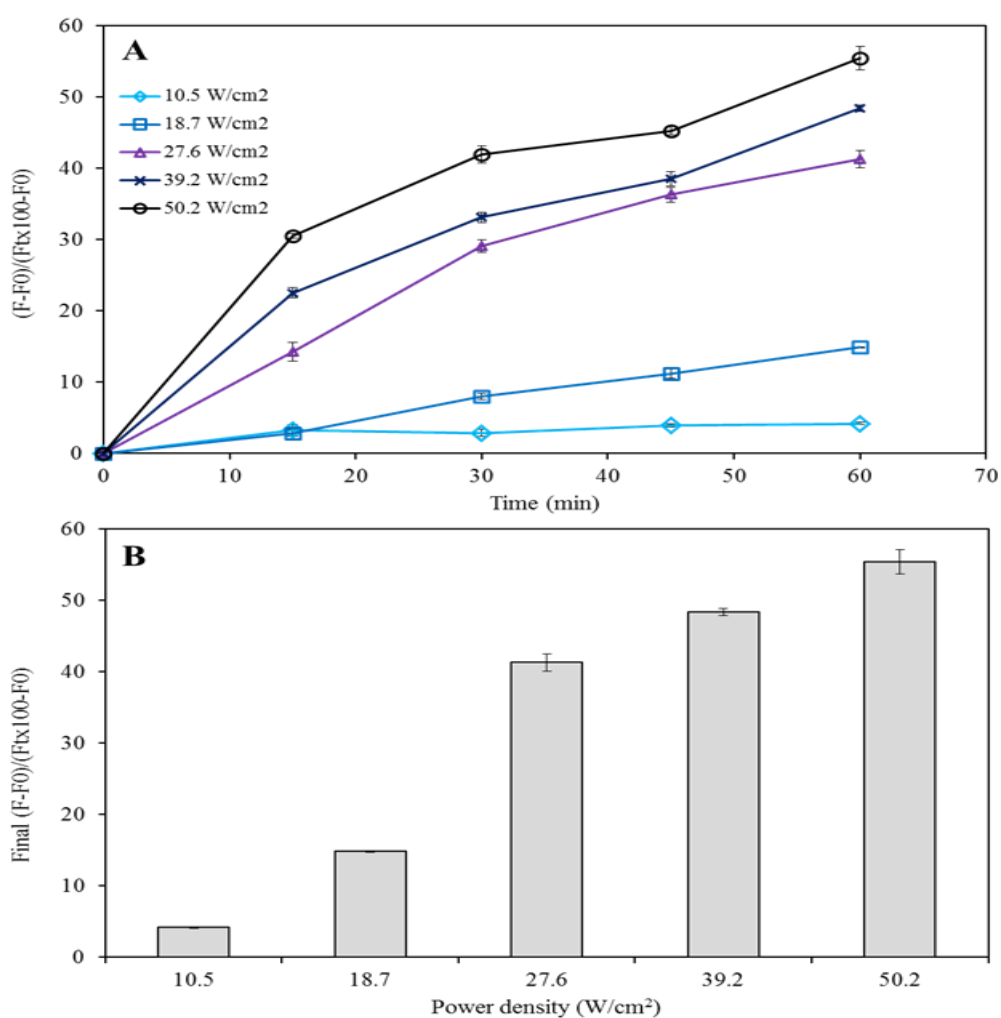


Figure 24. Calcein release kinetics from PEGylated liposomes at pH 7.4 using 1-MHz US. (A) Calcein release curves at different power (B) Final release (after 60 min insonation) as a function of power density.

Figure 25 shows the effect of increasing the power density on the rate of release at 3 MHz HFUS. Six different power densities, 50.6, 78.5, 94.3, 158.5, 173.3 and 183.0 W/cm², were used. The results showed a direct relation between intensity and percentage release for all power densities except for 158.5 and 173.3 W/cm², as there was a clear overlap between the two graphs. Otherwise, the results show a significant difference in drug release for the whole time of insonation at different intensities. The highest percentage release achieved using 3 MHz was around 68%, obtained at 183.0 W/cm².

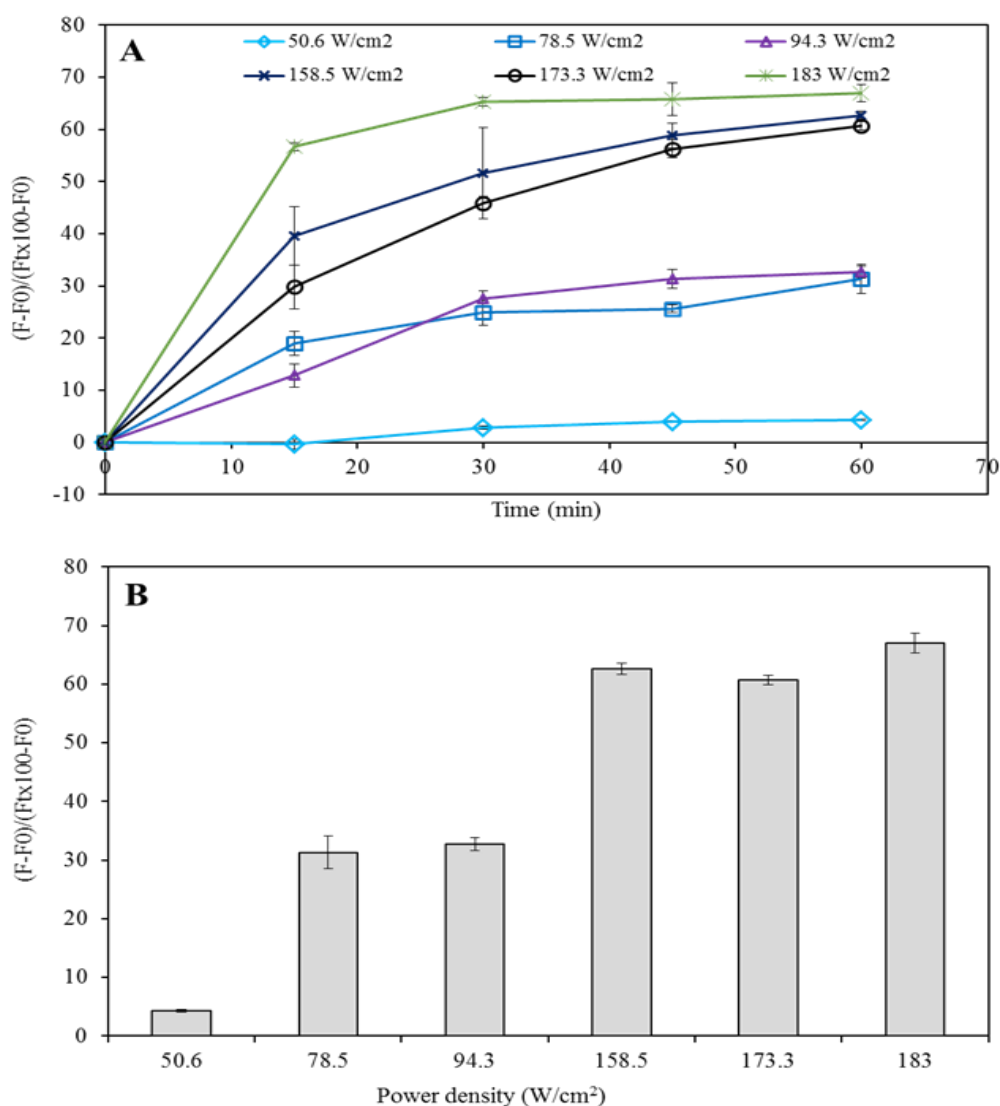


Figure 25. Calcein release kinetics from PEGylated liposomes at pH 7.4 using 3-MHz US. (A) Calcein release curves at different power densities; (B) Final release (after 60 min insonation) as a function of power density.

Nevertheless, when comparing the results obtained at 1 and 3 MHz HFUS, it was observed that a higher percentage release was obtained using the 3 MHz as the

power densities used at this frequency were significantly higher than the ones used for the 1 MHz experiments. That is, the 3 MHz probe yields intensities as high as 183 W/cm², whereas the highest intensity for the 1 MHz was 50.2 W/cm² (which is only comparable to the lowest intensity used at the 3 MHz HFUS). It can also be observed that the level of release obtained at 1 MHz for a certain power density, can only be obtained at 3 MHz when using a higher power intensity. As an example, the lowest percentage release obtained at 1 MHz was 4.18±0.15%, very similar to the one obtained at 3 MHz, 4.32±0.16%. However, the power density used at 1 MHz was about ten times lower than that at 3 MHz, 50.6 versus 10.5 W/cm². However, when comparing the results achieved at similar intensities, for example the highest power of the 1 MHz (50.2 W/cm²) and the lowest power of the 3 MHz (10.5 W/cm²), it is obvious that the maximum release was obtained when the lower US frequency was used (1 MHz). The difference is quite obvious (55.43±1.66% at 1 MHz compared to 4.34±0.16%, at 3 MHz), which highlights the advantage and effectivity of lower US frequencies as a means of inducing drug release. Therefore, higher release would be expected if higher power densities were used at the 1 MHz experiment.

6.3.3. Experimental procedure for the low frequency online experiments

The same initial procedure was used to prepare the liposomal sample, but instead of using an external insonation setup, the sample was loaded into a plastic cuvette which fits into the fluorometer and sonication was done directly from an opening in the top cover of the meter. The experiment here is done in a continuous online mode where the US was applied as the fluorescence level was being measured. For the first 60 seconds, US was kept off. During this period, the fluorescence level was being measured to serve as the baseline for the experiment. Then, ultrasound was turned on manually where it started to sonicate continuously for a period of a few seconds, then switched off for another few seconds. Then it repeats the on-off period until the maximum level of fluorescence is reached which is indicated by a plateau for at least 2 cycles. Figure 26 shows a sample of the online release curve. This experiment was done for different intensities and different on-off cycles to examine the effect of those two parameters on the general release trend.

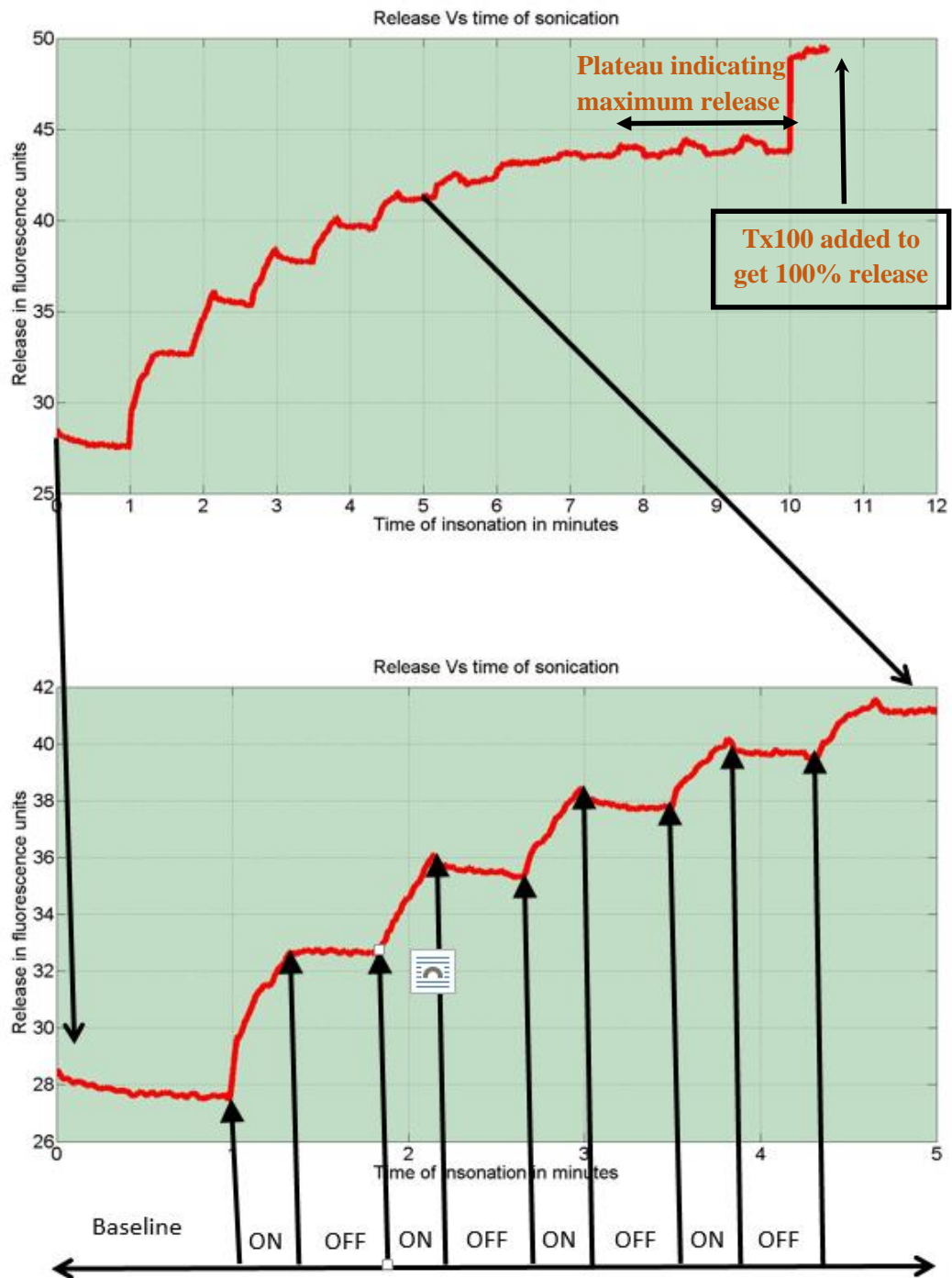


Figure 26. Calcein release curve versus time of sonication. Curve A shows a complete release curve with the addition of TX-100. Curve B shows a zoomed in version of the release curve for the first 5 minutes.

As can be seen from Figure 26, as the periodic sonication starts, the fluorescence level increases indicating drug release. For the period of the on cycle, the fluorescence increases, yet once the off cycle starts, the level stabilizes. This indicates that US is the main reason for the release from liposomes and once it is not available, no release occurs. Then, after a period of time, depending on the sonication intensity, the

fluorescence level plateaus for a few sonication cycles. This indicates that the US is no longer capable of inducing any further release from the liposomes. Therefore, the sonication is terminated and Tx100 is added to make sure any remaining liposomes are lysed and 100% of the loaded drug is released. For the specific example at hand, the sonication intensity was 30 % of the maximum amplitude equivalent to 11.83 W/cm². The sonication was done in 20 seconds on 30 seconds off cycles. The sonication was carried out until the plateaus took place which was after about 7 minutes of sonication. The sonication was kept for another 3 minutes to ensure there was no change in the fluorescence level. After the 10 minutes mark, sonication was terminated, Tx-100 was added, and the final fluorescence level was recorded. The results indicate that the baseline was around 27.84 units, the plateau was at around 44.56 units and the Tx-100 release was around 49.64 units. Hence, the percent release was 76.7 % after 10 minutes of sonication.

Results from other experiments showed behavior consistent with the sample shown in Figure 26. Differences were significant when intensity was changed especially in the time needed to reach the plateau stage and slight differences were noticed in the maximum release achieved. For example, Figure 27 shows another sample where an amplitude of 20 %, equivalent to 6.08 W/cm² was used in a 10 seconds on 10 seconds off cycles. As can be seen, it took 13 minutes of sonication at those settings to reach the plateau and 20 minutes to complete the whole experiment. The baseline was around 26.12 units, plateaued at 41.48 units, and Tx100 release was around 46.79 units. The first thing to notice is the consistency, as the baseline and the Tx100 release for the given two sample results are almost the same. Furthermore, the percent release for this case was around 74.31 % which is close to that of the first sample results. So, it can be concluded that the effect of lowering the sonication intensity is clear on the release rate and the time needed to reach maximum release.

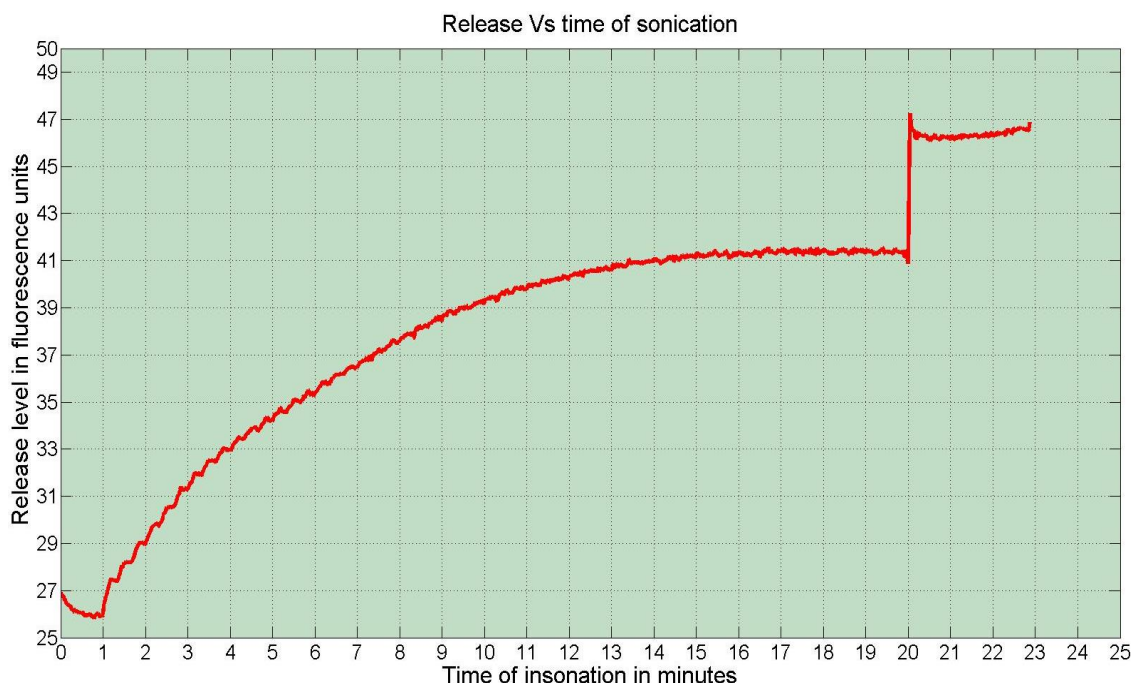


Figure 27. Calcein release curve when using ultrasound on/off cycle of 10/10 seconds.

6.3.4. Comparison between low and high frequency ultrasound as a triggering modality

Over all, both high and low frequency US proved to cause release from the synthesized liposomes; however, the differences are noticeable. When high frequency US was used, very high power densities were required to cause release, contrary to the case when 20 kHz was used. For example, in the case of the 1 MHz, the lowest intensity (10.5 W/cm^2) resulted in around 5 % release after 1 full hour of sonication, while an intensity of 11.83 W/cm^2 for the 20 kHz was able to reach 77% release after only 10 minutes of sonication. Hence, the higher the US frequency used, the higher the power densities needed to cause acceptable levels of release.

Another shortcoming of high frequency US is the long period of sonication needed. In the case of the 1 MHz, even after 60 minutes of sonication at all the intensities used, no clear plateau was reached. On the other hand, for the case of the 3 MHz, only the highest intensity used showed a clear plateau after 30 minutes while others did not even after 60 minutes of sonication. Furthermore, it was noticed that, unlike the case of low frequency, not all intensities for the high frequency converged to the same maximum release. Some of the power densities were not enough to cause much damage, while others were harsh on the liposomes leading to a somewhat fast release rate.

All in all, the results are in agreement with the fact that the release decreases as the US frequency increases (taking the intensity into consideration).[24, 269] As the frequency decreases, so does collapse cavitation, and thus, the mechanical index (MI; the peak negative pressure of the US wave divided by the square root of the centre frequency of the wave) increases, which leads to an increase in the rate of release (taking the intensity in consideration) [270]. It is clear from the sample results provided that using lower frequency US is better in terms of the time and power density needed to reach maximum release; also, between the 1 and 3 MHz US, the 1 MHz showed better results regarding that fact.

CHAPTER 7: Modeling and Control

So far in this thesis, the discussion was focused on the idea of synthesizing a liposomal carrier that is triggered using US and testing it against US of different frequencies and intensities. In this chapter and the one after however, the discussion will be shifted towards an application in which the experimental data can be used. This application is to develop a system in which drug release can be controlled automatically such that the output follows a desired target. To do this, a literature review on modeling and control is presented in this chapter and in the next chapter, the results of the control system are listed.

As was seen from the low frequency real time *in vitro* experiments, when the liposomes are sonicated, they release their content gradually following certain dynamics behavior. Using some modeling techniques, this behavior can be captured as a model that can be used to predict the drug release for a wider range of US frequencies, intensities, and drug concentrations. Such models can eliminate the need for further lab work to determine the behavior at any new operating conditions. In this thesis, the modeling technique of choice was an artificial neural network (ANN), the background of which is given below.

7.1. Background on Neural Networks Modeling

Neural networks is a technique developed around the middle of the 20th century thought to help scientists understand how the human nervous system functions. The idea that sensory sites distributed throughout the human body collected data and sent it to a centralized processing unit (the brain) was of a great interest and inspired many who were seeking to develop outstanding solutions to many of the everyday problems. Based on the collected data, the brain can identify a certain place, associate a certain scent with a specific perfume, classify different objects, and forecast possible events and many others. Hence, scientist tried to understand how the brain does that and the answer was it is trained based on the input data. That was the turning point at which the idea of artificial neural networks first originated in an attempt to develop mathematical processes capable of learning from input data and accordingly performing a certain activity. Soon, the applications that used ANN included system identification, pattern recognition, system control, classification and many others.

There are many types of ANNs based on their topology. ANNs can be classified into feedforward neural networks (FFNN), radial basis function network (RBFN), self-organizing network, recurrent neural network, physical neural network, and many others; nonetheless, FFNNs are the most widely used and are the topology of the network used in this work. There are two categories of FFNNs: single layer and multi-layer networks. The single layer FFNN is considered to be the simplest network of this type where there is only one output layer and the inputs are fed into it directly through a set of weights. The neurons in this output layer are referred to as linear threshold neurons as the output is either a 1 or a 0 based on the state of the neuron; 1 means the input activated the neuron, 0 means the neuron was not activated. This form of the FFNN is not very useful when dealing with complex processes. A more useful form is the multi-layer FFNN.

A multi-layer FFNN is composed of a multi-layered structure that has an input layer and an output layer with at least one intermediate layer referred to as a hidden layer. Each layer is composed of multiple neurons (weights) that are based on a certain activation function; the most widely used are tansig, logsig, pureline and Gaussian. The job of these activation functions is to give a hint to the NN about how the input data might look like. So, if the data is linear, the pureline activation function is the best one to use in terms of simplicity and performance. On the other hand, if the data is Gaussian and the activation function used is linear, the system might not be able to produce acceptable results. Some systems might have complex behavior that might not be modeled with a single activation function, therefore, more hidden layers can be added with different activation functions until the performance is satisfactory. Also, within the same hidden layer, neurons might have different activation functions as long as they enhance the performance (yet this is still not a so popular practice). So, by setting up a NN system with multiple layers, each layer should be connected to the next in away such that each neuron has at least one connection with another neuron from the next layer in a feedforward mode with no back propagated signals. An example of a simple multi-layer NN structure is given in Figure 28. In this work, there are two applications in which a FFNN is used. The first is to perform system identification and modeling and the second is to build a model predictive controller.

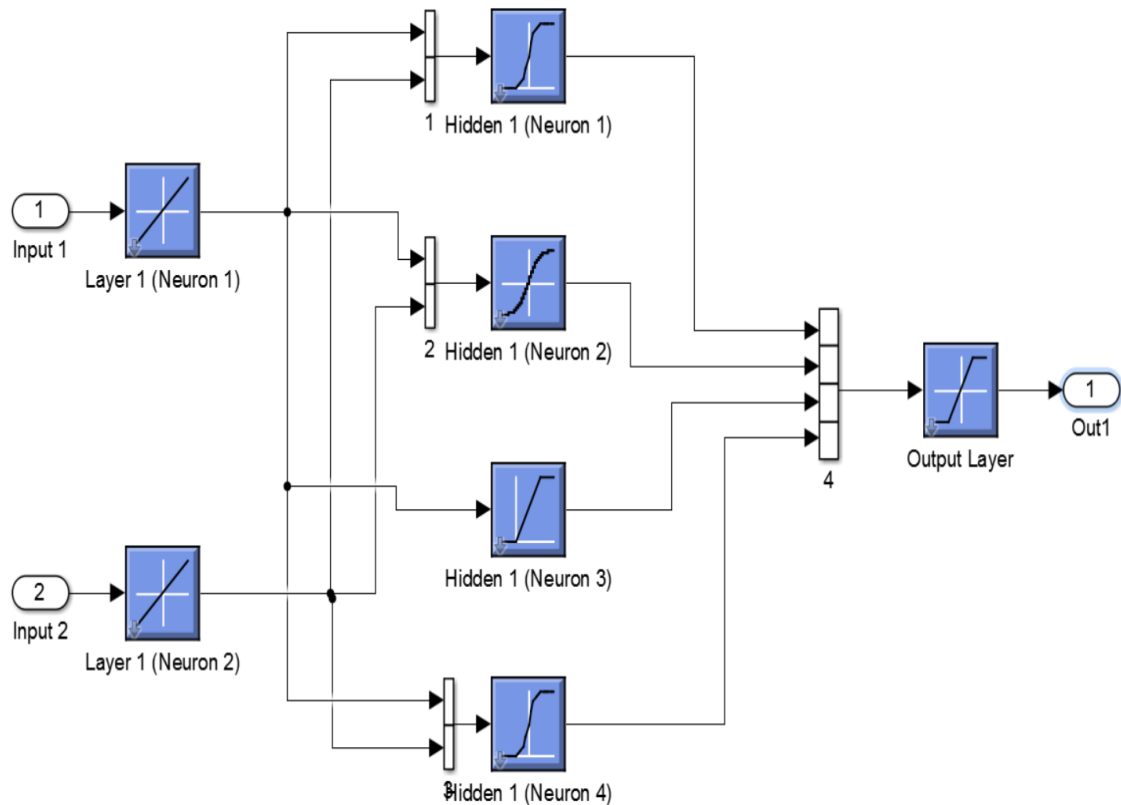


Figure 28. The structure of the simple neural network. This network has one input layer with two neurons, one output layer with one neuron and one hidden layer with 4 neurons with variable activation functions.

For the first application, the process by which an FFNN is used involves two stages. The first stage is the training stage. As is the case with any system identification, the system at hand is dealt with as a box that has input and output ports. To identify the system transfer function, the input is excited with a known input signal and the output is captured. Then by finding the output over the input equation, the transfer function of the box is identified.

The same procedure is followed when using NNs to do system identification. First, the system is excited with a known input then the corresponding output is captured. After that, the input and output data are used to train the NN. There are many methods by which the network can be trained. The most used method is based on backpropagation training. Initially, the data is divided into three sets: training, validation, and testing. The training data is first fed into the input layer of the NN. Then, based on the specified number of delays, at least 1, the output is fed back to the input layer from the output layer. While this process is running, the NN tries to adjust its neurons such that the output is similar to the intended output that was previously

captured from the actual system. This output is referred to as the targets. This process will keep going until all the training data is exhausted.

After that, the validation data is fed into the input layer of the trained network. The output due to the validation data is then compared with the corresponding targets and the error is calculated which is usually based on the mean squared error. If the error is above a specified threshold, the network is declared as usable and is then tested using the third set of data, the testing data for a final check. By this, the final tested network is considered to be equivalent to the transfer function of the real system and can be used as its model. It is worth mentioning that the more complex the system being identified, the more data needed to perform system identification using neural networks. An example of a back propagated training network is shown in Figure 29. Although, this training process might be enough for most application, a further training step called open loop training is usually utilized to assert the accuracy of the model compared to the actual system.

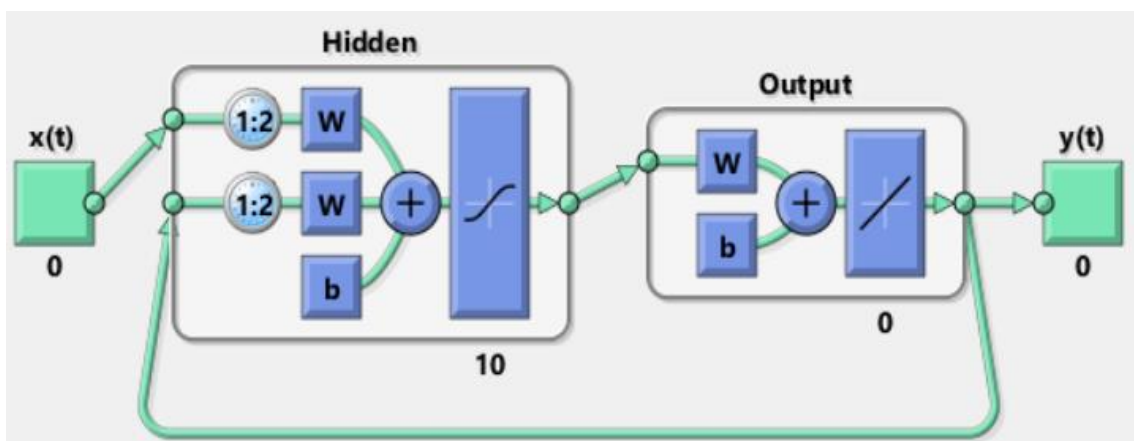


Figure 29. Back propagation training of neural networks with a delay of 2 samples.

As can be understood so far, the size of the network has to be determined before going into the training step. This is where the number of hidden layers and the number of neurons per layer are determined. Also, the type of activation functions have to be determined. All of those parameters are crucial to the network performance; hence, the structure must be optimized to best suit the input data while avoiding over fitting or under fitting. The number of layers and neurons affects the fitting of the system. If too many are used, over fitting may occur in which the performance of the network might be close to perfect for the training data while being almost useless for other data. On

the other hand, using an insufficient number of neurons might lead to under fitting which means the network performance is poor for training and testing data.

As for the second application in which FFNNs are used in this work (controller design), the same modeling procedure is used but the network is trained as a part of a whole system that has a plant model that is controlled by a predictive controller which tries to derive the output of the plant to follow a certain reference signal. This system is referred to as a model predictive controller and is introduced in the next section.

7.2. Model Predictive Controlling

As the name suggests, the controller predicts the proper movements based on a pre-loaded model. An MPC is made up of three main blocks namely: controlled plant, inverse plant model and optimizer. A schematic of a simple MPC is given in Figure 30. In essence, the way the controller works is based on feedback from the controlled plant which is compared to a reference input that the plant is supposed to follow. The controlling is done through creating an internal model which in some way can be regarded as an inverse model of the controlled plant. Hence, the output of the plant is fed back into the inverse model which then suggests the correct input that should be fed into the plant. The correction to the output of the controller is done through an optimization block which works as a match making device between the reference and the feedback signal.

First, the plant is initiated with an arbitrary input close to the starting values from the reference. Based on this input, the plant will produce an output which is fed into the inverse plant model through the feedback signal line. In the inverse model, the corresponding input will be calculated and fed into the optimizer. The optimizer however, already knows what the next input to the plant should be based on the reference given to it. However, this input is modified based on the signal coming from the inverse model to ensure the plant is following the targeted output.

For example, based on the reference, the first output to the plant should be 2 volts such that the plant will produce an output of 10 volts. Then, in the next step, the optimizer assumes the second input should be 5 volts as dictated by the reference signal. However, assume that from the previous feedback, the plant output was 8 volts instead of 10. This 8 is fed into the inverse model which calculates the corresponding input which happens to be 1.8 volt rather than the original 2 volts. So, these 1.8 volts are fed

to the optimizer which understands that the plant output is lagging the reference by a 2 volt difference. Therefore, the next input should be a value higher than the supposed 5 volts such that the output of the plant is forced back on track, so the plant is supplied by 6 volts instead. The optimizer then awaits the next feedback from the plant to see if there are any differences between it and the reference signal. If there is a difference, it tries to adjust the input again. This process is continued until the reference signal is completely covered. In practice though, the MPC is programmed to calculate more than one future controller step referred to as the controller prediction horizon. In this work, the MPC used has its inverse model designed using a FFNN hence the total system is called NN-MPC which is explained in the Chapter 8.

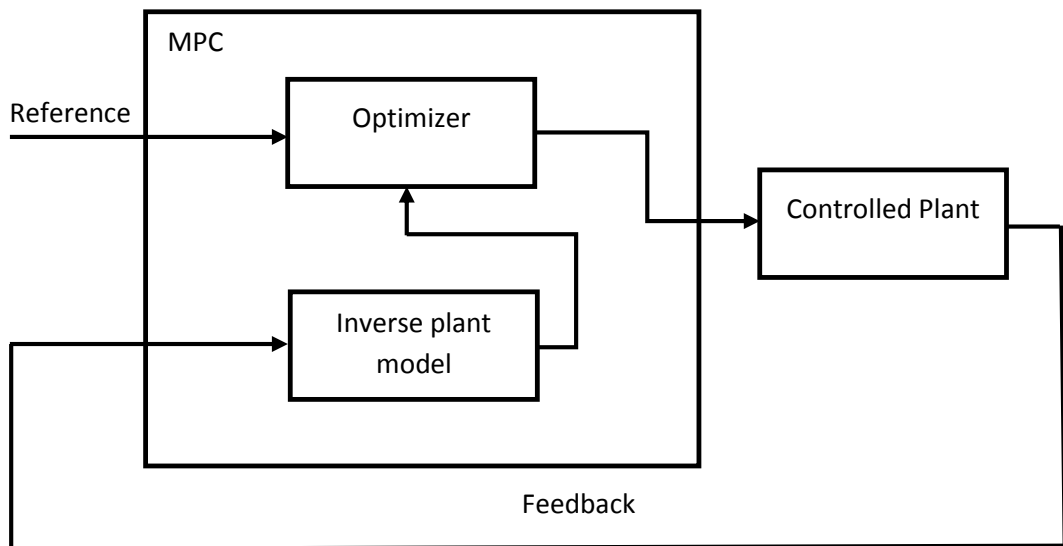


Figure 30. Basic components of a model predictive controller. It consists of a controlled plant from which an inverse model is derived to be used inside the MPC along with an optimizer such that the output follows the reference signal at the input.

CHAPTER 8: NN-MPC and Results

8.1. Procedure and Setup

As mentioned, the MPC that is designed for the purpose of this thesis is based on neural networks. To shed some light on the purpose of using an MPC, imagine the following example. A medical doctor diagnosed a patient with cancer and referred him to chemotherapy using liposomes as carriers and ultrasound as the trigger. However, the way the drug should be administered is subjected to the following requirements:

- The sonication power density should not exceed 10 W/cm^2
- The time of sonication should be around 3 minutes in total
- Based on the injected dosage, only 60 % of the content should be released at the end

To comply with the above constraints, experimental work should be conducted to figure out how the US should be operated throughout the sonication time. For example, sonicated for 1 minutes with a 30 on 30 off cycle and power density of 10 W/cm^2 , then for the next minute, sonicate at 5 W/cm^2 with 10 on 10 off cycles and for the third minute, sonicate continuously at 3 W/cm^2 . Unfortunately, if such lab work must be done to figure out the US behavior to achieve the required release, it won't be efficient. Even if the data collection is possible, the lab work is done *in vitro*. When moving to real life, many parameters could change making the assumed US trend inadequate. Furthermore, if the US settings are to be followed as suggested by the lab work, a control system with a feedback controller has to be used to make sure the release is on track which is why an NN-MPC is used here.

Hence, to explain the setup briefly, the patient will be treated with liposomes with a certain drug concentration out of which a certain percentage should be release through the use of US as a trigger. By employing an MPC the need for further experimentation is avoided. Everything can be automated. All that is needed is for the medical doctor to specify the constraints. Referring to Figure 30, the model of the body of the patient under treatment can be used as the plant. The feedback can be taken from a sensor that measures the instantaneous drug release level and sends it to the inverse plant model. The inverse plant model is a generalized model of the human body that is developed by using an FFNN trained with the experimental data collected for input-

output relation. Then, by finding a reference release curve to be fed to the optimizer, the NN-MPC is ready for work. Below is a step by step explanation of the developed system.

Step 1:

Since, in this work, everything is simulation, there was no patient to replace the plant. Therefore, a simulated model was used instead. This plant model was found using neural networks where the input was a square pulsed wave mimicking the periods during which US was on or off as shown in Figure 31.

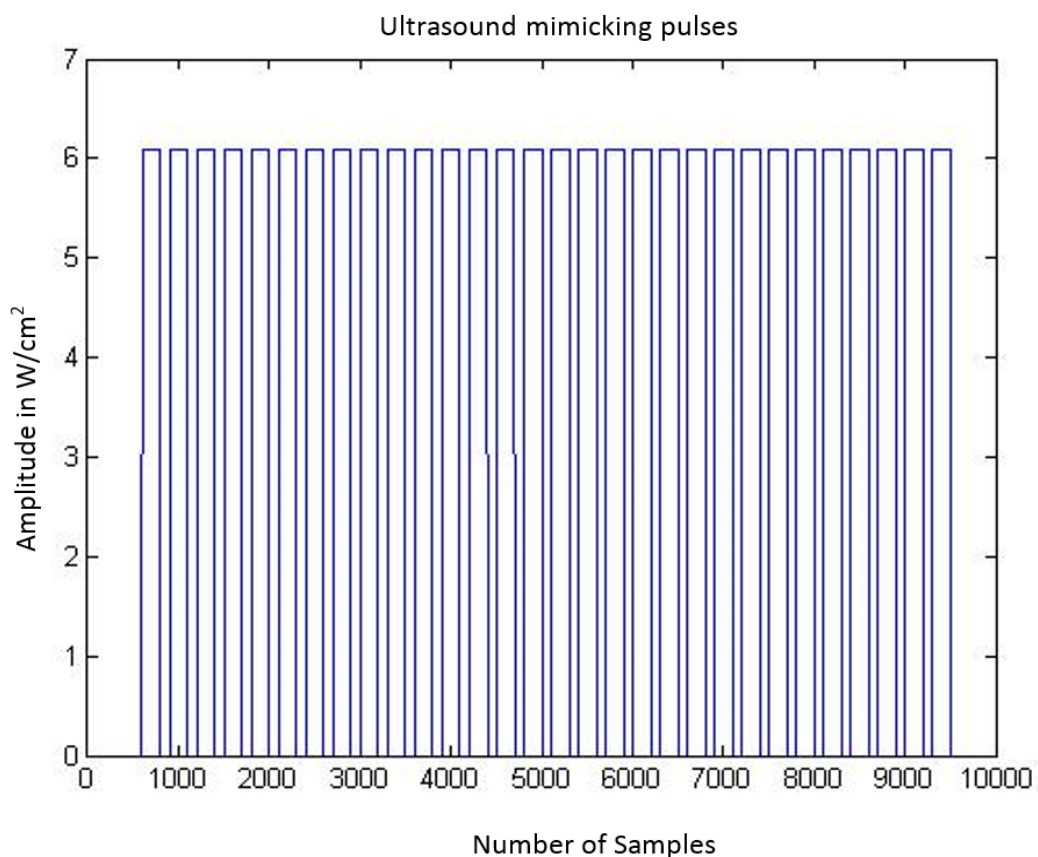


Figure 31. Square pulses indicating the periods at which the US is on or off as well as what power density is being used. The x-axis shows samples which can be converted into minutes and seconds by dividing by the sampling frequency 600.

Then, the corresponding release curve found in the lab from three runs is placed into an array along with the above pulses forming an input-output array. This array is fed to the neural network to find a model for this system where backpropagation was used in the training with a delay of 2 samples. Figure 32 shows the US pulses against the release curves.

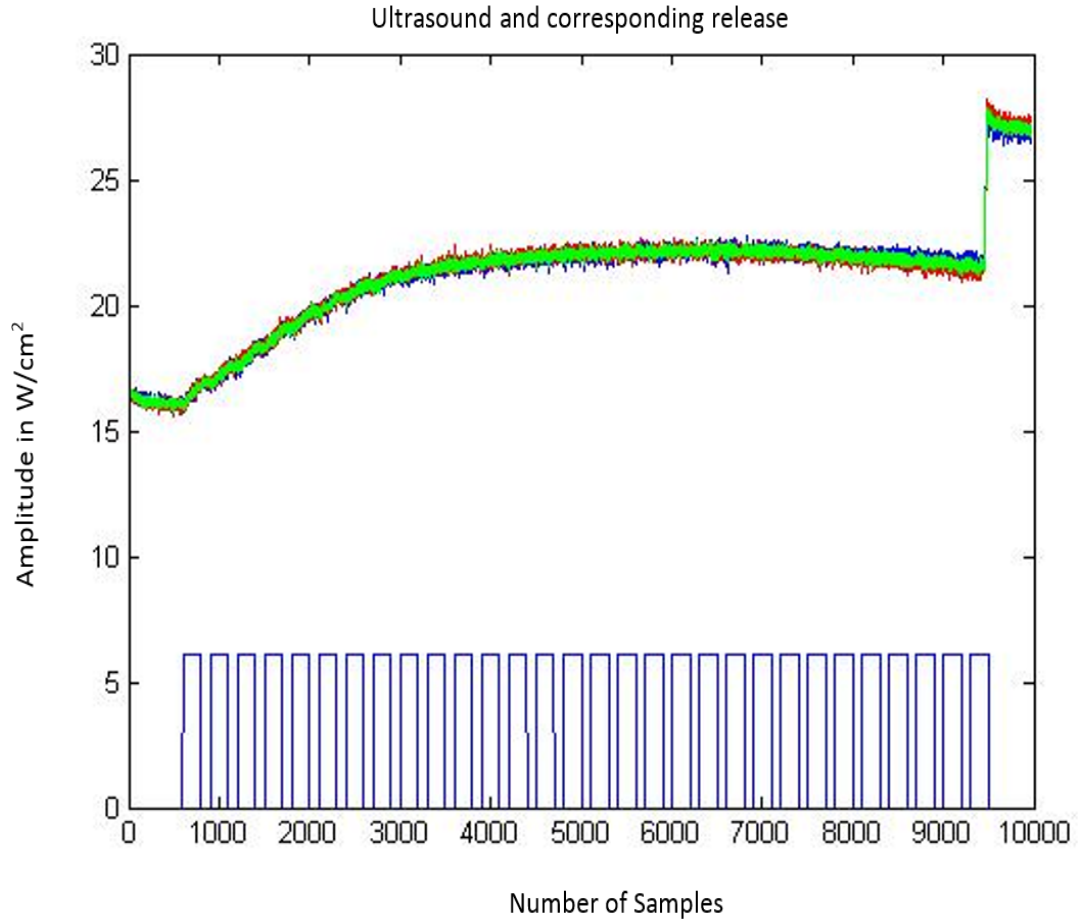


Figure 32. The mimicking US pulses plotted against the corresponding release curve. There are three release curve all were collected in vitro and they were consistent.

However, as can be seen, the collected release data is noisy which may cause trouble for the NN. Therefore, *sgolay* filter was used to clean and smooth the signal before the NN. Then the cleaned signal was fed to the NN and the developed model was found to have very minimal error. Figure 33 shows the final model with the error. The error was very minimal, in the range of 0.01 %, which indicates how well the model fits the system. This model was exported into Simulink to be used as the plant as a part of the final MPC. This model simulates the response of drug release in a real patient as it responds to US intensity as its input and produces the drug level as its output.

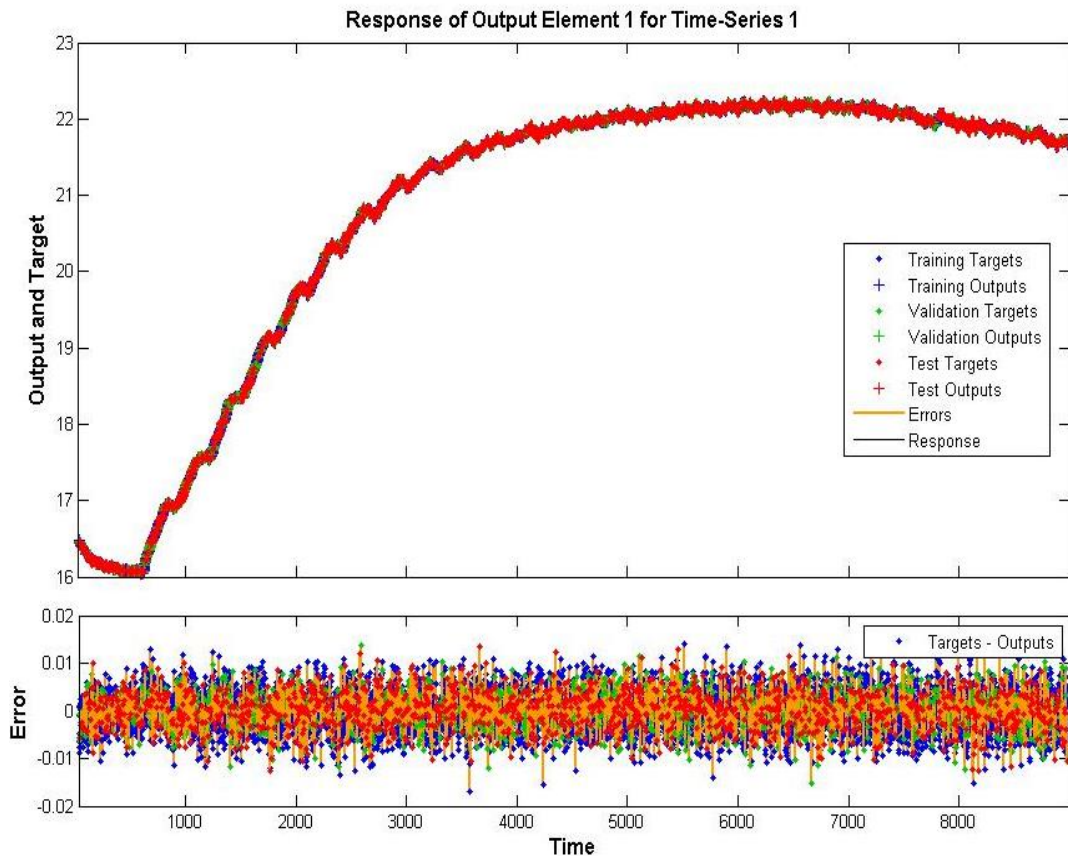


Figure 33. The release curve after cleaning and fitting using NN back propagated training. The error of the fitting is shown to be between 1%

Step 2:

The next part of this system is to find a way to predict the release curve for any doctors' defined constraints such as the example given earlier. In the database collected, only specific values of the parameters were tested, so any constraints that were not tested will not have a corresponding release curve. To estimate any curve from the existing curves, a MATLAB code was developed just to do that which is included in Appendix A. The code takes in an input that specifies the total sonication time in minutes and seconds as well as the expected final release. Then, using a lookup table, the curves that have the closest release value at the specified time are chosen and saved into a new array. Those curves will serve as the initial guess from which the correct release curve will be deduced. The program will then save the corresponding US parameters and behavior that caused each release curve (strictly speaking, the intensity and on/off periods). After that, through interpolation, new intermediate parameters are produced. From those parameters, a new US operation pattern will be created and

assumed to be the pattern that should be followed to fulfill the requirements of the doctor.

Step 3:

It is worth highlighting that the reference signal should be the signal that we wish the output of the plant to follow. Therefore, what was found in step 2 cannot serve as the reference rather the matching release curve is what is needed. To find this release curve, a generalized model is generated. This generalized model is created using all the collected data from different experiments. It incorporates US with different intensities and duty cycles as well as different sample concentrations. All the data was initially smoothed and then down sampled to reduce the mathematical complexity. All input signals were stored in an input matrix while all the output data were stored in another matrix. Then, with the aid of matrix inversion, the generalized model was found. The following equations help in understanding the process used.

$$Output = input * model \quad (47)$$

$$\therefore Model = \frac{Output}{input} \quad (48)$$

But since we are dealing with matrices, the division is done using matrix inversion

$$Model = Inverse(input) * Output \quad (49)$$

Consequently, the generalized model can be now used to predict the output of a given input. Hence, the interpolated US operating pattern is used as the input to the model to find the corresponding release curve which can be used as the reference to the optimizer of the MPC. All processing was done using a MATLAB code that can be found in Appendix A.

Step 4:

After finding the simulated plant and the reference signal, what is left is to find the inverse plant model which is placed inside the MPC. To do so, a release curve was recorded while varying the US intensity and duty cycle on the run. This curve allows for the development of a somewhat flexible model that can follow changes in the output and relate them to intensity and on/off cycle. Then, the input and output curves were

used to train the NN using the backpropagation method. This step was done by using the already made block in Simulink called NN-MPC shown in Figure 34.

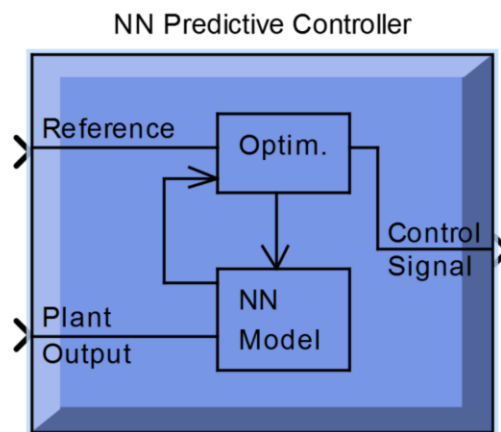


Figure 34. Simulink block of the NN predictive controller used to build the NN-MPC.

By combining the above four steps, a system was developed that can control US intensity and on-off cycles such that it follows a certain release behavior based on a feedback from a simulated plant. Figure 35 shows the full system.

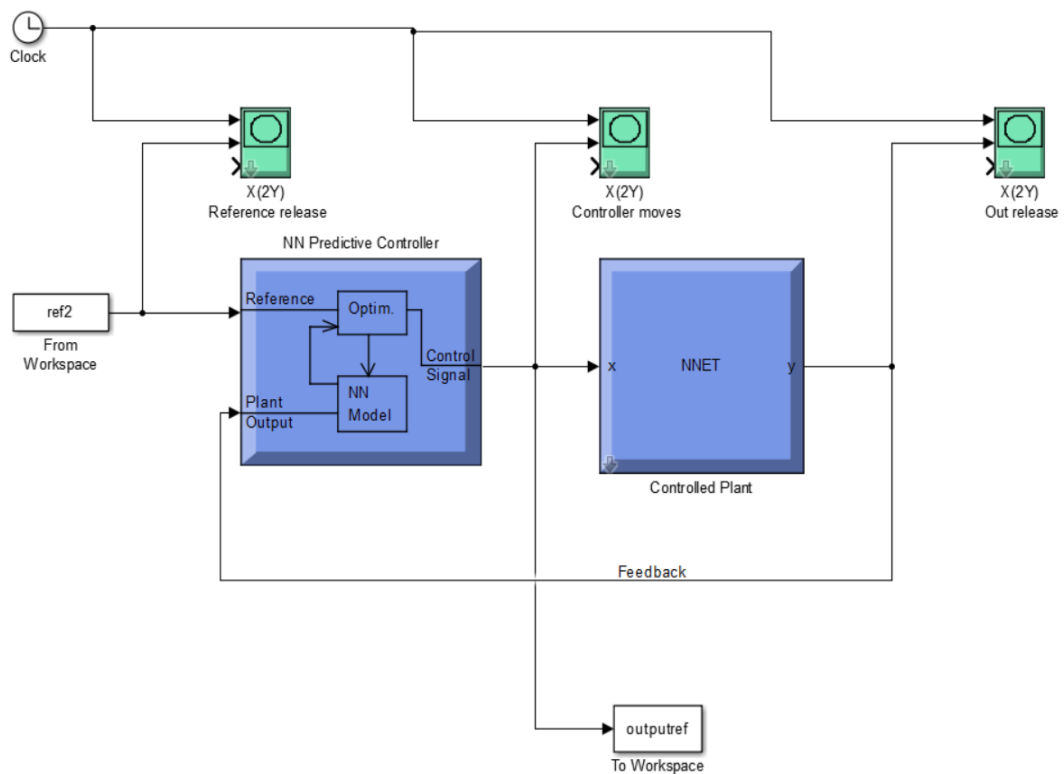


Figure 35. Full NN-MPC system setup. The system consists of an MPC block, an NN model of the controlled plant (patient's body) and the reference signal.

8.2. Sample results

For the following, the program was tested for the following constraints:

- US power density should not exceed 7 W/cm^2
- Final percent release should be around 46 %
- Total time of insonation should be 4 minutes and 10 seconds

First those constraints were fed into MATLAB code 1 to find the best matching release curves from the database. There happened to be two US settings that could achieve 46% release in 4 minutes and 10 seconds which are shown in Figure 37 (A). Based on the sampling frequency of the fluorometer used to create the database which was 10 samples per second, the 4 minutes and 10 seconds are equivalent to 2500 samples. As shown in the figure, at the 2500 mark, both curves are close to the 46 % release but not exactly at it. Therefore, by interpolating both curves based on proximity, an average curve can be found to better match the requirements which are shown in Figure 37 (B). This curve will be used as the reference curve in the MPC.

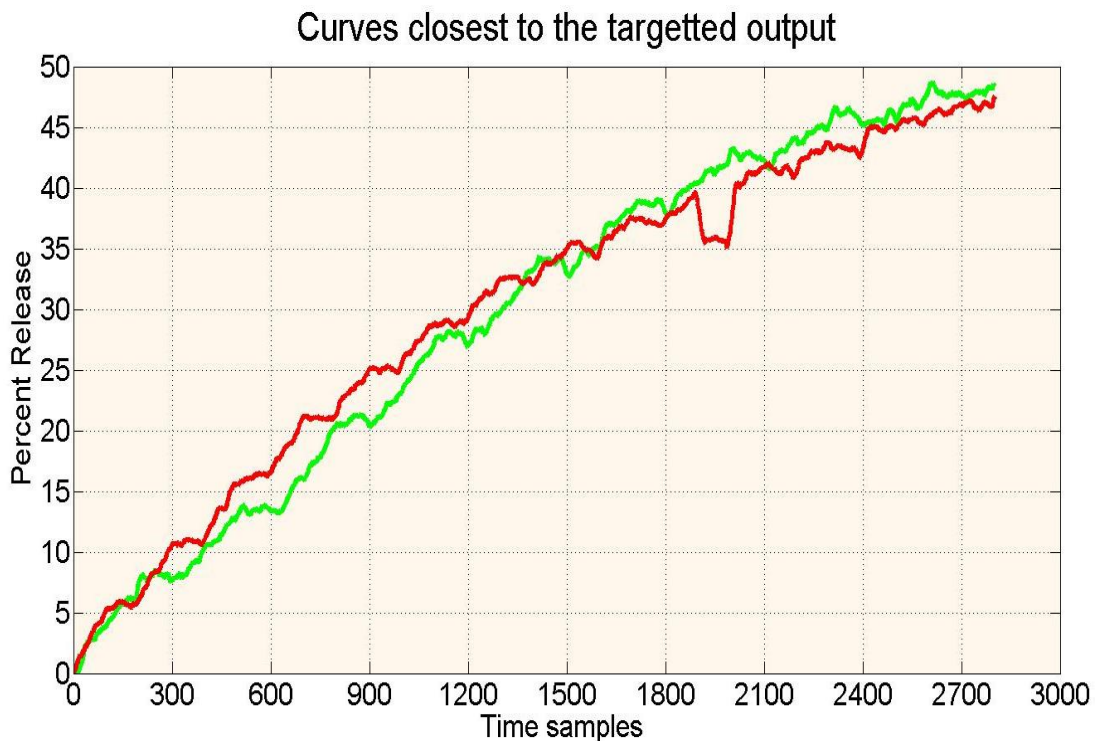


Figure 36. Finding the reference curve out from the data base of collected release curves. Shows the closest curves from the data base that satisfy the constraints of the doctor.

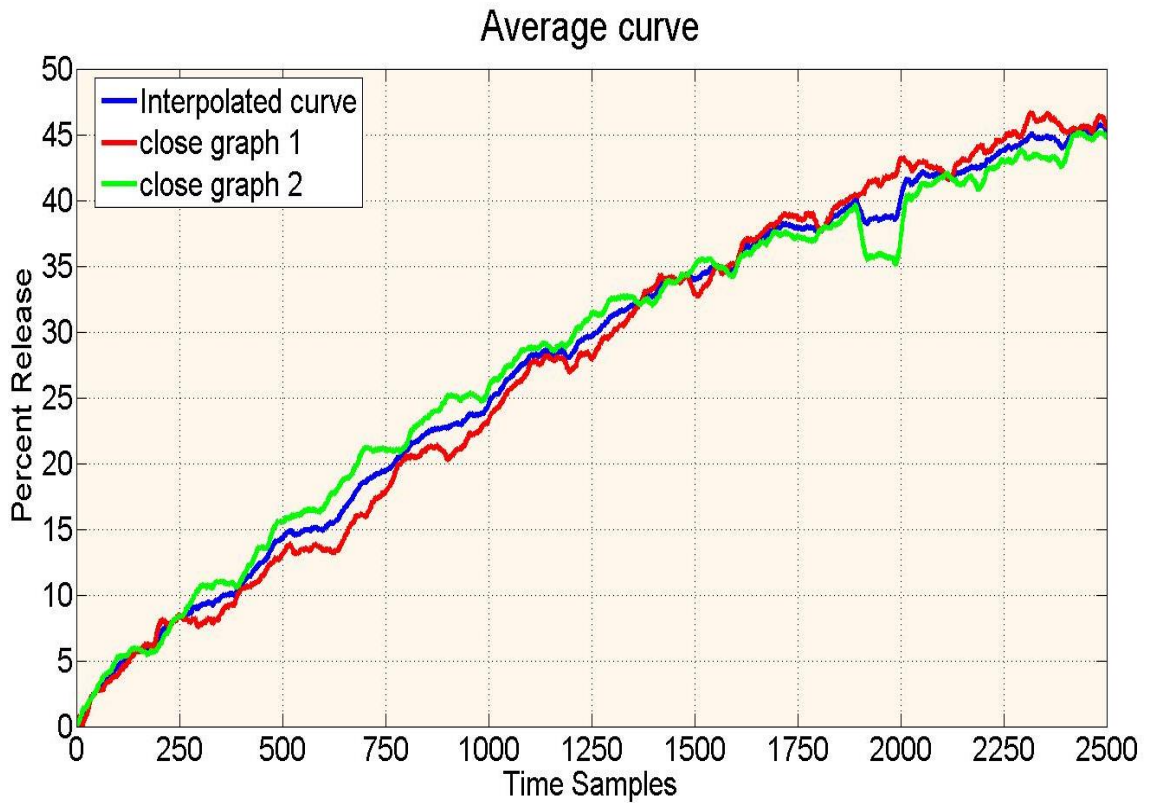


Figure 37. Finding the reference curve out from the data base of collected release curves. Shows the interpolated curve that shall be used as the proper reference in the MPC.

Furthermore, the corresponding US pattern was found using the generalized model explained in step 3 earlier. The pattern was as shown in Figure 38. This pattern is the ideal pattern by which the US should be operating under perfect conditions assuming the feedback signal from the controlled plant is exactly like the reference signal. Notice that the power density did not exceed 7 W/cm^2 which satisfies the constraints.

Now, after finding the plant model and the inverse plant model from which the complete MPC was constructed, the above reference curve was used as the input to the optimizer and the program was started. Figure 39 shows the reference signal, while Figure 40 shows the corresponding output signal from the plant. As for figure 41, it shows the US pattern used by the controller to create this output.

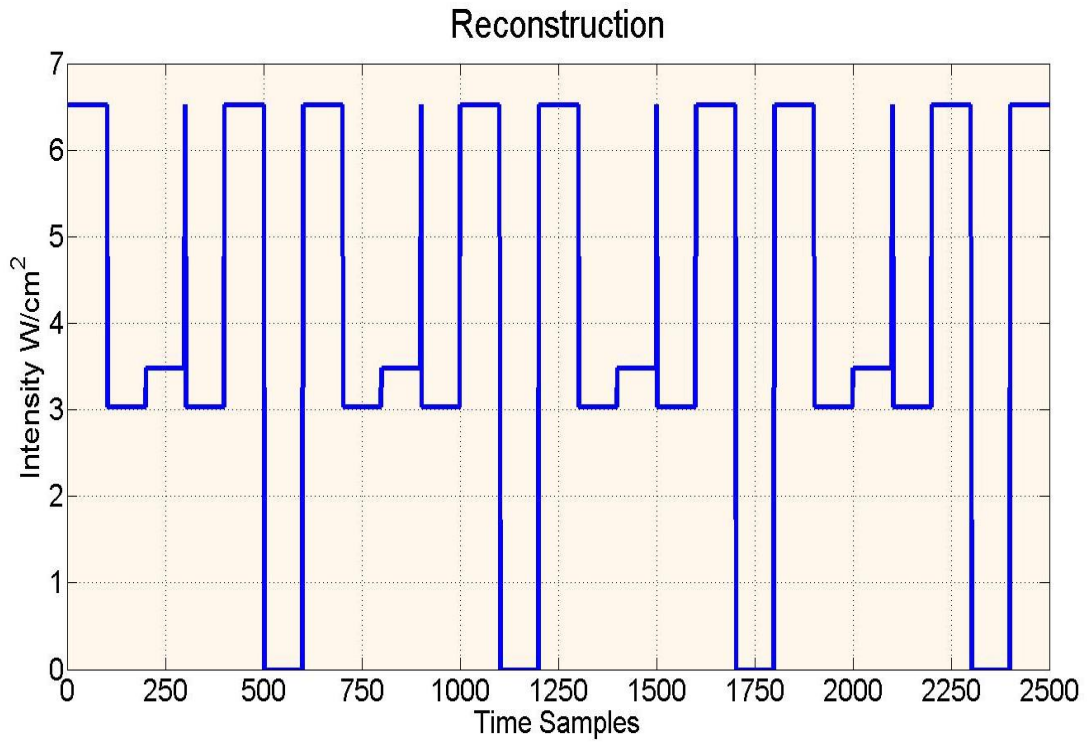


Figure 38. The proposed US pattern that shall be used in case of ideal performance to achieve an output that exactly follows the reference signal

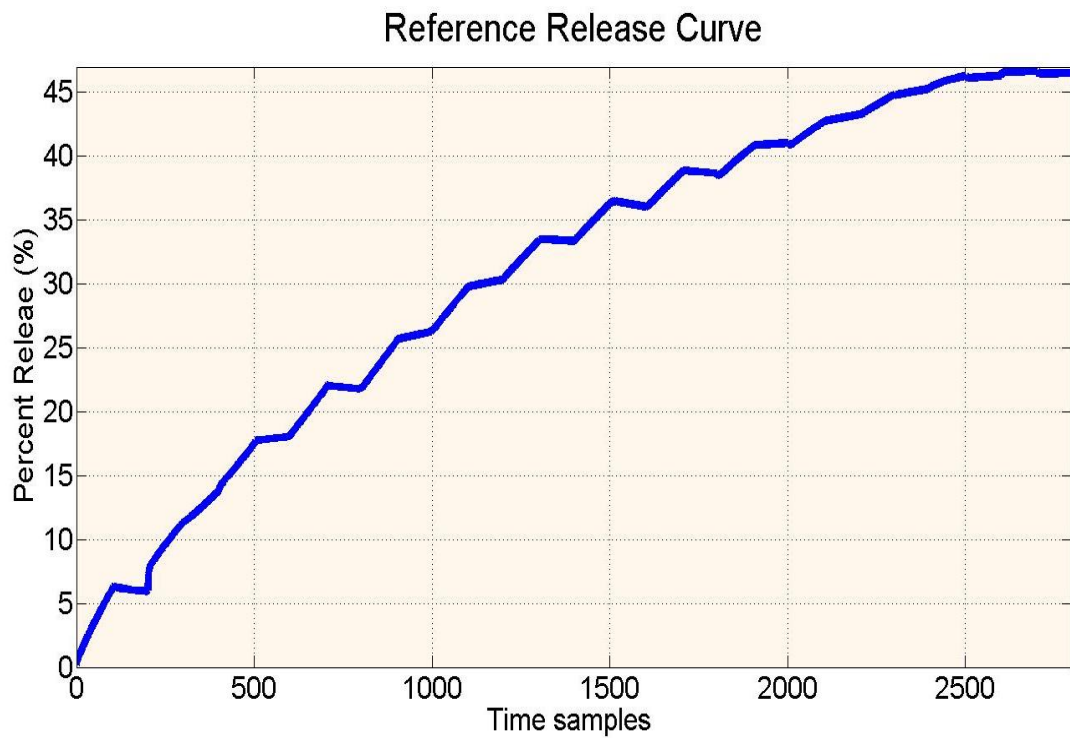


Figure 39. Sample results from the NN-MPC. Shows the reference signal according to which the controller shall produce the right US pattern that will ensure producing a matching output.

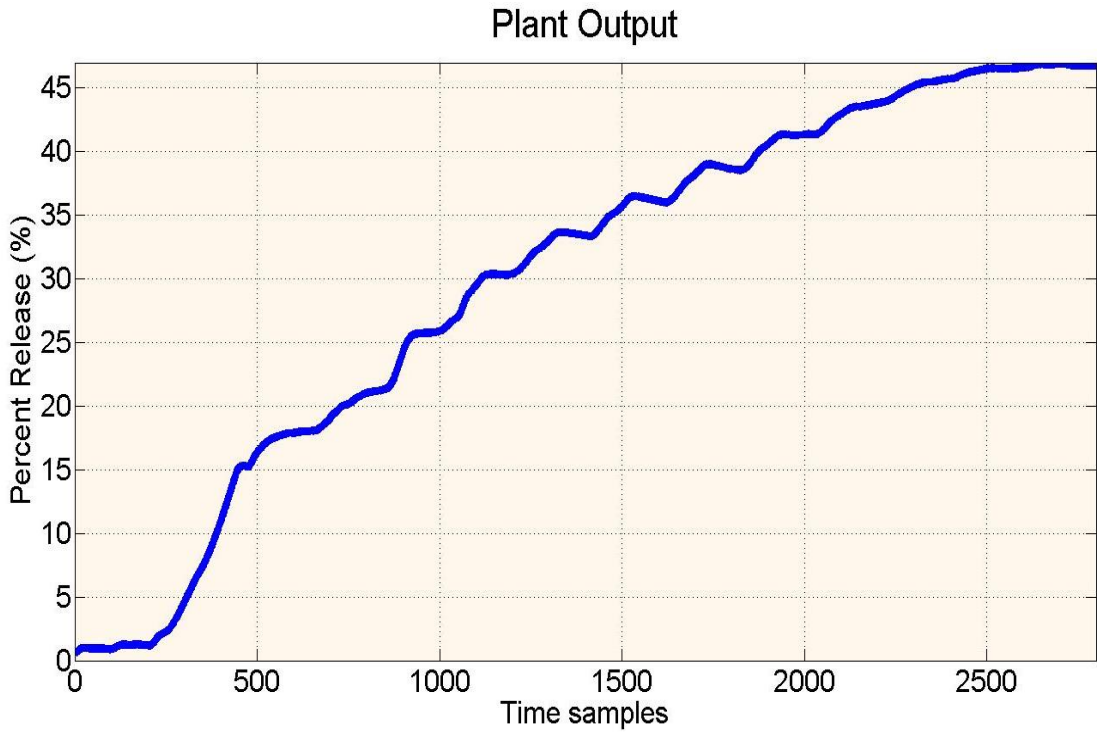


Figure 40. Sample results from the NN-MPC. Shows the corresponding system output from the controlled plant.

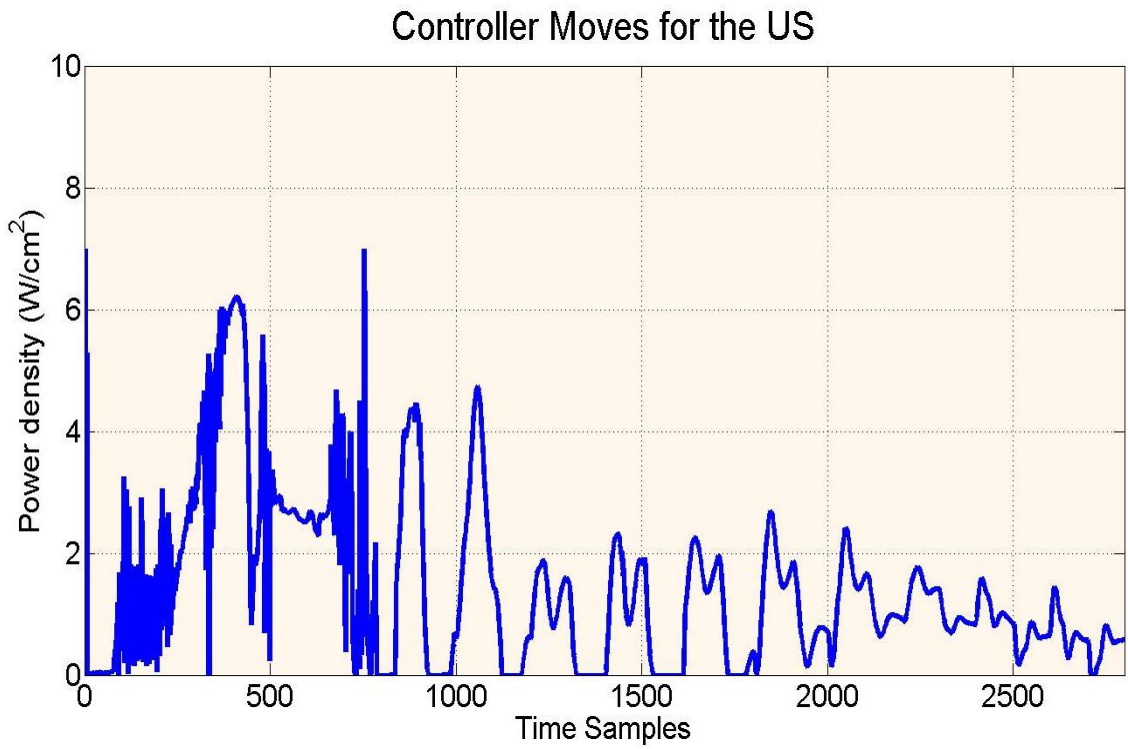


Figure 41. Sample results from the NN-MPC. Shows the controller moves based on the feedback and the reference.

The results show that the US intensity used did not exceed 7 W/cm². The controller was able to follow the reference and correct for any lags or differences as can be seen when comparing the reference and the output curves. Also, after the 2500 sample mark, which is equivalent to 4 minutes and 10 seconds, the output curve shows a release of exactly 46 %. However, the system kept running for around 30 more seconds just to make sure it totally followed the reference curve. Over all, the results show how accurate all the models are, as well as proving the competency of the designed controller.

CHAPTER 9: Conclusion and Recommendation

In this work, a full review on liposomal carriers and the different triggering techniques was presented with a focus on ultrasound as a potential trigger. Also, the work includes the development of a liposomal carrier in the labs of the university which were used to conduct *in vitro* experiments. The liposomes were loaded with the model drug calcein which is fluorescent. The liposomes were subjected to US with various intensities ranging from 6 to 150 W/cm² at various frequencies (20 kHz, 1 MHz and 3 MHz). The release was monitored for each setting and at the end the results were compared. It was found that at lower frequencies, less power density is needed to cause the release. This is why, the least and slowest release was achieved when using 3 MHz US and relatively high power densities. However, in the case of the 20 kHz, the maximum release was achieved in less than a quarter of the time and at comparatively low power densities. However, the advantage of high frequency US is the capability of focusing the beam. Furthermore, the work included modeling of the kinetics of the release as well as designing model predictive controller that will help in eliminating the need for exhaustive lab experiments.

As for the future of this work, more *in vitro* tests and data collection should be conducted to increase the database of release curves which will help in refining the modeling and control parts of the work. Hence, after finishing the *in vitro* tests (including experiments on cell cultures) and verifying the results, the data about the frequencies and the corresponding intensities shall be tabulated and saved to be used for further modeling. From this table, the required intensity at each frequency will be noted and, when combined with a proper model for the human body, can be used to determine the necessary power density that shall be sufficient to cause a certain release when conducting *in vivo* studies and animal work. The applied intensity should take into account the losses that will happen as the wave propagates through the layers of the body until it reaches the tumor site and cause the liposomes to release. As shown in Figure 9, the applied ultrasound will have to penetrate the skin layer, then the fat and muscle layers before it reaches the tumor especially in the case of breast, colorectal and cervical tumors. A detailed analysis of the reflection losses that happen due to impedance mismatches between those different layers shall be done even if only on a simplified model just to serve as an initial guess for the correct intensity.

Also, other transducer arrangements might be considered in an attempt to decrease the hyperthermia effect that can be induced along the way if a single element transducer is used. For example, instead of using a single transducer perpendicular to the surface of the skin, multiple transducers can be used at different locations where their produced waves add destructively everywhere except at the tumor site. This will stop the layers of the body from absorbing enough energy and converting it into heat that may cause tissue ablation.

Furthermore, other frequencies and intensities might be tried and compared to the results of this work in a search for optimal US settings. Also, it is very critical to take into consideration the range of frequencies and intensities that are classified as safe to be used on the human body and the maximum time of sonication that the human body can tolerate. All those factors will affect the future of this work. Assuming, from in vitro studies, the frequency and power density required to induce release from the synthesized liposomes are not within the usable ranges, then what was developed is not usable on humans. So, other intensities and frequencies should be tried as well as different liposomal compositions that might prove to be more sensitive to the acoustic waves.

References

- [1] D. M. Parkin, P. Pisani, and J. Ferlay, "Global cancer statistics," *Ca : a Cancer Journal for Clinicians*, vol. 49, pp. 33-64, 1999.
- [2] R. H. Bradbury, "Overview," in *Topics in Medicinal Chemistry: Cancer*. vol. 1, R. H. Bradbury, Ed., ed Berlin. Heidelberg.: Springer-Verlag, 2007, pp. 1-17.
- [3] V. T. DeVita, Jr. and E. Chu, "A history of cancer chemotherapy," *Cancer Res*, vol. 68, pp. 8643-53, Nov 1 2008.
- [4] A. Jemal, F. Bray, M. M. Center, J. Ferlay, E. Ward, and D. Forman, "Global cancer statistics," *CA Cancer J Clin*, vol. 61, pp. 69-90, Mar-Apr 2011.
- [5] E. K. Lim, E. Jang, K. Lee, S. Haam, and Y. M. Huh, "Delivery of cancer therapeutics using nanotechnology," *Pharmaceutics*, vol. 5, pp. 294-317, 2013.
- [6] M. R. Mozafari, A. Pardakhty, S. Azarmi, J. A. Jazayeri, A. Nokhodchi, and A. Omri, "Role of nanocarrier systems in cancer nanotherapy," *J Liposome Res*, vol. 19, pp. 310-21, 2009.
- [7] V. P. Torchilin, "Micellar nanocarriers: pharmaceutical perspectives," *Pharm Res*, vol. 24, pp. 1-16, Jan 2007.
- [8] S. Bibi, E. Lattmann, A. R. Mohammed, and Y. Perrie, "Trigger release liposome systems: local and remote controlled delivery?," *J Microencapsul*, vol. 29, pp. 262-76, 2012.
- [9] F. Alexis, "Nanoparticle technologies for cancer therapy," in *Handbook of Experimental Pharmacology: Drug Delivery*, M. Schafer-Korting, Ed., ed Berlin. Heidelberg.: Springer-Verlag, 2010, pp. 55-86.
- [10] T. Benvegnu, L. Lemiegre, and S. Cammas-Marion, "New generation of liposomes called archaeosomes based on natural or synthetic archaeal lipids as innovative formulations for drug delivery," *Recent Pat Drug Deliv Formul*, vol. 3, pp. 206-20, Nov 2009.
- [11] M. Rawat, D. Singh, and S. Saraf, "Nanocarriers: promising vehicle for bioactive drugs," *Biol Pharm Bull*, vol. 29, pp. 1790-8, Sep 2006.
- [12] N. Bertrand, J. Wu, X. Xu, N. Kamaly, and O. C. Farokhzad, "Cancer nanotechnology: the impact of passive and active targeting in the era of modern cancer biology," *Adv Drug Deliv Rev*, vol. 66, pp. 2-25, Feb 2014.
- [13] S. Gujral and S. Khatri, "A review on basic concept of drug targeting and drug carrier system," *Int. J. Adv. Pharm. Biol. Chem.*, vol. 2, pp. 130-136, 2013.
- [14] Y. Matsumura and H. Maeda, "A new concept for macromolecular therapeutics in cancer chemotherapy: mechanism of tumoritropic accumulation of proteins and the antitumor agent smancs," *Cancer Res*, vol. 46, pp. 6387-92, Dec 1986.
- [15] H. Maeda, "The enhanced permeability and retention (EPR) effect in tumor vasculature: the key role of tumor-selective macromolecular drug targeting," *Adv Enzyme Regul*, vol. 41, pp. 189-207, 2001.
- [16] H. Maeda, J. Wu, T. Sawa, Y. Matsumura, and K. Hori, "Tumor vascular permeability and the EPR effect in macromolecular therapeutics: a review," *J Control Release*, vol. 65, pp. 271-84, Mar 1 2000.
- [17] N. H. Bergstrand, "Liposomes for drug delivery: From physico-chemical studies to applications.," Ph.D., Department of Physical Chemistry, Uppsala University, Uppsala, 2003.
- [18] N. T. Huynh, E. Roger, N. Lautram, J. P. Benoit, and C. Passirani, "The rise and rise of stealth nanocarriers for cancer therapy: passive versus active targeting," *Nanomedicine (Lond)*, vol. 5, pp. 1415-33, Nov 2010.

- [19] S. E. Leucuta, "Subcellular drug targeting, pharmacokinetics and bioavailability," *J Drug Target*, vol. 22, pp. 95-115, Feb 2014.
- [20] L. Rajendran, H. J. Knolker, and K. Simons, "Subcellular targeting strategies for drug design and delivery," *Nat Rev Drug Discov*, vol. 9, pp. 29-42, Jan 2010.
- [21] A. Akbarzadeh, R. Rezaei-Sadabady, S. Davaran, S. W. Joo, N. Zarghami, Y. Hanifehpour, *et al.*, "Liposome: classification, preparation, and applications," *Nanoscale Res Lett*, vol. 8, p. 102, 2013.
- [22] D. W. Deamer, "From "banghasomes" to liposomes: a memoir of Alec Bangham, 1921-2010," *FASEB J*, vol. 24, pp. 1308-10, May 2010.
- [23] D. Lasic, "Liposomes: synthetic lipid microspheres serve as multipurpose vehicles for the delivery of drugs, genetic material and cosmetics.," *American Scientist*, vol. 80, pp. 20-31, 1992.
- [24] A. Schroeder, J. Kost, and Y. Barenholz, "Ultrasound, liposomes, and drug delivery: principles for using ultrasound to control the release of drugs from liposomes," *Chem Phys Lipids*, vol. 162, pp. 1-16, Nov 2009.
- [25] O. Garbuzenko, Y. Barenholz, and A. Prievo, "Effect of grafted PEG on liposome size and on compressibility and packing of lipid bilayer," *Chem Phys Lipids*, vol. 135, pp. 117-29, Jun 2005.
- [26] V. V. Kumar, "Complementary molecular shapes and additivity of the packing parameter of lipids," *Proc Natl Acad Sci U S A*, vol. 88, pp. 444-8, Jan 15 1991.
- [27] A. S. Ulrich, "Biophysical aspects of using liposomes as delivery vehicles," *Biosci Rep*, vol. 22, pp. 129-50, Apr 2002.
- [28] V. P. Torchilin, "Recent advances with liposomes as pharmaceutical carriers," *Nat Rev Drug Discov*, vol. 4, pp. 145-60, Feb 2005.
- [29] M. L. Immordino, F. Dosio, and L. Cattel, "Stealth liposomes: review of the basic science, rationale, and clinical applications, existing and potential," *Int J Nanomedicine*, vol. 1, pp. 297-315, 2006.
- [30] D. D. Lasic, "Novel applications of liposomes," *Trends Biotechnol*, vol. 16, pp. 307-21, Jul 1998.
- [31] D. D. Lasic and D. Needham, "The "Stealth" Liposome: A Prototypical Biomaterial," *Chem Rev*, vol. 95, pp. 2601-2628, 1995.
- [32] M. C. Woodle and D. D. Lasic, "Sterically stabilized liposomes," *Biochim Biophys Acta*, vol. 1113, pp. 171-99, Aug 14 1992.
- [33] N. W. Moore and T. L. Kuhl, "The role of flexible tethers in multiple ligand-receptor bond formation between curved surfaces," *Biophys J*, vol. 91, pp. 1675-87, Sep 1 2006.
- [34] X. Li, L. Ding, Y. Xu, Y. Wang, and Q. Ping, "Targeted delivery of doxorubicin using stealth liposomes modified with transferrin," *Int J Pharm*, vol. 373, pp. 116-23, May 21 2009.
- [35] M. Javadi, W. G. Pitt, D. M. Belnap, N. H. Tsosie, and J. M. Hartley, "Encapsulating nanoemulsions inside eLiposomes for ultrasonic drug delivery," *Langmuir*, vol. 28, pp. 14720-9, Oct 16 2012.
- [36] M. Javadi, W. G. Pitt, C. M. Tracy, J. R. Barrow, B. M. Willardson, J. M. Hartley, *et al.*, "Ultrasonic gene and drug delivery using eLiposomes," *J Control Release*, vol. 167, pp. 92-100, Apr 10 2013.
- [37] J. R. Lattin, D. M. Belnap, and W. G. Pitt, "Formation of eLiposomes as a drug delivery vehicle," *Colloids Surf, B*, vol. 89, pp. 93-100, Jan 1 2012.
- [38] J. R. Lattin, W. G. Pitt, D. M. Belnap, and G. A. Hussein, "Ultrasound-induced calcein release from eLiposomes," *Ultrasound Med Biol*, vol. 38, pp. 2163-73, Dec 2012.

- [39] C. Y. Lin, M. Javadi, D. M. Belnap, J. R. Barrow, and W. G. Pitt, "Ultrasound sensitive eLiposomes containing doxorubicin for drug targeting therapy," *Nanomedicine*, vol. 10, pp. 67-76., Jul 9 2014.
- [40] S. L. Huang and R. C. MacDonald, "Acoustically active liposomes for drug encapsulation and ultrasound-triggered release," *Biochim Biophys Acta*, vol. 1665, pp. 134-41, Oct 11 2004.
- [41] Y. Z. Zhao, L. N. Du, C. T. Lu, Y. G. Jin, and S. P. Ge, "Potential and problems in ultrasound-responsive drug delivery systems," *Int J Nanomedicine*, vol. 8, pp. 1621-33, 2013.
- [42] P. P. Deshpande, S. Biswas, and V. P. Torchilin, "Current trends in the use of liposomes for tumor targeting," *Nanomedicine (Lond)*, vol. 8, pp. 1509-28, Sep 2013.
- [43] H. P. Schwan, "Electromagnetic and ultrasonic induction of hyperthermia in tissue-like substances," *Radiat Environ Biophys*, vol. 17, pp. 189-203, 1980.
- [44] E. Amstad, J. Kohlbrecher, E. Muller, T. Schweizer, M. Textor, and E. Reimhult, "Triggered release from liposomes through magnetic actuation of iron oxide nanoparticle containing membranes," *Nano Lett*, vol. 11, pp. 1664-70, Apr 13 2011.
- [45] B. M. Dicheva and G. A. Koning, "Targeted thermosensitive liposomes: an attractive novel approach for increased drug delivery to solid tumors," *Expert Opin Drug Deliv*, vol. 11, pp. 83-100, Jan 2014.
- [46] H. Grull and S. Langereis, "Hyperthermia-triggered drug delivery from temperature-sensitive liposomes using MRI-guided high intensity focused ultrasound," *J Control Release*, vol. 161, pp. 317-27, Jul 20 2012.
- [47] B. Kneidl, M. Peller, G. Winter, L. H. Lindner, and M. Hossann, "Thermosensitive liposomal drug delivery systems: state of the art review," *Int J Nanomedicine*, vol. 9, pp. 4387-4398, 2014.
- [48] C. S. Kumar and F. Mohammad, "Magnetic nanomaterials for hyperthermia-based therapy and controlled drug delivery," *Adv Drug Deliv Rev*, vol. 63, pp. 789-808, Aug 14 2011.
- [49] T. Ta and T. M. Porter, "Thermosensitive liposomes for localized delivery and triggered release of chemotherapy," *J Control Release*, vol. 169, pp. 112-125, July 28 2013.
- [50] M. de Smet, S. Langereis, S. van den Bosch, and H. Grull, "Temperature-sensitive liposomes for doxorubicin delivery under MRI guidance," *J Control Release*, vol. 143, pp. 120-7, Apr 2 2010.
- [51] A. Gasselhuber, M. R. Dreher, A. Partanen, P. S. Yarmolenko, D. Woods, B. J. Wood, *et al.*, "Targeted drug delivery by high intensity focused ultrasound mediated hyperthermia combined with temperature-sensitive liposomes: computational modelling and preliminary in vivo validation," *Int J Hyperthermia*, vol. 28, pp. 337-48, 2012.
- [52] A. Gasselhuber, M. R. Dreher, F. Rattay, B. J. Wood, and D. Haemmerich, "Comparison of Conventional Chemotherapy, Stealth Liposomes and Temperature-Sensitive Liposomes in a Mathematical Model," *PLoS ONE*, vol. 7, 2012.
- [53] S.-J. Lim, C.-J. Carling, C. C. Warford, D. Hsiao, B. D. Gates, and N. R. Branda, "Multifunctional photo- and thermo-responsive copolymer nanoparticles," *Dyes Pigments*, vol. 89, pp. 230-235, 2011.
- [54] S. M. Park, M. S. Kim, S.-J. Park, E. S. Park, K.-S. Choi, Y.-s. Kim, *et al.*, "Novel temperature-triggered liposome with high stability: Formulation, in

- vitro evaluation, and in vivo study combined with high-intensity focused ultrasound (HIFU)," *J Control Release*, vol. 170, pp. 373-379, 2013.
- [55] A. E. Deatsch and B. A. Evans, "Heating efficiency in magnetic nanoparticle hyperthermia," *J Magn Magn Mater*, vol. 354, pp. 163-172, 2014.
- [56] K. Demura, S. Morikawa, K. Murakami, K. Sato, H. Shiomi, S. Naka, *et al.*, "An easy-to-use microwave hyperthermia system combined with spatially resolved MR temperature maps: phantom and animal studies," *J Surg Res*, vol. 135, pp. 179-86, Sep 2006.
- [57] N. A. Forbes and J. A. Zasadzinski, "Localized Photothermal Heating of Temperature Sensitive Liposomes," *Biophys J*, vol. 98, p. 274a, 2010.
- [58] M. J. Ernsting, A. Worthington, J. P. May, T. Tagami, M. C. Kolios, and S.-D. Li, "Ultrasound drug targeting to tumors with thermosensitive liposomes," in *2011 IEEE Int Ultrasonics Symp.*, 2011, pp. 1-4.
- [59] M. B. Yatvin, J. N. Weinstein, W. H. Dennis, and R. Blumenthal, "Design of liposomes for enhanced local release of drugs by hyperthermia," *Science*, vol. 202, pp. 1290-3, Dec 22 1978.
- [60] M. H. Gaber, K. Hong, S. K. Huang, and D. Papahadjopoulos, "Thermosensitive sterically stabilized liposomes: formulation and in vitro studies on mechanism of doxorubicin release by bovine serum and human plasma," *Pharm Res*, vol. 12, pp. 1407-16, Oct 1995.
- [61] S. Unezaki, K. Maruyama, N. Takahashi, M. Koyama, T. Yuda, A. Suginaka, *et al.*, "Enhanced delivery and antitumor activity of doxorubicin using long-circulating thermosensitive liposomes containing amphipathic polyethylene glycol in combination with local hyperthermia," *Pharm Res*, vol. 11, pp. 1180-5, Aug 1994.
- [62] D. Needham, G. Anyarambhatla, G. Kong, and M. W. Dewhirst, "A new temperature-sensitive liposome for use with mild hyperthermia: characterization and testing in a human tumor xenograft model," *Cancer Res*, vol. 60, pp. 1197-201, Mar 1 2000.
- [63] K. Kono, "Thermosensitive polymer-modified liposomes," *Adv Drug Deliv Rev*, vol. 53, pp. 307-19, Dec 31 2001.
- [64] K. Kono, R. Nakai, K. Morimoto, and T. Takagishi, "Thermosensitive polymer-modified liposomes that release contents around physiological temperature," *Biochim Biophys Acta* vol. 1416, pp. 239-250, 1999.
- [65] H. G. Schild, "Poly(N-isopropylacrylamide): experiment, theory and application," *Prog Polym Sci*, vol. 17, pp. 163-249, 1992.
- [66] K. Kono, H. Hayashi, and T. Takagishi, "Temperature-sensitive liposomes: liposomes bearing poly (N-isopropylacrylamide)," *J Control Release*, vol. 30, pp. 69-75, 1994.
- [67] K. Kono, A. Henmi, and T. Takagishi, "Temperature-controlled interaction of thermosensitive polymer-modified cationic liposomes with negatively charged phospholipid membranes," *Biochim Biophys Acta*, vol. 1421, pp. 183-197, 1999.
- [68] K. Kono, A. Henmi, H. Yamashita, H. Hayashi, and T. Takagishi, "Improvement of temperature-sensitivity of poly(N-isopropylacrylamide)-modified liposomes," *J Control Release*, vol. 59, pp. 63-75, May 1 1999.
- [69] J.-C. Kim and J.-D. Kim, "Release property of temperature-sensitive liposome containing poly(N-isopropylacrylamide)," *Colloids Surf, B*, vol. 24, pp. 45-52, 2002.

- [70] T. Nishita, "Heat-sensitive liposomes containing cisplatin and localized hyperthermia in treatment of murine tumor," *Osaka City Med J*, vol. 44, pp. 73-83, Jun 1998.
- [71] L. Paasonen, B. Romberg, G. Storm, M. Yliperttula, A. Urtti, and W. E. Hennink, "Temperature-sensitive poly(N-(2-hydroxypropyl)methacrylamide mono/dilactate)-coated liposomes for triggered contents release," *Bioconjug Chem*, vol. 18, pp. 2131-6, Nov 12 2007.
- [72] M. Vollmer, "Physics of the microwave oven," *Physics Education*, vol. 39, pp. 74-81, 2003.
- [73] C. Gabriel, S. Gabriel, E. Grant, B. Halstead, D. Michael, and P. Mingos, "Dielectric parameters relevant to microwave dielectric heating," *Chem. Soc. Rev.*, vol. 27, pp. 213-224, 1998.
- [74] S. M. Bradshaw, E. J. van Wyk, and J. B. de Swardt, "Microwave heating principles and the application to the regeneration of granular activated carbon," *The Journal of The South African Institute of Mining and Metallurgy*, vol. July/August 1998, pp. 201-212, 1998.
- [75] A. G. van der Heijden, L. A. Kiemeney, O. N. Gofrit, O. Nativ, A. Sidi, Z. Leib, *et al.*, "Preliminary European results of local microwave hyperthermia and chemotherapy treatment in intermediate or high risk superficial transitional cell carcinoma of the bladder," *Eur Urol*, vol. 46, pp. 65-71; discussion 71-2, July 2004.
- [76] Z. Popovic and B. D. Popovic, "The Skin Effect," in *Introductory Electromagnetics*, M. Horton, Ed., ed New Jersey: Prentice Hall, 2010, pp. 382-392.
- [77] D. H. Staelin, "Electromagnetic Waves," in *Electromagnetics and Applications*, D. H. Staelin, Ed., ed Cambridge, MA: Massachusetts Institute of Technology 2011, pp. 255-298.
- [78] F. Vatansever and M. R. Hamblin, "Far infrared radiation (FIR): its biological effects and medical applications," *Photonics Lasers Med*, vol. 4, pp. 255-266, Nov 1 2012.
- [79] R. K. Gilchrist, R. Medal, W. D. Shorey, R. C. Hanselman, J. C. Parrott, and C. B. Taylor, "Selective inductive heating of lymph nodes," *Ann Surg*, vol. 146, pp. 596-606, Oct 1957.
- [80] M. Babincova, P. Cicmanec, V. Altanerova, C. Altaner, and P. Babinec, "AC-magnetic field controlled drug release from magnetoliposomes: design of a method for site-specific chemotherapy," *Bioelectrochemistry*, vol. 55, pp. 17-9, Jan 2002.
- [81] P. Pradhan, J. Giri, F. Rieken, C. Koch, O. Mykhaylyk, M. Doblinger, *et al.*, "Targeted temperature sensitive magnetic liposomes for thermo-chemotherapy," *J Control Release*, vol. 142, pp. 108-21, Feb 25 2010.
- [82] L. A. Tai, P. J. Tsai, Y. C. Wang, Y. J. Wang, L. W. Lo, and C. S. Yang, "Thermosensitive liposomes entrapping iron oxide nanoparticles for controllable drug release," *Nanotechnology*, vol. 20, p. 135101, Apr 1 2009.
- [83] F. Danhier, O. Feron, and V. Preat, "To exploit the tumor microenvironment: Passive and active tumor targeting of nanocarriers for anti-cancer drug delivery," *J Control Release*, vol. 148, pp. 135-146, 2010.
- [84] R. de la Rica, D. Aili, and M. M. Stevens, "Enzyme-responsive nanoparticles for drug release and diagnostics," *Adv Drug Deliv Rev*, vol. 64, pp. 967-978, 2012.

- [85] A. Arouri, A. H. Hansen, T. E. Rasmussen, and O. G. Mouritsen, "Lipases, liposomes and lipid-prodrugs," *Curr Opin Colloid Interface Sci*, vol. 18, pp. 419-431, 2013.
- [86] A. S. Luk, E. W. Kaler, and S. P. Lee, "Phospholipase C-induced aggregation and fusion of cholesterol-lecithin small unilamellar vesicles," *Biochemistry*, vol. 32, pp. 6965-73, Jul 13 1993.
- [87] J. L. Nieva, F. M. Goni, and A. Alonso, "Liposome fusion catalytically induced by phospholipase C," *Biochemistry*, vol. 28, pp. 7364-7367, 1989.
- [88] T. Abe, K. Sakamoto, H. Kamohara, Y. Hirano, N. Kuwahara, and M. Ogawa, "Group II phospholipase A2 is increased in peritoneal and pleural effusions in patients with various types of cancer," *Int J Cancer*, vol. 74, pp. 245-50, Jun 20 1997.
- [89] S. Yamashita, J. Yamashita, K. Sakamoto, K. Inada, Y. Nakashima, K. Murata, *et al.*, "Increased expression of membrane-associated phospholipase A2 shows malignant potential of human breast cancer cells," *Cancer*, vol. 71, pp. 3058-64, May 15 1993.
- [90] J. Davidsen, K. Jorgensen, T. L. Andresen, and O. G. Mouritsen, "Secreted phospholipase A2 as a new enzymatic trigger mechanism for localised liposomal drug release and absorption in diseased tissue," *Biochim Biophys Acta*, vol. 1609, pp. 95-101, 2003.
- [91] J. Davidsen, C. Vermehren, S. Frokjaer, O. G. Mouritsen, and K. Jorgensen, "Drug delivery by phospholipase A2 degradable liposomes," *Int J Pharm*, vol. 214, pp. 67-69, 2001.
- [92] T. Kaasgaard, T. L. Andresen, S. S. Jensen, R. O. Holte, L. T. Jensen, and K. Jorgensen, "Liposomes containing alkylated methotrexate analogues for phospholipase A2 mediated tumor targeted drug delivery," *Chem Phys Lipids*, vol. 157, pp. 94-103, 2009.
- [93] T. L. Andresen, S. S. Jensen, and K. Jorgensen, "Advanced strategies in liposomal cancer therapy: problems and prospects of active and tumor specific drug release," *Prog Lipid Res*, vol. 44, pp. 68-97, Jan 2005.
- [94] Y. Chau, J. Zhong, and M. Moo-Young, "Enzyme-Sensitive Biomaterials for Drug Delivery," in *Comprehensive Biotechnology*, M. Moo-Young, Ed., 2nd ed Burlington: Academic Press, 2011, pp. 605-624.
- [95] M. J. A. de Jonge, M. Slingerland, W. J. Loos, E. A. C. Wiemer, H. Burger, R. H. J. Mathijssen, *et al.*, "Early cessation of the clinical development of LiPlaCis, a liposomal cisplatin formulation," *Eur J Cancer*, vol. 46, pp. 3016-3021, 2010.
- [96] P. Meers, "Enzyme-activated targeting of liposomes," *Adv Drug Deliv Rev*, vol. 53, pp. 265-72, Dec 31 2001.
- [97] J. C. Powers, B. F. Gupton, A. D. Harley, N. Nishino, and R. J. Whitley, "Specificity of porcine pancreatic elastase, human leukocyte elastase and cathepsin G Inhibition with peptide chloromethyl ketones," *Biochimica et Biophysica Acta*, vol. 485, pp. 156-166, 1977.
- [98] T. Sato, S. Takahashi, T. Mizumoto, M. Harao, M. Akizuki, M. Takasugi, *et al.*, "Neutrophil elastase and cancer," *Surg Oncol*, vol. 15, pp. 217-22, Dec 2006.
- [99] S. C. Davis and F. C. Szoka, Jr., "Cholesterol phosphate derivatives: synthesis and incorporation into a phosphatase and calcium-sensitive triggered release liposome," *Bioconjug Chem*, vol. 9, pp. 783-92, Nov 1998.
- [100] D. C. Drummond, M. Zignani, and J. Leroux, "Current status of pH-sensitive liposomes in drug delivery," *Prog Lipid Res*, vol. 39, pp. 409-60, Sep 2000.

- [101] D. D. S. Ferreira, S. C. Lopes, M. S. Franco, and M. C. Oliveira, "pH-sensitive liposomes for drug delivery in cancer treatment," *Ther Deliv*, vol. 4, pp. 1099-123, Sep 2013.
- [102] H. Karanth and R. S. Murthy, "pH-sensitive liposomes--principle and application in cancer therapy," *J Pharm Pharmacol*, vol. 59, pp. 469-83, Apr 2007.
- [103] S. Simoes, J. Moreira, C. Fonseca, N. Duzqunes, and M. Pedroso de Lima, "On the formulation of pH-sensitive liposomes with long circulation times," *Adv Drug Deliv Rev*, vol. 56, pp. 947-965, 2004.
- [104] M. B. Yatvin, W. Kreutz, B. A. Horwitz, and M. Shinitzky, "pH-sensitive liposomes: possible clinical implications," *Science*, vol. 210, pp. 1253-5, Dec 12 1980.
- [105] R. M. Straubinger, N. Duzqunes, and D. Papahadjopoulos, "pH-sensitive liposomes mediate cytoplasmic delivery of encapsulated macromolecules," *FEBS Letters*, vol. 179, pp. 148-154, 1985.
- [106] V. Torchilin, "Multifunctional and stimuli-sensitive pharmaceutical nanocarriers," *Eur J Pharm Biopharm*, vol. 71, pp. 431-44, Mar 2009.
- [107] A. D. Carvalho Junior, F. P. Vieira, V. J. Melo, M. T. Lopes, J. N. Silveira, G. A. Ramaldes, *et al.*, "Preparation and cytotoxicity of cisplatin-containing liposomes," *Braz J Med Biol Res*, vol. 40, pp. 1149-57, Aug 2007.
- [108] M. C. de Oliveira, V. Rosilio, P. Lesieur, C. Bourgaux, P. Couvreur, M. Ollivon, *et al.*, "pH-sensitive liposomes as a carrier for oligonucleotides: a physico-chemical study of the interaction between DOPE and a 15-mer oligonucleotide in excess water," *Biophys Chem*, vol. 87, pp. 127-37, Oct 30 2000.
- [109] P. R. Cullis and B. de Kruijff, "Lipid polymorphism and the functional roles of lipids in biological membranes," *Biochimica et Biophysica Acta*, vol. 559, pp. 399-420, Dec 20 1979.
- [110] D. C. Litzinger and L. Huang, "Phosphatidylethanolamine liposomes: drug delivery, gene transfer and immunodiagnostic applications," *Biochim Biophys Acta*, vol. 1113, pp. 201-27, Aug 14 1992.
- [111] D. Liu and L. Huang, "pH-sensitive, plasma-stable liposomes with relatively prolonged residence in circulation," *Biochimica et Biophysica Acta*, vol. 1022, pp. 348-54, Mar 1990.
- [112] V. A. Slepishkin, S. Simoes, P. Dazin, M. S. Newman, L. S. Guo, M. C. Pedroso de Lima, *et al.*, "Sterically stabilized pH-sensitive liposomes. Intracellular delivery of aqueous contents and prolonged circulation in vivo," *J Biol Chem*, vol. 272, pp. 2382-8, Jan 24 1997.
- [113] G. Shi, W. Guo, S. M. Stephenson, and R. J. Lee, "Efficient intracellular drug and gene delivery using folate receptor-targeted pH-sensitive liposomes composed of cationic/anionic lipid combinations," *J Control Release*, vol. 80, pp. 309-19, Apr 23 2002.
- [114] R. A. Parente, S. Nir, and F. C. Szoka, Jr., "pH-dependent fusion of phosphatidylcholine small vesicles. Induction by a synthetic amphipathic peptide," *J Biol Chem*, vol. 263, pp. 4724-30, Apr 5 1988.
- [115] J. D. Almeida, D. C. Edwards, C. M. Brand, and T. D. Heath, "Formation of virosomes from influenza subunits and liposomes," *Lancet*, vol. 2, pp. 899-901, Nov 8 1975.
- [116] A. E. Felber, M.-H. Dufresne, and J.-C. Leroux, "pH-sensitive vesicles, polymeric micelles, and nanospheres prepared with polycarboxylates," *Adv Drug Deliv Rev*, vol. 64, pp. 979-992, 2012.

- [117] G. Chen and A. S. Hoffman, "Graft copolymers that exhibit temperature-induced phase transitions over a wide range of pH," *Nature*, vol. 373, pp. 49-52, 1995.
- [118] S. Hirotsu, Y. Hirokawa, and T. Tanaka, "Volume-phase transitions of ionized N-isopropylacrylamide gels," *J Chem Phys*, vol. 87, pp. 1392-1395, 1987.
- [119] N. Bertrand, P. Simard, and J.-C. Leroux, "Serum-Stable and Long-Circulating, PEGylated, pH-Sensitive Liposomes," in *Liposomes - Methods in Molecular Biology*. vol. 605, V. Weissig, Ed., ed Totowa: Humana Press, 2010, pp. 545-558.
- [120] B. Brazdova, N. Zhang, V. V. Samoshin, and X. Guo, "trans-2-Aminocyclohexanol as a pH-sensitive conformational switch in lipid amphiphiles," *Chem Commun*, pp. 4774-4776, 2008.
- [121] X. Liu, Y. Zheng, N. M. Samoshina, A. H. Franz, X. Guo, and V. V. Samoshin, "Fliposomes: pH-triggered conformational flip of new trans-2-aminocyclohexanol-based amphiphiles causes instant cargo release in liposomes," *J Liposome Res*, vol. 22, pp. 319-28, Dec 2012.
- [122] A. V. Samoshin, I. S. Veselov, V. A. Chertkov, A. A. Yaroslavov, G. V. Grishina, N. M. Samoshina, *et al.*, "Fliposomes: new amphiphiles based on trans-3,4-bis(acyloxy)-piperidine able to perform a pH-triggered conformational flip and cause an instant cargo release from liposomes," *Tetrahedron Lett*, vol. 54, pp. 5600-5604, 2013.
- [123] N. M. Samoshina, X. Liu, B. Brazdova, A. H. Franz, V. V. Samoshin, and X. Guo, "Fliposomes: pH-Sensitive Liposomes Containing a trans-2-morpholinocyclohexanol-Based Lipid That Performs a Conformational Flip and Triggers an Instant Cargo Release in Acidic Medium," *Pharmaceutics*, vol. 3, pp. 379-405, 2011.
- [124] Y. Zheng, X. Liu, N. M. Samoshina, V. A. Chertkov, A. H. Franz, X. Guo, *et al.*, "Fliposomes: pH-controlled release from liposomes containing new trans-2-morpholinocyclohexanol-based amphiphiles that perform a conformational flip and trigger an instant cargo release upon acidification," *Nat Prod Commun*, vol. 7, pp. 353-8, Mar 2012.
- [125] E. Mamasheva, C. O'Donnell, A. Bandekar, and S. Sofou, "Heterogeneous liposome membranes with pH-triggered permeability enhance the in vitro antitumor activity of folate-receptor targeted liposomal doxorubicin," *Mol Pharm*, vol. 8, pp. 2224-32, Dec 5 2011.
- [126] A. D. Carvalho-Junior, L. G. Mota, E. A. Nunan, A. J. Wainstein, A. P. Wainstein, A. S. Leal, *et al.*, "Tissue distribution evaluation of stealth pH-sensitive liposomal cisplatin versus free cisplatin in Ehrlich tumor-bearing mice," *Life Sci*, vol. 80, pp. 659-64, Jan 23 2007.
- [127] E. A. Leite, A. M. Lana, A. D. Junior, L. G. Coelho, and M. C. De Oliveira, "Acute toxicity study of cisplatin loaded long-circulating and pH-sensitive liposomes administered in mice," *J Biomed Nanotechnol*, vol. 8, pp. 229-39, Apr 2011.
- [128] E. A. Leite, C. M. Souza, A. D. Carvalho-Junior, L. G. Coelho, A. M. Lana, G. D. Cassali, *et al.*, "Encapsulation of cisplatin in long-circulating and pH-sensitive liposomes improves its antitumor effect and reduces acute toxicity," *Int J Nanomedicine*, vol. 7, pp. 5259-69, 2012.
- [129] S. R. Paliwal, R. Paliwal, H. C. Pal, A. K. Saxena, P. R. Sharma, P. N. Gupta, *et al.*, "Estrogen-anchored pH-sensitive liposomes as nanomodule designed for

- site-specific delivery of doxorubicin in breast cancer therapy," *Mol Pharm*, vol. 9, pp. 176-86, Jan 1 2012.
- [130] S, Amarnath, and U. S. Sharma. "Liposomes in drug delivery: progress and limitations." *International Journal of Pharmaceutics*, vol. 154, pp. 123-140, 1997.
- [131] T. Ishida, Y. Okada, T. Kobayashi, and H. Kiwada, "Development of pH-sensitive liposomes that efficiently retain encapsulated doxorubicin (DXR) in blood," *Int J Pharm*, vol. 309, pp. 94-100, Feb 17 2006.
- [132] O. V. Gerasimov, J. A. Boomer, M. M. Qualls, and D. H. Thompson, "Cytosolic drug delivery using pH- and light-sensitive liposomes," *Adv Drug Deliv Rev*, vol. 38, pp. 317-338, 1999.
- [133] S. J. Leung and M. Romanowski, "Light-activated content release from liposomes," *Theranostics*, vol. 2, pp. 1020-36, 2012.
- [134] A. Yavlovich, A. Singh, R. Blumenthal, and A. Puri, "A novel class of photo-triggerable liposomes containing DPPC:DC(8,9)PC as vehicles for delivery of doxorubicin to cells," *Biochim Biophys Acta*, vol. 1808, pp. 117-26, Jan 2011.
- [135] V. C. Anderson and D. H. Thompson, "Triggered release of hydrophilic agents from plasmalogen liposomes using visible light or acid," *Biochim Biophys Acta*, vol. 1109, pp. 33-42, Aug 10 1992.
- [136] D. H. Thompson, O. V. Gerasimov, J. J. Wheeler, Y. Rui, and V. C. Anderson, "Triggerable plasmalogen liposomes: improvement of system efficiency," *Biochim Biophys Acta* vol. 1279, pp. 25-34, 1996.
- [137] R. H. Bisby, C. Mead, A. C. Mitchell, and C. G. Morgan, "Fast laser-induced solute release from liposomes sensitized with photochromic lipid: effects of temperature, lipid host, and sensitizer concentration," *Biochem Biophys Res Commun*, vol. 262, pp. 406-10, Aug 27 1999.
- [138] R. H. Bisby, C. Mead, and C. G. Morgan, "Wavelength-programmed solute release from photosensitive liposomes," *Biochem Biophys Res Commun*, vol. 276, pp. 169-73, Sep 16 2000.
- [139] A. Yavlovich, A. Singh, S. Tarasov, J. Capala, R. Blumenthal, and A. Puri, "Design of liposomes containing photopolymerizable phospholipids for triggered release of contents " *J Therm Anal Calorim*, vol. 98, pp. 97-104, Oct 1 2009.
- [140] A. Aygun, K. Torrey, A. Kumar, and L. D. Stephenson, "Investigation of factors affecting controlled release from photosensitive DMPC and DSPC liposomes," *Appl Biochem Biotechnol*, vol. 167, pp. 743-57, Jun 2012.
- [141] L. Paasonen, T. Laaksonen, C. Johans, M. Yliperttula, K. Kontturi, and A. Urtili, "Gold nanoparticles enable selective light-induced contents release from liposomes," *J Control Release*, vol. 122, pp. 86-93, Sep 11 2007.
- [142] M. M. Mady, M. M. Fathy, T. Youssef, and W. M. Khalil, "Biophysical characterization of gold nanoparticles-loaded liposomes," *Phys Med*, vol. 28, pp. 288-95, Oct 2012.
- [143] L. Paasonen, T. Sipila, A. Subrizi, P. Laurinmaki, S. J. Butcher, M. Rappolt, *et al.*, "Gold-embedded photosensitive liposomes for drug delivery: Triggering mechanism and intracellular release," *J Control Release*, vol. 147, pp. 136-143, 2010.
- [144] Z. Zhang, J. Wang, and C. Chen, "Near-Infrared Light-Mediated Nanoplatforams for Cancer Thermo-Chemotherapy and Optical Imaging," *Advanced Materials*, vol. 25, pp. 3869-3880, 2013.

- [145] K. A. Carter, S. Shao, M. I. Hoopes, D. Luo, B. Ahsan, V. M. Grigoryants, *et al.*, "Porphyrin-phospholipid liposomes permeabilized by near-infrared light," *Nat Commun*, vol. 5, 2014.
- [146] A. Puri, "Phototriggerable Liposomes: Current Research and Future Perspectives," *Pharmaceutics*, vol. 6, pp. 1-25, 2014.
- [147] P. Shum, J.-M. Kim, and D. H. Thompson, "Phototriggering of liposomal drug delivery systems," *Adv Drug Deliv Rev*, vol. 53, pp. 273-284, 2001.
- [148] A. Lavi, H. Weitman, R. T. Holmes, K. M. Smith, and B. Ehrenberg, "The depth of porphyrin in a membrane and the membrane's physical properties affect the photosensitizing efficiency," *Biophys J*, vol. 82, pp. 2101-10, Apr 2002.
- [149] Q. Xu, S. Geng, Y. Dai, G. Qin, and J. Y. Wang, "CDBA-liposome as an effective sunscreen with longer UV protection and longer shelf life," *J Photochem Photobiol B*, vol. 129, pp. 78-86, Dec 5 2013.
- [150] R. Subramaniam, Y. Xiao, Y. Li, S. Y. Qian, W. Sun, and S. Mallik, "Light-mediated and H-bond facilitated liposomal release: the role of lipid head groups in release efficiency," *Tetrahedron Lett*, vol. 51, pp. 529-532, 2010.
- [151] M. W. Freeman, A. Arrott, and J. H. L. Watson, "Magnetism in Medicine," *J Appl Phys*, vol. 31, pp. S404-S405, 1960.
- [152] K. Hayashi, K. Ono, H. Suzuki, M. Sawada, M. Moriya, W. Sakamoto, *et al.*, "High-Frequency, Magnetic-Field-Responsive Drug Release from Magnetic Nanoparticle/Organic Hybrid Based on Hyperthermic Effect," *ACS Applied Materials & Interfaces*, vol. 2, pp. 1903-1911, 2010.
- [153] R. Hergt and S. Dutz, "Magnetic particle hyperthermia - biophysical limitations of a visionary tumour therapy," *J Magn Magn Mater*, vol. 311, pp. 187-192, 2007.
- [154] T. Hoare, B. P. Timko, J. Santamaria, G. F. Goya, S. Irusta, S. Lau, *et al.*, "Magnetically Triggered Nanocomposite Membranes: A Versatile Platform for Triggered Drug Release," *Nano Letters*, vol. 11, pp. 1395-1400, 2011.
- [155] T.-Y. Liu, K.-H. Liu, D.-M. Liu, S.-Y. Chen, and I. W. Chen, "Temperature-Sensitive Nanocapsules for Controlled Drug Release Caused by Magnetically Triggered Structural Disruption," *Adv Funct Mater*, vol. 19, pp. 616-623, 2009.
- [156] K. Hayashi, M. Nakamura, H. Miki, S. Ozaki, M. Abe, T. Matsumoto, *et al.*, "Magnetically responsive smart nanoparticles for cancer treatment with a combination of magnetic hyperthermia and remote-control drug release," *Theranostics*, vol. 4, pp. 834-44, 2014.
- [157] K. Hayashi, M. Nakamura, W. Sakamoto, T. Yogo, H. Miki, S. Ozaki, *et al.*, "Superparamagnetic nanoparticle clusters for cancer theranostics combining magnetic resonance imaging and hyperthermia treatment," *Theranostics*, vol. 3, pp. 366-76, 2013.
- [158] S. J. Soenen, M. Hodenius, and M. De Cuyper, "Magnetoliposomes: versatile innovative nanocolloids for use in biotechnology and biomedicine," *Nanomedicine (Lond)*, vol. 4, pp. 177-91, Feb 2009.
- [159] S. Behnia, F. Ghalichi, A. Bonabi, and A. Jafari, "Ultrasound Thermotherapy of Breast: Theoretical Design of Transducer and Numerical Simulation of Procedure," *Jpn J Appl Phys*, vol. 45, p. 1856, 2006.
- [160] P. L. Carson and A. Fenster, "Anniversary paper: evolution of ultrasound physics and the role of medical physicists and the AAPM and its journal in that evolution," *Med Phys*, vol. 36, pp. 411-28, Feb 2009.

- [161] Y. Cui, J. U. E. Peng, H. U. Tang, T. Wang, and S. Chen, "New focused ultrasound transducer for fat cell disruption " *J Innov Opt Health Sci*, vol. 05, p. 1250001, 2012.
- [162] C. E. de Lucena, J. L. Dos Santos Junior, C. A. de Lima Resende, V. F. do Amaral, A. de Almeida Barra, and J. H. Reis, "Ultrasound-guided core needle biopsy of breast masses: How many cores are necessary to diagnose cancer?," *J Clin Ultrasound*, vol. 35, pp. 363-6, Sep 2007.
- [163] T. Kang, L. Horton, P. Emery, and R. J. Wakefield, "Value of ultrasound in rheumatologic diseases," *J Korean Med Sci*, vol. 28, pp. 497-507, Apr 2013.
- [164] J. C. R. Rippey and A. G. Royse, "Ultrasound in trauma," *Best Pract Res Cl Anaesthesiol*, vol. 23, pp. 343-362, 2009.
- [165] F. M. Abu-Zidan, A. F. Hefny, and P. Corr, "Clinical ultrasound physics," *J Emerg Trauma Shock*, vol. 4, pp. 501-3, Oct 2011.
- [166] G. Arthurs, "The Physics of Ultrasound," in *AAGBI Core Topics in Anaesthesia*, I. Johnston, W. Harrop-Griffiths, and L. Gemmell, Eds., ed Oxford: Wiley-Blackwell, 2011, pp. 1-16.
- [167] E. U. Buddemeyer, "The physics of diagnostic ultrasound," *Radiol Clin North Am*, vol. 13, pp. 391-402, Dec 1975.
- [168] H. L. Frankel, B. P. deBoisblanc, S. Murthi, M. Ferguson, and A. Sisley, "Ultrasound Physics and Equipment," in *Bedside Procedures for the Intensivist*, H. Frankel, Ed., ed: Springer New York, pp. 57-80, 2010.
- [169] J. Shriki, "Ultrasound Physics," *Crit Care Clin*, vol. 30, pp. 1-24, 2014.
- [170] M. D. Coltrera, "Ultrasound physics in a nutshell," *Otolaryngol Clin North Am*, vol. 43, pp. 1149-59, , Dec 2010.
- [171] M. Yogeshkumar, M. Loizidou, and A. M. Seifalian. "Liposomes and nanoparticles: nanosized vehicles for drug delivery in cancer." *Trends in pharmacological sciences*, vol 30, 11th edition, pp. 592-599, 2009.
- [172] R. N. Baird, "Doppler ultrasound – physics, instrumentation and clinical applications," *Br J Surg*, vol. 77, pp. 355-355, 1990.
- [173] W. R. Hendee and E. R. Ritenour, *Medical Imaging Physics*, 4th Edition ed.: John Wiley & Sons, Inc., 2003.
- [174] H. Azhari, *Basics of Biomedical Ultrasound for Engineers*. Hoboken, New Jersey: John Wiley and Sons, Inc., 2010.
- [175] D. Dalecki, "Mechanical bioeffects of ultrasound," *Annu Rev Biomed Eng*, vol. 6, pp. 229-48, 2004.
- [176] H.-L. Liu and C.-M. Hsieh, "Single-transducer dual-frequency ultrasound generation to enhance acoustic cavitation," *Ultrason Sonochem*, vol. 16, pp. 431-438, 2009.
- [177] N. Vadivelu, R. D. Urman, R. L. Hines, and T. Halaszynski, "Principles of Ultrasound Techniques," in *Essentials of Pain Management*, ed: Springer New York, pp. 469-500, 2011.
- [178] L. Ziegler and R. T. O'Brien, "Harmonic ultrasound: a review," *Vet Radiol Ultrasound*, vol. 43, pp. 501-9, Nov-Dec 2002.
- [179] J. E. Aldrich, "Basic physics of ultrasound imaging," *Crit Care Med*, vol. 35, pp. S131-7, May 2007.
- [180] E. N. Carlsen, "Ultrasound physics for the physician. A brief review," *J Clin Ultrasound*, vol. 3, pp. 69-75, Mar 1975.
- [181] D. O. Hall and A. R. Selfridge, "Multi-frequency ultrasound therapy systems and methods," USA Patent, 1995.

- [182] F. Ahmadi, I. V. McLoughlin, S. Chauhan, and G. ter-Haar, "Bio-effects and safety of low-intensity, low-frequency ultrasonic exposure," *Prog Biophys Mol Biol*, vol. 108, pp. 119-38, Apr 2012.
- [183] J. E. Aldrich, "Basic physics of ultrasound imaging," *Critical care medicine*, vol. 35, pp. S131-S137, 2007.
- [184] W. R. Hendee and E. R. Ritenour, *Medical Imaging Physics*: John Wiley & Sons, Inc., 2003.
- [185] G. Kossoff, "Basic physics and imaging characteristics of ultrasound," in *World Journal of Surgery* vol. 24, ed, pp. 134-142, 2000.
- [186] F. M. Abu-Zidan, A. F. Hefny, and P. Corr, "Clinical ultrasound physics," *Journal of emergencies, trauma, and shock*, vol. 4, pp. 501-3, 2011.
- [187] P. L. Carson and A. Fenster, "Anniversary paper: evolution of ultrasound physics and the role of medical physicists and the AAPM and its journal in that evolution," *Medical physics*, vol. 36, pp. 411-428, 2009.
- [188] A. Schroeder, J. Kost, and Y. Barenholz, "Ultrasound, liposomes, and drug delivery: principles for using ultrasound to control the release of drugs from liposomes," *Chemistry and Physics of Lipids*, vol. 162, pp. 1-16, 2009.
- [189] R. Belmonte, M. Tejero, M. Ferrer, J. M. Muniesa, E. Duarte, O. Cunillera, *et al.*, "Efficacy of low-frequency low-intensity electrotherapy in the treatment of breast cancer-related lymphoedema: a cross-over randomized trial," *Clin Rehabil*, vol. 26, pp. 607-18, Jul 2012.
- [190] G. S. Chen, H. C. Liu, Y. C. Lin, and Y. L. Lin, "Experimental analysis of 1-3 piezocomposites for high-intensity focused ultrasound transducer applications," *IEEE Trans Biomed Eng*, vol. 60, pp. 128-34, Jan 2013.
- [191] D. Horvath and N. A. Lesica, "The effects of interaural time difference and intensity on the coding of low-frequency sounds in the mammalian midbrain," *J Neurosci*, vol. 31, pp. 3821-7, Mar 9 2011.
- [192] J. W. Jenne, T. Preusser, and M. Gunther, "High-intensity focused ultrasound: principles, therapy guidance, simulations and applications," *Z Med Phys*, vol. 22, pp. 311-22, Dec 2012.
- [193] E. M. Khedr, F. Gilio, and J. Rothwell, "Effects of low frequency and low intensity repetitive paired pulse stimulation of the primary motor cortex," *Clin Neurophysiol*, vol. 115, pp. 1259-63, Jun 2004.
- [194] G. Kossoff, "Basic Physics and Imaging Characteristics of Ultrasound," *World J Surg*, vol. 24, pp. 134-142, 2000.
- [195] J. Man, R. M. Shelton, P. R. Cooper, and B. A. Scheven, "Low-intensity low-frequency ultrasound promotes proliferation and differentiation of odontoblast-like cells," *J Endod*, vol. 38, pp. 608-13, May 2012.
- [196] M. A. Buldakov, M. A. Hassan, Q. L. Zhao, L. B. Feril, Jr., N. Kudo, T. Kondo, *et al.*, "Influence of changing pulse repetition frequency on chemical and biological effects induced by low-intensity ultrasound in vitro," *Ultrason Sonochem*, vol. 16, pp. 392-7, Mar 2009.
- [197] R. Karshafian, P. D. Bevan, R. Williams, S. Samac, and P. N. Burns, "Sonoporation by ultrasound-activated microbubble contrast agents: effect of acoustic exposure parameters on cell membrane permeability and cell viability," *Ultrasound Med Biol*, vol. 35, pp. 847-60, May 2009.
- [198] J. J. Choi, K. Selert, Z. Gao, G. Samiotaki, B. Baseri, and E. E. Konofagou, "Noninvasive and localized blood-brain barrier disruption using focused ultrasound can be achieved at short pulse lengths and low pulse repetition frequencies," *J Cereb Blood Flow Metab*, vol. 31, pp. 725-37, Feb 2011.

- [199] D. Lieu, "Ultrasound physics and instrumentation for pathologists," *Arch Pathol Lab Med*, vol. 134, pp. 1541-56, Oct 2010.
- [200] E. C. Pua and P. Zhong, "Ultrasound-mediated drug delivery," *IEEE Eng Med Biol* vol. 28, pp. 64-75, 2009.
- [201] N. Rapoport, "Ultrasound-mediated micellar drug delivery," *Int J Hyperthermia*, vol. 28, pp. 374-385, 2012.
- [202] E. U. Buddemeyer, "The physics of diagnostic ultrasound," *Radiologic clinics of North America*, vol. 13, pp. 391-402, 1975.
- [203] M. D. Coltrera, "Ultrasound Physics in a Nutshell," in *Otolaryngologic Clinics of North America* vol. 43, pp. 1149-1159, 2010.
- [204] H. Edwards, "Ultrasound Physics and Technology: How, Why and When," in *Ultrasound* vol. 18, pp. 100-100, 2010.
- [205] D. Lieu, "Ultrasound physics and instrumentation for pathologists," in *Archives of Pathology and Laboratory Medicine* vol. 134, pp. 1541-1556, 2010.
- [206] S. B. Murthi, M. Ferguson, and A. C. Sisley, "Ultrasound physics and equipment," in *Bedside Procedures for the Intensivist*, ed: Springer, pp. 57-80, 2010.
- [207] E. N. Carlsen, "Ultrasound physics for the physician. A brief review," *Journal of clinical ultrasound : JCU*, vol. 3, pp. 69-75, 1975.
- [208] D. R. Wagner, "Ultrasound as a tool to assess body fat," in *Journal of Obesity* vol. 2013, ed, 2013.
- [209] H. Azhari, *Basics of Biomedical Ultrasound for Engineers*: John Wiley and Sons, 2010.
- [210] L. Schmerr, Jr., "Reflection and Refraction of Bulk Waves," in *Fundamentals of Ultrasonic Nondestructive Evaluation*, ed: Springer US, 1998, pp. 91-140.
- [211] L. W. Schmerr, S.-J. Song, and SpringerLink, *Ultrasonic Nondestructive Evaluation Systems: Models and Measurements*. Boston, MA: Springer Science+Business Media, LLC, 2007.
- [212] T. F. Johansen and T. Rommetveit, "Characterization of ultrasound transducers," in *Proc. of the 33rd Scandinavian Symposium on Physical Acoustics*, 2010.
- [213] A. E. Farjat and J. I. Etcheverry, "Mathematical modeling of the radiated acoustic field of ultrasonic transducers," ed, 2007.
- [214] L. W. Schmerr Jr., "Fundamentals of Ultrasonic Nondestructive Evaluation: A Modeling Approach," in *Mechanical Engineering* vol. 120, ed. New York: American Society of Mechanical Engineers, 1998, p. 95.
- [215] A. Arnau and SpringerLink, *Piezoelectric Transducers and Applications*. Berlin, Heidelberg: Springer Berlin Heidelberg, 2008.
- [216] L. Schmerr, Jr., "Near-Field Measurement Models," in *Fundamentals of Ultrasonic Nondestructive Evaluation*, ed: Springer US, 1998, pp. 435-456.
- [217] L. Schmerr, Jr., "Ultrasonic Transducer Radiation," in *Fundamentals of Ultrasonic Nondestructive Evaluation*, ed: Springer US, 1998, pp. 157-282.
- [218] M. de Smet, E. Heijman, S. Langereis, N. M. Hijnen, and H. Grull, "Magnetic resonance imaging of high intensity focused ultrasound mediated drug delivery from temperature-sensitive liposomes: an in vivo proof-of-concept study," *J Control Release*, vol. 150, pp. 102-110, Feb 28 2011.
- [219] L. Li, T. L. ten Hagen, M. Hossann, R. Suss, G. C. van Rhoon, A. M. Eggermont, *et al.*, "Mild hyperthermia triggered doxorubicin release from optimized stealth thermosensitive liposomes improves intratumoral drug delivery and efficacy," *J Control Release*, vol. 168, pp. 142-50, Jun 10 2013.

- [220] D. Chen and J. Wu, "An in vitro feasibility study of controlled drug release from encapsulated nanometer liposomes using high intensity focused ultrasound," *Ultrasonics*, vol. 50, pp. 744-9, Aug 2010.
- [221] J. J. Lagendijk, J. Crezee, and J. W. Hand, "Dose uniformity in scanned focused ultrasound hyperthermia," *Int J Hyperthermia*, vol. 10, pp. 775-84, Nov-Dec 1994.
- [222] R. J. Lalonde and J. W. Hunt, "Optimizing ultrasound focus distributions for hyperthermia," *IEEE Trans Biomed Eng*, vol. 42, pp. 981-990, 1995.
- [223] S. Wang, V. Frenkel, and V. Zderic, "Optimization of pulsed focused ultrasound exposures for hyperthermia applications," *J Acoust Soc Am*, vol. 130, pp. 599-609, Jul 2011.
- [224] N. M. Tole, "Interaction of Ultrasound with Matter," in *Basic Physics of Ultrasonographic Imaging.*, H. Ostensen, Ed., ed: World Health Organization., 2005.
- [225] C. Damianou, "MRI monitoring of the effect of tissue interfaces in the penetration of high intensity focused ultrasound in kidney in vivo," *Ultrasound Med Biol*, vol. 30, pp. 1209-15, Sep 2004.
- [226] G. F. Baronzio and E. D. Hager, *Hyperthermia in Cancer Treatment: A Primer*. Boston, MA: Landes Bioscience and Springer Science+Business Media, LLC, 2006.
- [227] N. Saniei, "Hyperthermia and Cancer Treatment," *Heat Transfer Eng*, vol. 30, pp. 915-917, 2009.
- [228] P. Wust, B. Hildebrandt, G. Sreenivasa, B. Rau, J. Gellermann, H. Riess, *et al.*, "Hyperthermia in combined treatment of cancer," *Lancet Oncol*, vol. 3, pp. 487-97, Aug 2002.
- [229] T. G. Leighton, "What is ultrasound?," *Prog Biophys Mol Biol*, vol. 93, pp. 3-83, Jan-Apr 2007.
- [230] K. Y. Bilah and R. H. Scanian, "Resonance, Tacoma Narrows bridge failure and undergraduate physics textbooks," *Am. J. Phys.*, vol. 59, pp. 118-124, 1991.
- [231] B. Wolfrum, "Cavitation and Shock Wave Effects on Biological Systems.," Ph.D., University of Gottingen Gottingen, 2004.
- [232] M. Afadzi, S. P. Strand, E. A. Nilssen, S. E. Masoy, T. F. Johansen, R. Hansen, *et al.*, "Mechanisms of the ultrasound-mediated intracellular delivery of liposomes and dextrans," *IEEE Trans Ultrason Ferroelectr Freq Control*, vol. 60, pp. 21-33, Jan 2013.
- [233] M. A. Diaz de la Rosa, G. A. Hussein, and W. G. Pitt, "Mathematical modeling of microbubble cavitation at 70 kHz and the importance of the subharmonic in drug delivery from micelles," *Ultrasonics*, vol. 53, pp. 97-110, Jan 2012.
- [234] S. Hernot and A. L. Klibanov, "Microbubbles in ultrasound-triggered drug and gene delivery," *Adv Drug Deliv Rev*, vol. 60, pp. 1153-66, Jun 30 2008.
- [235] P. Zhong, Y. Zhou, and S. Zhu, "Dynamics of bubble oscillation in constrained media and mechanisms of vessel rupture in SWL," *Ultrasound Med Biol*, vol. 27, pp. 119-34, Jan 2001.
- [236] W. G. Pitt, G. A. Hussein, and B. J. Staples, "Ultrasonic drug delivery--a general review," *Expert Opin Drug Deliv*, vol. 1, pp. 37-56, Nov 2004.
- [237] J. Wu and W. L. Nyborg, "Ultrasound, cavitation bubbles and their interaction with cells," *Adv Drug Deliv Rev*, vol. 60, pp. 1103-16, Jun 30 2008.
- [238] M. A. Diaz-De-La-Rosa, "High-frequency ultrasound drug delivery and cavitation," M.Sc., Brigham Young University, Provo, UT, 2007.

- [239] S. L. Huang, "Liposomes in ultrasonic drug and gene delivery," *Adv Drug Deliv Rev*, vol. 60, pp. 1167-76, Jun 30 2008.
- [240] C. C. Church and X. Yang, "The mechanical index and cavitation in tissue," *J Acoust Soc Am* vol. 117, pp. 2530-2530, 2005.
- [241] J.-P. Franc and J.-M. Michel, *Fundamentals of Cavitation*. Dordrecht: Springer Science + Business Media, Inc., 2005.
- [242] S. Mehier-Humbert, F. Yan, P. Frinking, M. Schneider, R. H. Guy, and T. Bettinger, "Ultrasound-mediated gene delivery: influence of contrast agent on transfection," *Bioconjug Chem*, vol. 18, pp. 652-62, May-Jun 2007.
- [243] C. Oerlemans, R. Deckers, G. Storm, W. E. Hennink, and J. F. Nijsen, "Evidence for a new mechanism behind HIFU-triggered release from liposomes," *J Control Release*, vol. 168, pp. 327-33, Jun 28 2013.
- [244] P.-A. Boucher, B. Joos, M. J. Zuckermann, and L. Fournier, "Pore Formation in a Lipid Bilayer under a Tension Ramp: Modeling the Distribution of Rupture Tensions," *Biophys J*, vol. 92, pp. 4344-4355, 2007.
- [245] R. R. Netz and M. Schick, "Pore formation and rupture in fluid bilayers," *Phys Rev E Stat Phys Plasmas Fluids Relat Interdiscip Topics*, vol. 53, pp. 3875-3885, Apr 1996.
- [246] H. Y. Lin and J. L. Thomas, "PEG-Lipids and oligo(ethylene glycol) surfactants enhance the ultrasonic permeabilizability of liposomes," *Langmuir*, vol. 19, pp. 1098-1105, 2003.
- [247] E. L. Yuh, S. G. Shulman, S. A. Mehta, J. Xie, L. Chen, V. Frenkel, *et al.*, "Delivery of systemic chemotherapeutic agent to tumors by using focused ultrasound: study in a murine model," *Radiology*, vol. 234, pp. 431-7, Feb 2005.
- [248] S. Dromi, V. Frenkel, A. Luk, B. Traughber, M. Angstadt, M. Bur, *et al.*, "Pulsed-high intensity focused ultrasound and low temperature-sensitive liposomes for enhanced targeted drug delivery and antitumor effect," *Clin Cancer Res*, vol. 13, pp. 2722-7, May 1 2007.
- [249] A. Schroeder, Y. Avnir, S. Weisman, Y. Najajreh, A. Gabizon, Y. Talmon, *et al.*, "Controlling liposomal drug release with low frequency ultrasound: mechanism and feasibility," *Langmuir*, vol. 23, pp. 4019-4025, 2007.
- [250] A. Schroeder, R. Honen, K. Turjeman, A. Gabizon, J. Kost, and Y. Barenholz, "Ultrasound triggered release of cisplatin from liposomes in murine tumors," *J Control Release*, vol. 137, pp. 63-8, Jul 1 2009.
- [251] W. G. Pitt, G. A. Hussein, B. L. Roeder, D. J. Dickinson, D. R. Warden, J. M. Hartley, *et al.*, "Preliminary results of combining low frequency low intensity ultrasound and liposomal drug delivery to treat tumors in rats," *J Nanosci Nanotechnol*, vol. 11, pp. 1866-70, Mar 2011.
- [252] T. J. Evjen, E. Hagtvet, A. Moussatov, S. Rognvaldsson, J. L. Mestas, R. A. Fowler, *et al.*, "In vivo monitoring of liposomal release in tumours following ultrasound stimulation," *Eur J Pharm Biopharm*, vol. 84, pp. 526-31, Aug 2013.
- [253] K. Ninomiya, S. Kawabata, H. Tashita, and N. Shimizu, "Ultrasound-mediated drug delivery using liposomes modified with a thermosensitive polymer," *Ultrason Sonochem*, vol. 21, pp. 310-316, 2014.
- [254] S. Rizzitelli, P. Giustetto, C. Boffa, D. Delli Castelli, J. C. Cutrin, S. Aime, *et al.*, "In vivo MRI visualization of release from liposomes triggered by local application of pulsed low-intensity non-focused ultrasound," *Nanomedicine*, Mar 21 2014.

- [255] P. Wang, Y. Li, X. Wang, L. Guo, X. Su, and Q. Liu, "Membrane damage effect of continuous wave ultrasound on K562 human leukemia cells," *J Ultrasound Med*, vol. 31, pp. 1977-86, Dec 2012.
- [256] (2015, 15/02). *High intensity focused ultrasound (HIFU) for prostate cancer*. Available:<http://www.cancerresearchuk.org/about-cancer/type/prostate-cancer/treatment/high-intensity-focused-ultrasound-for-prostate-cancer>[Feb. 12, 2014]
- [257] B. T. Hayes, M. A. Merrick, M. A. Sandrey, and M. L. Cordova, "Three-MHz Ultrasound Heats Deeper Into the Tissues Than Originally Theorized," *Journal of Athletic Training*, vol. 39, pp. 230-234, Jul-Sep 2004.
- [258] C. Rodgers, "Questions about Prenatal Ultrasound and the Alarming Increase in Autism," *Midwifery Today*, vol. 80, 2006.
- [259] E. S. B. C. Ang, V. Gluncic, A. Duque, M. E. Schafer, and P. Rakic, "Prenatal exposure to ultrasound waves impacts neuronal migration in mice," *Proceedings of the National Academy of Sciences*, vol. 103, pp. 12903-12910, August 22, 2006.
- [260] T. M. Allen and P. R. Cullis, "Liposomal drug delivery systems: from concept to clinical applications," *Adv Drug Deliv Rev*, vol. 65, pp. 36-48, Jan 2013.
- [261] L. Zhang, F. X. Gu, J. M. Chan, A. Z. Wang, R. S. Langer, and O. C. Farokhzad, "Nanoparticles in medicine: therapeutic applications and developments," *Clin Pharmacol Ther*, vol. 83, pp. 761-9, May 2008.
- [262] A. Babu, A. K. Templeton, A. Munshi, and R. Ramesh, "Nanoparticle-Based Drug Delivery for Therapy of Lung Cancer: Progress and Challenges," *Journal of Nanomaterials*, vol. 2013, p. 11, 2013.
- [263] J. T. Thigpen, C. A. Aghajanian, D. S. Alberts, S. M. Campos, A. N. Gordon, M. Markman, *et al.*, "Role of pegylated liposomal doxorubicin in ovarian cancer," *Gynecol Oncol*, vol. 96, pp. 10-8, Jan 2005.
- [264] G. Pillai, "Nanomedicines for Cancer Therapy: An Update of FDA Approved and Those under Various Stages Development," *SOJ Pharm Pharm Sci*, vol. 1, pp. 1-13, 2014.
- [265] S. Koudelka and J. Turanek, "Liposomal paclitaxel formulations," *J Control Release*, vol. 163, pp. 322-34, Nov 10 2012.
- [266] C. Nehate, S. Jain, A. Saneja, V. Khare, N. Alam, R. D. Dubey, *et al.*, "Paclitaxel formulations: challenges and novel delivery options," *Curr Drug Deliv*, vol. 11, pp. 666-86, 2014.
- [267] H. Sun, B. Guo, R. Cheng, F. Meng, H. Liu, and Z. Zhong, "Biodegradable micelles with sheddable poly(ethylene glycol) shells for triggered intracellular release of doxorubicin," *Biomaterials*, vol. 30, pp. 6358-66, Oct 2009.
- [268] V. P. Torchilin, T. S. Levchenko, A. N. Lukyanov, B. A. Khaw, A. L. Klibanov, R. Rammohan, *et al.*, "p-Nitrophenylcarbonyl-PEG-PE-liposomes: fast and simple attachment of specific ligands, including monoclonal antibodies, to distal ends of PEG chains via p-nitrophenylcarbonyl groups," *Biochim Biophys Acta*, vol. 1511, pp. 397-411, Apr 2 2001.
- [269] D. Cohen-Levi, "Ultrasound for targeted delivery of cytotoxic drugs from liposomes.," M.Sc. M.Sc., Faculty of Engineering Sciences, Ben Gurion University, Beer Sheva, Israel, 2000.
- [270] H. Y. Lin and J. L. Thomas, "Factors affecting responsivity of unilamellar liposomes to 20 kHz ultrasound," *Langmuir*, vol. 20, pp. 6100-6, Jul 20 2004.

Appendix A

```
%MATLAB code 1 used to find the right reference curve for the NN-
MPC

clc
close all
lookup =[run1(:,3) run2(:,3) run3(:,3) run4(:,3) run5(:,3)
run6(:,3) run7(:,3) run8(:,3) run9(:,3)];

r = input('please specify the time in minutes and second and the
release out of 100 in square brakets like [3 50 45] ')

s = 1;
while(s~=0)
if (r(1,3)<65 && r(1,3)>0) && (r(1,1)<=4 && r(1,1)>0) &&
(r(1,2)>59 || r(1,2)<0)
    disp('please make sure the seconds is between 0 and 59')
    r(1,2) = input('please specify adjust the seconds ')
elseif (r(1,3)<100 && r(1,3)>20) && (r(1,1)>4 || r(1,1)<0) &&
(r(1,2)<59 && r(1,2)>=0)
    disp('please make sure minutes is between 0 and 4')
    r(1,1) = input('please specify min ')
elseif (r(1,3)>65 || r(1,3)<0) && (r(1,1)<=4 && r(1,1)>0) &&
(r(1,2)<59 && r(1,2)>=0)
    disp('please make sure the release is a number out of
65')
    r(1,3) = input('please specify the release out of 65 ')
elseif (r(1,3)>65 || r(1,3)<0) && (r(1,1)>4 || r(1,1)<0) &&
(r(1,2)<59 && r(1,2)>=0)
    disp('please make sure the release is a number out of 65
and the minutes is between 0 and 4')
    rm = input('please specify the minuts and the release
[minutes release]')
    r(1,1) = rm(1,1);
    r(1,3) = rm(1,2);
elseif (r(1,3)>65 || r(1,3)<0) && (r(1,1)<=4 && r(1,1)>0) &&
(r(1,2)>59 || r(1,2)<0)
    disp('please make sure the release is a number out of 65
and the seconds is between 0 and 59')
    rs = input('please specify the seconds and the release
[seconds release]')
    r(1,2) = rs(1,1);
    r(1,3) = rs(1,2);
elseif (r(1,3)<65 && r(1,3)>0) && (r(1,1)>4 || r(1,1)<0) &&
(r(1,2)>59 || r(1,2)<0)
    disp('please make sure the min is between 0 and 4 and the
seconds is between 0 and 59')
    ms = input('please specify the minutes and seconds
[minutes seconds]')
    r(1,1) = ms(1,1);
    r(1,2) = ms(1,2);
else
    s = 0;
end
end
```

```

##### time conversion #####
if r(1,1) == 4 && r(1,2)>40
    disp('The maximum allowed time is 4:40 min and the requested is
larger than that')
    disp(' so the value will be assumed to be 4:40 min automatically')
    r(1,2) = 40
end
tim = r(1,1)*600+r(1,2)*10;
lookinto = lookup(tim,:);
for i = 1:length(lookinto)
    diff(i) = abs(r(1,3)-lookinto(i));

end
[row column] = min(diff)
diff(1,column) = 100;
[row2 column2] = min(diff)

closest = [column column2];

intensity = [max(run1(:,2)) max(run2(:,2)) max(run3(:,2))
max(run4(:,2)) max(run5(:,2)) max(run6(:,2)) max(run7(:,2))
max(run8(:,2)) max(run9(:,2))];
### diff in percentage ###
diff_per =row+row2;
per1 = row/diff_per;
per2= row2/diff_per;
merged_intens = intensity(column) * per1 + intensity(column2) *
per2;

##### duty cycle merged #####
dutyon = [20 20 20 20 10 10 10 10 10];
duty_merg_on = (dutyon(column)*per1+dutyon(column2)*per2)*10;
duty_merg_on = round(duty_merg_on);
dutyoff = [10 10 10 10 10 10 10 10 10];
duty_merg_off = (dutyoff(column)*per1+dutyoff(column2)*per2)*10;
duty_merg_off = round(duty_merg_off);
totalduty = duty_merg_on+duty_merg_off;
##### reconstruction #####
number_of_pulses = round(tim/totalduty);
matr = zeros(1,totalduty);
matr(:,1:duty_merg_on) = merged_intens;
pulsedsignal = repmat(matr,1,number_of_pulses);
figure
plot(pulsedsignal)

##### construct method 2 #####
xrecon =[run1(:,2) run2(:,2) run3(:,2) run4(:,2) run5(:,2) run6(:,2)
run7(:,2) run8(:,2) run9(:,2)];
w = pinv(xrecon)*lookup';
z = run3(:,2)'*w;

w2 = pinv(lookup(1:tim,:))'*xrecon(1:tim,:);
averagecurve = (lookup(1:tim,column)+lookup(1:tim,column2))/2;
z2 = averagecurve'*w2;

```

```

##### Plotting results #####
figure
plot(lookup(:,column),'go')
hold on
plot(lookup(:,column2),'r')
title('Curves closest to the targetted output')
figure
plot(averagecurve)
hold on
plot(lookup(1:tim,column),'r')
plot(lookup(1:tim,column2),'g')
title('Averagecurve')
legend('Interpolated curve','close graph 1','close graph 2')
figure
plot(pulsedsignal)
title('Pulses of the refernce signal using weighted averaging')
figure
plot(z)
title('Just and Example of reverse model reconstruction')
figure
plot(z2)
title('reconstruction')
legend('reconstructed graph for the reference US signal')
xlabel('Time units')
ylabel('Intensity W/cm^2')

```

```

% MATLAB code 2 used to prepare the data for the controller

close all
T = averagecurve';
d =5;
X = z2;
figure
plot(X)
hold on
plot(T, 'r')
X = num2cell(X);
T = num2cell(T);

net = narxnet(1:d,1:d,[4,10]);
net.numLayers = 3;
net.layers{1}.transferFcn = 'logsig';
net.layers{2}.transferFcn = 'tansig';
net.layers{3}.transferFcn = 'purelin';
net.trainParam.epochs=10000;           % Maximum number of epochs
net.trainParam.show=50;                % Period of showing calculation
progress
net.trainParam.lr=0.1;                  % Algorithm learning rate
net.trainParam.goal=1e-9;              % Optimisation goal
net.trainParam.min_grad=1e-10;         % Minimum gradient
net.trainParam.mem_reduc=1;            % Memory reduction parameter
net.trainParam.mu_max=1e100;
[Xs,Xi,Ai,Ts] = preparets(net,X,{},T);
net = train(net,Xs,Ts,Xi,Ai);
% view(net)
yy = net(Xs,Xi,Ai);
% [yy,Xfo,Afo] = net(Xs,Xi,Ai);
netc = closeloop(net);
% [netc,Xic,Aic] = closeloop(net,Xfo,Afo);
% view(netc)
[Xs2,Xi2,Ai2,Ts] = preparets(netc,X,{},T);
yp = netc(Xs2,Xi2,Ai2);
% [yp,Xfc,Afc] = netc(Xs2,Xic,Aic);
figure
plot(cell2mat(yy))
figure
plot(cell2mat(yp), 'r')

[sysName,netName] = gensim(netc,'InputMode','Workspace',...
    'OutputMode','Workspace','SolverMode','Discrete');

```

Vita

Hesham Gamal Ali Moussa was born on February 24, 1992, in Alexandria, Egypt. He moved to Saudi Arabia in the same year where he completed his primary and elementary school in Riyadh city. Then he moved to Germany where he studied the first two years of high school then returned back to Saudi Arabia to graduate high school. Then, in year 2008, he joined the American university of Sharjah, UAE where he received a partial scholarship to graduate with a Bachelor of Science in Electrical Engineering with magna cum laude in 2013.

In the same year, Mr. Hesham joined the Master's program in Electrical Engineering at the American University of Sharjah, Sharjah, UAE in 2012, where he was awarded a graduate assistantship to continue his studies. The assistantship granted him an opportunity to work as a teaching assistant from January 2013 until January 2015, then he worked as a research assistant January 2015 until June 2015.

Mr. Hesham is the first author of a review article published in the *Journal of Drug Targeting*, April, 2015, entitled “*Review on Triggered Liposomal Drug Delivery with a Focus on Ultrasound*”. He is also the first author of another article submitted to the same journal (currently under review, up to the date this thesis was approved for online publication), entitled “*Release of calcein from stealth and normal liposomes using low- and high-frequency ultrasound: A comparative study*”. Moreover, Mr. Hesham is a co-author of an abstract, submitted to the XIII International Conference on Nanoscience and Nanotechnology, Copenhagen, 2015, entitled “*Release of calcein from liposomes using low- and high- frequency ultrasound*”. He has also a conference paper titled “*Visual Aid for Optic Nerve Hypoplasia Patients*” that he presented in Biomedical Engineering (MECBME), 2014 Middle East Conference, Doha, Qatar. He also participated in First IEEE EMBS International Students Conference that took place in Cairo University, Egypt, in which, as a group, was able to secure the second place with the paper titled “*Eye-Tracking Based Visual Aid for Vision Impairment*”